HETEROGENEOUS NETWORKS IN LTE

Teză destinată obţinerii
titlului ştiinţific de doctor inginer
la
Universitatea Politehnica Timişoara
în domeniul
INGINERIE ELECTRONICĂ, TELECOMUNICAȚII
ȘI TEHNOLOGII INFORMAȚIONALE
de către

Ing. Ionel Romeo Petruț

Conducător ştiinţific: prof.univ.dr.ing. Marius Oteșteanu
Referenţi ştiinţifici: prof.univ.dr.ing. Aldo De Sabata
prof.univ.dr.ing. Florin Alexa
conf.univ.dr.ing. Mârza Eugen

Ziua susţinerii tezei: 13.06.2019

Seriile Teze de doctorat ale UPT sunt:

1. Automatică
2. Chimie
3. Energetică
4. Ingineria Chimică
5. Inginerie Civilă
6. Inginerie Electrică
7. Inginerie Electronică și Telecomunicații
8. Inginerie Industrială
9. Inginerie Mecanică
10. Știința Calculatoarelor
11. Știința și Ingineria Materialelor
12. Ingineria sistemelor
13. Inginerie energetică
14. Calculatoare şi tehnologia informației
15. Ingineria materialelor
16. Inginerie şi Management
17. Arhitectură
18. Inginerie civilă și instalații

Universitatea Politehnica din Timişoara a inițiat seriile de mai sus în scopul diseminării expertizei, cunoştinţelor şi rezultatelor cercetărilor întreprinse în cadrul școlii doctorale a universității. Seriile conțin, potrivit H.B.Ex.S Nr. 14 / 14.07.2006, tezele de doctorat susținute în universitate începând cu 1 octombrie 2006.

România, 300159 Timișoara, Bd. Republicii 9,

tel. 0256 403823, fax. 0256 403221

e-mail: editura@edipol.upt.ro

Cuvânt înainte

Teza de doctorat a fost elaborată pe parcursul activității mele de cercetare atât în cadrul Facultății de Electronică și Telecomunicații a Universității „Politehnica” din Timișoara, cât și in cadrul companiei Alcatel-Lucent România.

Lucrarea se adresează tuturor celor interesați a cunoaște aspectele principale legate de rețelele eterogene LTE și cum pot celulele de tip small cell să crească performanțele rețelelor de comunicații mobile.

O decizie cu privire la ce arhitectură de rețea va fi utilizată, pentru fiecare rețea mobilă în parte, va fi luată de către fiecare operator pe baza particularităților mediului și a nevoilor utilizatorilor. Rezultatele prezentate în această teză creează premisele pentru dezvoltarea unor rețelele eterogene native, în special prin prisma specificități tehnologiilor IoT și 5G.

Timișoara, iunie 2019 PETRUȚ Ionel Romeo

This work was partially supported by the strategic grant POSDRU/159/1.5/S/137516 of the Ministry of National Education, Romania, co-financed by the European Social Fund – Investing in People, within the Sectorial Operational Program Human Resources Development 2007-2013.

Finalizarea acestei lucrări a fost posibilă datorită tuturor celor care m-au îndrumat și sprijinit pe durata acestor ani: colectivul catedrei de Comunicații din cadrul Facultății de Electronică și Telecomunicații a Universității „Politehnica” din Timișoara și colegii de serviciu pe plan profesional; familia mea, pe plan personal.

Sămânța începerii activității mele în cercetare, a fost sădită de prof.dr.ing Calin Doru, care prin încrederea ce mi-a oferit-o pe parcursul anilor în care am colaborat, m-a făcut să cred că voi reuși.

Tuturor le mulțumesc că au fost alături de mine și îmi doresc ca și pe viitor să îmi rămână aproape.

Petruț, Ionel Romeo

HETEROGENEOUS NETWORKS IN LTE

Teze de doctorat ale UPT, Seria 19, Nr. 1, Editura Politehnica, 2019, 130 pagini, 69 figuri, 5 tabele.

ISSN:2668-425X
ISSN-L:2668-425X
ISBN: 978-606-35-0295-8

Cuvinte cheie: LTE, HetNet, MIMO, Beamfoarming, eICIC, optimizare,SAR

Rezumat,

Celulele mici sunt stații de bază low-cost, cu putere redusă destinate să îmbunătățească acoperirea și capacitatea rețelelor fără fir. Prin implementarea unor celule mici în completarea rețelelor tradiționale macro-celulare, operatorii se află într-o poziție mult mai bună de a oferi utilizatorilor finali o calitate mai bună și mai bună a experienței (QoE).

Rezultatele obținute pe parcursul cercetării validează creșterea performanțelor rețelelor mobile prin introducerea celulelor de putere mică și a celor cu capabilități de beamfoarming.

O decizie cu privire la ce arhitectură de rețea va fi utilizată pentru rețeaua mobilă va fi luată de fiecare operator de rețea pe baza particularităților mediului și a nevoilor utilizatorilor, dor că rezultatele prezentate în această teză creează premisele pentru dezvoltarea unor rețelele eterogene native, în special prin prisma specificităților IoT și 5G.

Contents

Acronyms

1xEV-DO	1x Evolution for Data Optimized
3GPP	Third Generation Partnership Project
3GPP2	Third Generation Partnership Project 2
4G	Fourth Generation Wireless Systems
5G	Fifth Generation Wireless Systems
AAA	Authentication, Authorization and Accounting
AAS	Adaptive Antenna System
ACK	Acknowledge or Acknowledgement
AM	Acknowledged Mode
AMBR	Aggregate Maximum Bit Rate
AMC	Adaptive Modulation and Coding
AN	Access Network
APN	Access Point Name
ARP	Address Resolution Protocol
ARP	Allocation and Retention Priority
ARQ	Automatic Repeat Request
BCCH	Broadcast Control Channel
BCH	Broadcast Channel
BER	Bit Error Rate
BLER	Block Error Rate
BPSK	Binary Phase Shift Keying
BW	Bandwidth
C-RNTI	Cell Radio Network Temporary Identity
CDMA	Code Division Multiple Access
CFI	Channel Format Indicator
CP	Cyclic Prefix
CN	Core Network
CQI	Channel Quality Indicator
DCCH	Dedicated Control Channel
DCI	Downlink Control Information
DHCP	Dynamic Host Configuration Protocol
DL	Downlink
E-UTRAN	Evolved UMTS Terrestrial Radio Access Network
eNodeB	E-UTRAN Node B
EPC	Evolved Packet Core
EPS	Evolved Packet System
EUTRAN	Evolved UTRAN
EV-DO	Evolution for Data Optimized

FDD	Frequency Division Duplex
FDM	Frequency Division Multiplexing
FDMA	Frequency Division Multiple Access
FEC	Forward Error Correction
GPRS	General Packet Radio Service
GSM	Global System for Mobile Communication
GW	Gateway
H-ARQ	Hybrid ARQ
HDTV	Hi Definition TV
HetNet	Heterogeneous Networks
HLR	Home Location Register
HO	Handover
HPLMN	Home PLMN
HSDPA	High Speed Downlink Packet Access
HSPA	High Speed Packet Access
HSS	Home Subscriber Server
HSUPA	High Speed Uplink Packet Access
ICI	Inter-Carrier Interference
ICIC	Inter-cell Interference Coordination
IEEE	Institute of Electrical and Electronics Engineers
IoT	Internet of Things
IP	Internet Protocol
IPSec	Internet Protocol Security
IPv4	Internet Protocol version 4
IPv6	Internet Protocol version 6
ISI	Inter-Symbol Interference
ITU	International Telecommunication Union
kbps	kilo-bits per second
kHz	Kilo Hertz
L1	Layer 1 (physical layer)
L3	Layer 3 (network layer)
LTE	Long Term Evolution
MAC	Medium Access Control
MBR	Maximum Bit Rate
MCH	Multicast Channel
MCM	Multi-Carrier Modulation
ME	Mobile Equipment
MGW	Media Gateway
MHz	Mega Hertz
MIB	Master Information Block
MIMO	Multiple Input Multiple Output
MIP	Mobile IP
MISO	Multiple Input Single Output
MME	Mobility Management Entity
MMS	Multimedia Messaging Service

MS	Mobile Station
MSC	Mobile Switching Center
NACK	Negative ACK
NAS	Non-Access Stratum
OFDM	Orthogonal Frequency Division Multiplexing
OFDMA	Orthogonal Frequency Division Multiple Access
OSS	Operations System Support
P-GW	PDN Gateway
PCFICH	Physical Control Format Indicator Channel
PCRF	Policy and Charging Rule Function
PDCCH	Physical Dedicated Control Channel
PDCP	Packet Data Convergence Protocol
PDN	Packet Data Network
PDP	Packet Data Protocol
PDSCH	Physical Downlink Shared Channel
PDU	Protocol Data Unit
PHY	Physical Layer
PLMN	Public Land Mobile Network
PRACH	Physical Random Access Channel
PRB	Physical Resource Block
PSTN	Public Switched Telephone Network
PUCCH	Physical Uplink Control Channel
PUSCH	Physical Uplink Shared Channel
QAM	Quadrature Amplitude Modulation
QCI	QoS Class Identifiers
QoE	Quality of Experience
QoS	Quality of Service
QPSK	Quadrature Phase Shift Keying
RACH	Random Access Channel
RAN	Radio Access Network
RAT	Radio Access Technology
RB	Resource Block
RF	Radio Frequency
RLC	Radio Link Control
RRC	Radio Resource Control
RRM	Radio Resource Management
RSRP	Reference Symbol Received Power
RSRQ	Reference Symbol Received Quality
RSSI	Received Signal Strength Indicator
S-GW	Serving Gateway
S1-U	S1 - User Plane
SAE	System Architecture Evolution
SAR	Specific Absorption Rate
SC	Single Carrier
SC-FDMA	Single Carrier - Frequency Division Multiple Access

SCH	Synchronization Channel
SIB	System Information Block
SIMO	Single Input Multiple Output
SIP	Session Initiation Protocol
SIR	Signal-to-Interference Ratio
SNR	Signal-to-Noise Ratio
TA	Tracking Area
TDD	Time Division Duplex
TM	Transmission Mode
TTI	Transmission Time Interval
UCI	Uplink Control Information
UDP	User Datagram Protocol
UE	User Equipment
UL	Uplink
UL-SCH	Uplink Shared Channel
UM	Unacknowledged Mode
UMA	Unlicensed Mobile Access
UMTS	Universal Mobile Telecommunications System
VoIP	Voice over Internet Protocol
VRB	Virtual Resource Blocks
WCDMA	Wideband Code Division Multiple Access
Wi-Fi	Wireless Fidelity
WiMAX	Worldwide Interoperability for Microwave Access
WLAN	Wireless Local Area Networks

List of Figures

List of Tables

1 Introduction

Today it's hard to imagine a world without connectivity, without access to various services from voice to 4K resolution broadcast movies, from web browsing to chat. The connectivity asset becomes more powerful in association with mobility, at that time when the location, moving speed and access technology are no longer a barrier to be an online entity. In current era, everything is developing fast, new technologies are born every day and new customer expectations appears.

Enabling technology for mobile phones was first developed in the 1940s but it was not until the mid-1980s that they became widely available. Since 1980s, the development processes went through many phases and generations driving the mobile networks to better performance, coverage, capacity, continues increasing the end user experience in parallel with a cost-effectiveness [1]. Mobile network providers make considerable efforts to adapt existing infrastructure to accommodate new requirements and combine new technologies with legacy technologies to shape future mobile communication networks. Taking into consideration all these aspects the evolution from a single layer / technology network to a Heterogeneous Network multi-layers/ multi-technology is imposed.

1.1 Problem statement

Based on "World Cellular Information Service (WCIS)" studies, in 2016 more than 75% of mobile calls were made in an indoor environment [2]. The trend of increased indoor power consumption induces a natural action from many countries' sides: enlarge health safety norms [3]. Lowering the maximum allowed power complicates the network planning and makes it more difficult to compliant with these requirements using only macro equipment. A low power and most cost-effective solution is offered by small cells.

Nowadays the data traffic in the mobile network is rising and the subscribers' performance expectations are growing, so supplementing the existing macro networks with small cells is an effective way to provide a better coverage and a higher capacity in the indoor environment and outdoor area; in the public space, enterprises and in homes.

In addition, small cells that are deployed in strategic areas are the perfect solution to bring network innovation such as value-adding applications, local contextual applications and IoT services.

Small cells are low-cost, low-power base stations designed to improve coverage and capacity of the wireless networks. By deploying small cells on top and in complement to the traditional macro cellular networks, operators are in a much better

position to provide the end users with a more uniform and improved Quality of Experience (QoE) [4]. Small cells deployment is subject to service delivery requirements, as well as to the actual constraints specific to the targeted areas. For a good uniformity of service, in dense populated areas where presence of buildings is the main reason for significant radio signal attenuation, small cells may need to be closely spaced, e.g. within a couple of hundred meters from each other. Naturally, the performance of small cells is highly dependent on the environment specific characteristics, such as materials used for building construction, their specific propagation properties and surroundings. It is particularly important to have a proper characterization of an environment where small cells are deployed [4].

Taking into consideration all the challenges that come with "always online statement, the evolution from a single layer / technology network to a Heterogeneous Network multi-layers/ multi-technology is imposed. The multi-layer networks can take many forms, from the first used criteria, where inside the same radio access technology we play with the size of the cell, up to mixtures of cells size and technologies inside the same system.

Once combining indoor and outdoor cells need to take care of particularities such as: different rage of transmitted power, processing capacity and specific interferences.

1.2 Thesis objectives

The main goal of this thesis is to bring new and relevant contributions in the area of LTE Heterogeneous Networks. The contribution presented in this thesis correspond to several different research directions which will be described below.

The study of in-building performance and feasibility of LTE Small Cells with Beamforming capabilities was the first deliverable of my research. After the first encouraging results, I continued to explore the subject by discovering various ways to improve LTE indoor coverage using also MIMO capabilities of the small cells.

Next main topic addressed was HetNet performance analysis and performance improvement studies on several directions:

- Handover mechanism optimization by replacing signal strength indicator - RSRP with signal quality indicator - RSRQ as main trigger in handover mechanism.
- Improvement of overall uplink throughput by performing a network densification using small cells
- Reducing interference effects and cluster capacity increase through eICIC technology and parameter customization for a HetNet.

The third addressed topic was to analyze the end user experience in mobile networks and to determine the mobile networks influences against the human bodies (analyzed the impact of electromagnetic radiation, SAR - Specific Absorption Rate).

1.3 Thesis outline

After a brief introduction, the thesis starts by presenting the background and motivation of this work in Chapter 2. During this chapter I made a LTE overview followed by key feature presentations, parameters definitions, Heterogeneous Network design and applications.

The remainder of the thesis holds the main contributions and the conclusions.

A performance analysis of single layer LTE network, from indoor coverage point of view, along with indoor LTE service improvements achievable when using MIMO capable small cells are presented in Chapter 3.

In Chapter 4 HetNet benefits were analyzed the and this chapter presents several improvement ways from handover, uplink throughput and interference mitigation parts. HO optimization is analyzed from HO trigger parameters perspective: RSRQ and RSRP; The UL throughput improvement is addressed through network densification using small cells and the interference mitigations is addressed through eICIC parameters optimization.

In Chapter 5 the results of a set of experiments are described, conducted on a commercial mobile network, to determine the end user experience and how HetNet technology can reduce the electromagnetic radiation effect on our bodies.

Finally, Chapter 6 is dedicated to the conclusions of this work.

2 Background and motivation

We are living in the communication generation, massive networking and internet computing, where everything is connected everywhere. Everything is developing fast: new technologies are born every day as more capable users equipment's are developed and users are constantly demanding a higher data traffic and getting a better performance. Since the introduction of the first mobile network up to now, the mobile networks evolved to better performances, better coverage, higher capacity, higher throughput per user and clean architecture, easily deployable and cost effective [5].

In the last years many operators where migrating to Long Term Evolution (LTE) to answer to market requirements:

- a significant increase of number of connected devices
- a massive growth in traffic volume
- an increased wide range of applications with varying requirements and characteristics

The LTE is one of the latest milestones achieved in advancing series of mobile telecommunication systems by the Third Mobile Generation Partnership Project (3GPP) from a commercial network point of view.

3GPP technologies have evolved from global system for mobile communication (GSM)- to Enhanced data for GSM evolution (EDGE), to Universal Mobile Telecommunications System (UMTS)- to High Speed Packet Access (HSPA)- to evolved HSPA (HSPA+), to LTE and Finally to Long Term Evolution Advanced (LTE-A) and in near future will go to 5G in order to provide increased capacity and new features as can be seen in Figure 1 [6].

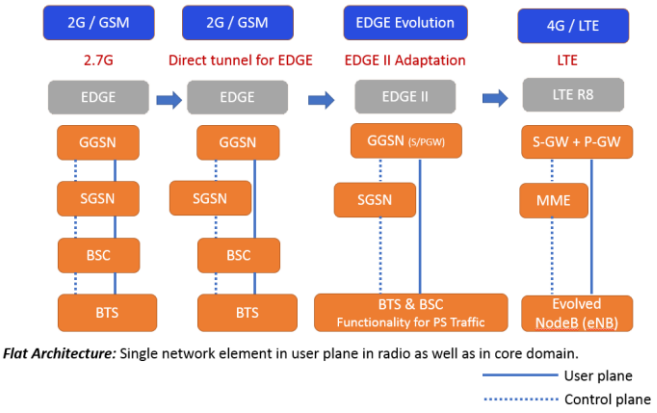

Figure 1: Wireless networks evolutions

LTE employs Orthogonal Frequency Division Multiplexing (OFDM) as its radio access technology, together with advanced antenna techniques like Multiple-Input-Multiple-Output (MIMO), spatial multiplexing and beam-forming. The choice of OFDM technology not only helps LTE to fulfill the requirements for spectrum flexibility but also enables cost-efficient solutions for very wide carriers with high peak data rates.

2.1 LTE Network Architecture

In contrast to the circuit-switched model of previous cellular systems, Long Term Evolution (LTE) has been designed to support only packet-switched services. It aims to provide seamless Internet Protocol (IP) connectivity between user equipment (UE) and the packet data network (PDN), without any disruption to the end users' applications during mobility.

While the term "LTE" encompasses the evolution of the Universal Mobile Telecommunications System (UMTS) radio access through the Evolved UTRAN (E-UTRAN), it is accompanied by an evolution of the non-radio aspects under the term "System Architecture Evolution" (SAE), which includes the Evolved Packet Core (EPC) network. Together LTE and SAE comprise the Evolved Packet System (EPS) [7].

At a high level, the network is comprised of the core network (EPC) and the access network E-UTRAN. While the CN consists of many logical nodes, the access network is made up of essentially just one node, the evolved NodeB (eNodeB), which connects to the UEs. The eNodeB is the only network element on the radio side, replacing the previous NodeB / RNC combination from UMTS and providing all the radio management functions. Each of these network elements is interconnected by means of interfaces that are standardized to allow multi-vendor interoperability. This gives network operators the possibility to source different network elements from different vendors. In fact, network operators may choose in their physical implementations to split or merge these logical network elements depending on commercial considerations. The EPS network elements are shown in Figure 2 [8].

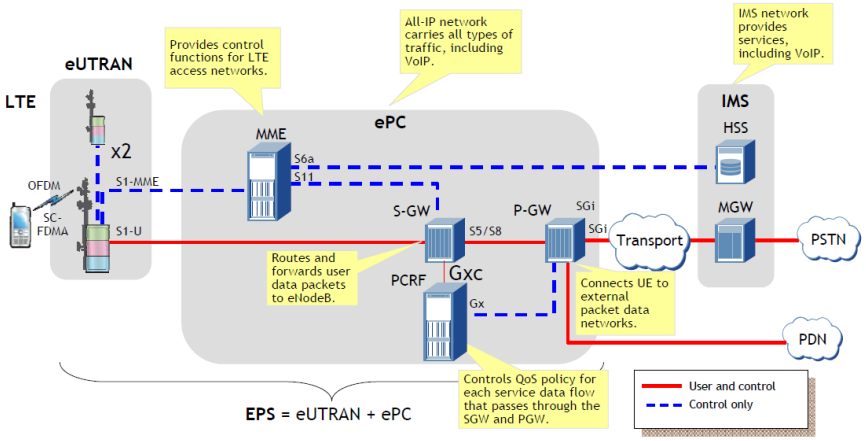

Figure 2: LTE network architecture

LTE network elements definitions and functionalities are presented below:

- User equipment (UE):
  - Sends initial attach requests to eNodeB
  - Registers with the network to request services

- Evolved NodeB (eNodeB):
  - Radio Resource Management (RRM) functionalities like radio bearer control and radio admission control.
  - IP header compression and encryption of the user data stream.
  - Radio resource allocation in both uplink and downlink.
  - Transfer of paging messages over the air.
  - Transfer of BCCH information over the air.
  - Selection of the MME during a call.
  - Mobility control in the LTE_ACTIVE state.
  - Measurement collection and evaluation
  - User data routing to the S-GW/P-GW
  - Security: Ciphering and Integrity protection on the radio interface
  - IP header (de)compression
  - Connection Management Control: UE state management

- Mobility Management Entity (MME):
  - MME is the control node that processes the signaling between the UE and the EPC. The protocols running between the UE and the EPC are known as the Non-Access Stratum (NAS) protocols.
  - The main functions supported by the MME can be classified as:
    - Functions related to bearer management – This includes the establishment, maintenance and release of the bearers and is handled by the session management layer in the NAS protocol.
    - Functions related to connection management – This includes the establishment of the connection and security between the network and UE

- The Home Subscriber Server (HSS):
  - Permanent and central subscriber database containing mobility and service data for each subscriber.
  - The Home Subscriber Server contains users' SAE subscription data such as the EPS-subscribed QoS profile and any access restrictions for roaming. It also holds information about the PDNs to which the user can connect.
  - In addition, the HSS holds dynamic information such as the identity of the MME to which the user is currently attached or registered. The HSS may also integrate the authentication center (AUC), which generates the vectors for authentication and security keys.

- Serving gateway (S-GW):
  - Manages the user data in the EPC. Receives packet data from the eNodeB and sends packet data to it.

- All user IP packets are transferred through the Serving Gateway, which serves as the local mobility anchor for the data bearers when the UE moves between eNodeB' s.
- It also retains the information about the bearers when the UE is in the idle state and temporarily buffers downlink data while the MME initiates paging of the UE to reestablish the bearers.
- It also serves as the mobility anchor for interworking with other 3GPP technologies such as general packet radio service (GPRS) and UMTS.

- Packet Gateway (P-GW or PDN-GW):
  - Connection between EPC and external Packet Data Networks (PDN). Comparable in functionality with the GGSN in 2G/3G networks.
  - It is responsible for IP address allocation for the UE, as well as QoS enforcement and flow-based charging according to rules from the PCRF.
  - It is also responsible for the filtering of downlink user IP packets into the different QoS-based bearers.
  - The P-GW performs QoS enforcement for guaranteed bit rate (GBR) bearers.
  - It also serves as the mobility anchor for interworking with non-3GPP technologies such as CDMA2000 and WiMAX® networks.

- Policy Control and Charging Rules Function (PCRF):
  - The PCRF is responsible for policy control decision-making, as well as for controlling the flow-based charging functionalities in the Policy Control Enforcement Function (PCEF), which resides in the P-GW.
  - The PCRF provides the QoS authorization (QoS class identifier [QCI] and bit rates) that decides how a certain data flow will be treated in the PCEF and ensures that this is in accordance with the user's subscription profile.

The main logical interfaces that connect the LTE network elements are S1 and X2 and can be seen in Figure 3:

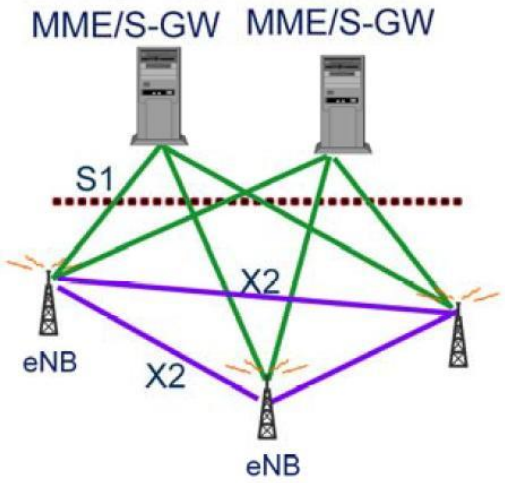

Figure 3: LTE network logical interfaces

The S1 interface is the interface between the E-UTRAN and EPC. The S1 functionalities are split into C-plane and U-plane functionalities.

- S1-UP applies to the interface between the eNodeB and the S-GW. The S1-UP interface is responsible for delivering user data between the eNodeB and the S-GW.
- S1-CP applies to the interface between the eNodeB and the MME and is also called S1-MME interface. It is responsible for delivering a signaling protocol between the eNodeB and the MME and for EPS bearer setup/release procedures, the handover signaling procedure, the paging procedure, tracking area updates, authentication and the NAS transport procedure.

The X2 interface is the logical interface between eNodeB's since it does not need direct site-to-site connection. It can be routed via core network as well. It is used during inter eNodeB handovers avoiding the involvement of the core network during the handover and forwarding the data between source and target eNodeB.

X2 functionalities are split into control-plane (C-plane) and user-plane (U-plane) functionalities.

- X2-CP protocol functions include Intra LTE-Access-System mobility support for the UE, context transfer from source eNodeB to target eNodeB, control of user plane tunnels between source eNodeB and target eNodeB, handover cancellation, uplink load management, general X2 management and error handling functions.
- The X2-UP protocol tunnels end-user packets between the eNodeB's. The tunneling functions supported are identifications of packets with the tunnels and packet loss management.

2.2 LTE Characteristics

2.2.1 Air Interface Protocol Stack

The LTE air interface protocol stack contains the following layers:

- Physical layer:

It is responsible for the actual radio transmission, and includes coding for forward error correction, modulation, bit interleaving, scrambling and other functions needed to minimize errors over the radio link. The PHY layer also manages the operation of Hybrid Automatic Repeat Request (HARQ), which provides a fast error correction mechanism through incremental redundancy [9].

Along with the other usual functions, the physical layer in LTE supports the HARQ with soft combining, uplink power control and multi-stream transmission and reception (MIMO).

- MAC layer:

The Medium Access Control (MAC) layer handles the scheduling of uplink and downlink resources and determines the transport format to be used. It also takes care of multiplexing packets into a single transmission and insert padding bits as required.

Along with scheduling, it performs error correction through HARQ, priority handling across UEs as well as across different logical channels of a UE, traffic volume measurement reporting, and multiplexing/demultiplexing of different RLC radio bearers into/from the physical layer on transport channels [10].

- RLC layer:

Radio Link Control (RLC) performs segmentation and concatenation to optimize the use of the available resources, and tracks which packets were sent and received.

Along with transferring upper layer PDUs, the RLC does error correction through ARQ, in-sequence delivery of upper layer PDUs, duplicate detection, and flow control and concatenation/re-assembly of packets [11].

- PDCP layer:

Packet Data Convergence Protocol (PDCP) implements Robust Header Compression (ROHC) and any required ciphering (encryption) functions. The PDCP layer is also included in the control plane and is used for ciphering and integrity protection. In addition, it is used for control plane data transmission, i.e., the PDCP receives PDCP SDUs from the RRC and forwards them to the RLC layer and vice versa [10].

- RRC layer:

The Radio Resource Control layer performs broadcasting, paging, connection management, radio bearer control, mobility functions and UE measurement reporting and control.

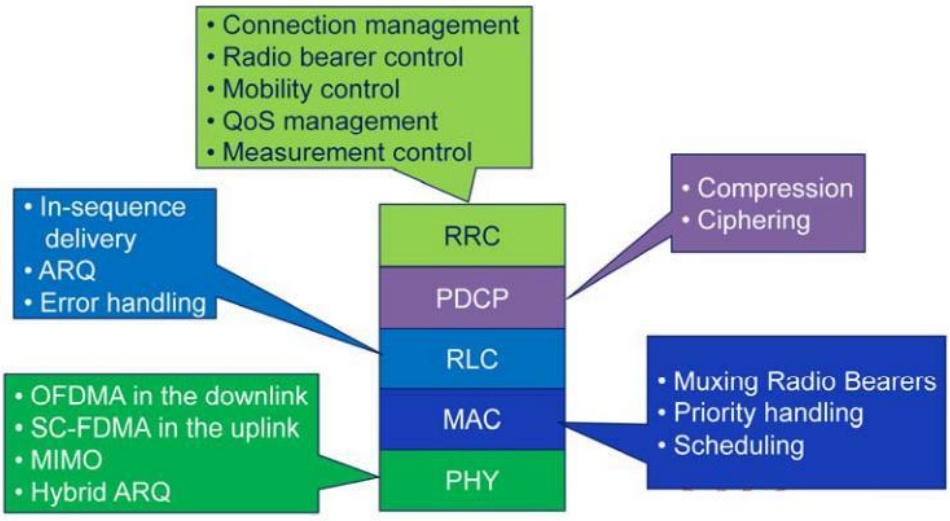

Figure 4: Air Interface protocol stack

2.2.2 Channel Architecture

In LTE several types of channels are defined, they are detailed bellow:

A **Logical Channel** is defined by the type of information it carries. Logical channels are classified into control and traffic channels. It answers the question: what is it being transported? [10]

A **Transport Channel** is defined by how and with what characteristics the information is transmitted. It answers the question: how is it being transported?

A **Physical Channel** is defined by the physical resources used to transmit the data. At the physical level, a distinction can be made between:

- The physical channel on which transport channels are mapped.
- The physical signal, which does not carry information but is used for synchronization or measurement.

The following logical control channels have been defined by 3GPP:

- **BCCH** - Broadcast Control Channel, used for the transmission of system control information. An UE needs to decode it before requesting a connection.
- **PCCH** - Paging Control Channel is a downlink channel that transfers paging information and system information change notifications. This channel is used for paging when the network does not know the location cell of the UE.
- **CCCH** - Common Control Channel is a channel for transmitting control information between UEs and network. This channel is used for UEs having no RRC connection with the network.
- **DCCH** - Dedicated Control Channel is a point-to-point bi-directional channel that transmits dedicated control information between a UE and the network. Used by UEs having an RRC connection.
- **MCCH** - Multicast Control Channel is a point-to-multipoint downlink channel used for transmitting MBMS control information from the network to the UE, for one or several MTCHs. This channel is only used by UEs that receive MBMS.

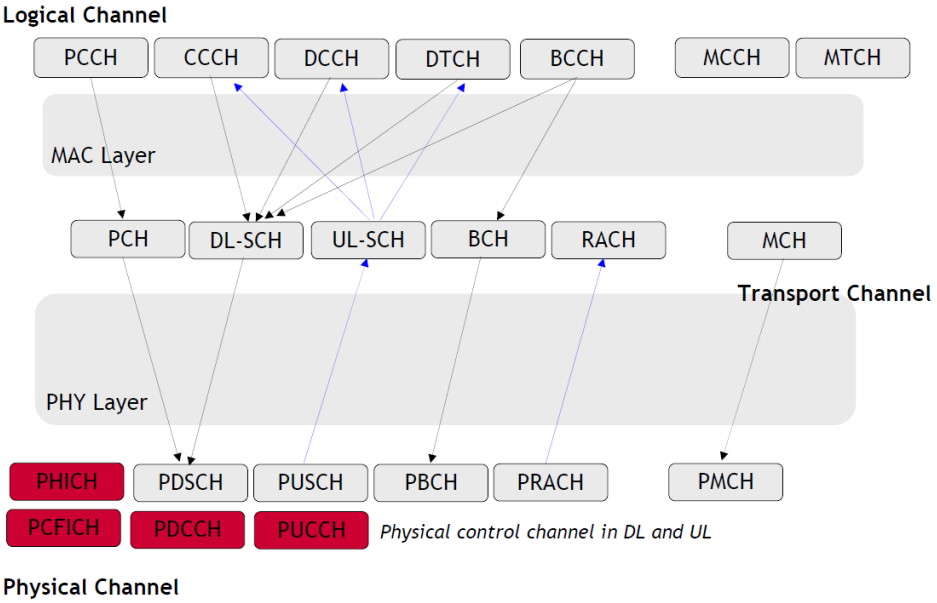

Figure 5: Channel mapping in LTE technology

The following logical traffic channels have been defined by 3GPP:

- **DTCH** - Dedicated Traffic Channel is a point-to-point channel, dedicated to one UE, for the transfer of user information. A DTCH can exist both in uplink and downlink.
- **MTCH** - Multicast Traffic Channel is a point-to-multipoint downlink channel for transmitting traffic data from the network to the UE. This channel is only used by UEs that receive MBMS.

The following DL transport channels have been defined by 3GPP:

- **BCH** - Broadcast Channel characterized by a fixed, pre-defined transport format with a robust modulation to be broadcast in the entire coverage area of the cell. DL-SCH - Downlink Shared Channel characterized by a dynamic link adaptation by varying the modulation, coding and transmit power support for ARQ (radio retransmission).
- **PCH** - Paging Channel: requirement to be broadcast in the entire cell.
- **MCH** - Multicast Channel: requirement to be broadcast in the entire coverage area of the cell.

The following UL transport channels have been defined by 3GPP:

- **UL-SCH** - Uplink Shared Channel characterized by:
  - support for dynamic link adaptation by varying the transmit power and potentially
  - modulation and coding
  - support for H-ARQ
  - support for both dynamic and semi-static resource allocation.
- **RACH** - Random Access Channel characterized by:

- limited control information
- collision risk

The DL physical channels are:

- **PDSCH** - Physical DL Shared Channel - It is a shared channel used to carry user data, radio & core network, system information (BCH), paging message. PDCCH - Physical DL Control Channel - It is a shared signaling channel to carry the allocation of the resources (PDSCH).
- **PBCH** - Physical Broadcast Channel - It is the channel used to broadcast the system information.

The UL physical channels are:

- **PRACH** - Physical Random Access Channel - It is a shared channel used for the access procedure.
- **PUSCH** - Physical UL Shared Channel - It is a shared channel used to carry user data, radio & core network.
- **PUCCH** - Physical UL Control Channel - It is a UL shared signaling channel used to allow the UE to request resources on the PUSCH.

2.2.3 LTE access technologies

LTE standard defines two access technologies to be supported: Time Division Duplex (TDD) and Frequency Division Duplex (FDD).

In **FDD mode,** Figure 6**,** a pair of frequency spectrum is provided for the uplink and downlink. The uplink and the downlink transmissions are separated by frequency. Two bandwidths are used.

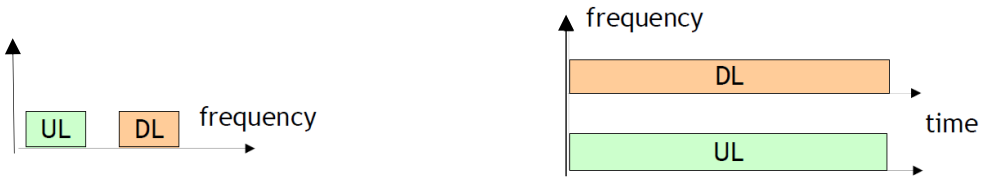

Figure 6: Frequency Division Duplexing

In **TDD mode**, Figure 7 , the available frame duration is divided into two parts in time domain for the uplink and downlink. The Uplink and the downlink transmissions are separated by the time. Only one bandwidth (carrier frequency) is used. The number of uplink and downlink time slots is varied in TDD mode based on traffic profile. Theoretically spectrum utilization is greater in TDD than in FDD.

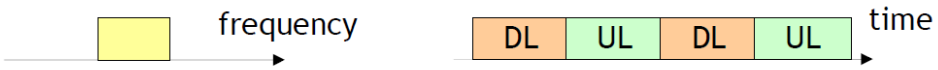

Figure 7: Time Division Duplexing

All the experiments and studies run in this thesis are done for LTE FDD mode.

2.2.4 Modulation in LTE

The LTE uses three different modulation schemes - Quadrature Amplitude Modulations (QAMs) depending on the radio quality. QAM is a modulation method that modifies the phase and the amplitude of the carrier signal. QAM symbols are represented by the carrier signal being transmitted with specific phase/amplitude (dictated by the message), for finite periods of time. One symbol is identified by a Q and an I value.

To increase the bit per sec (bps) capacity of a channel, while keeping the number of symbols per second (Baud rate) at the low values imposed by the channel bandwidth, the symbols carry (represent) more than one single bit.

The drawback is the presence of multiple symbols in the channel, increasing the probability of incorrect symbol identification at the receiver.

Depending on the radio quality, the eNodeB selects the most adapted modulation for the data transmissions.

QPSK Modulation - is the most robust modulation. It can be represented by the constellation below. The radius, *R*, represents the amplitude and the angle; *φ*, represents the phase.

There is one amplitude but four phases for 4 different states. Two bits can be coded using one QPSK symbol as can be seen in Figure 8.

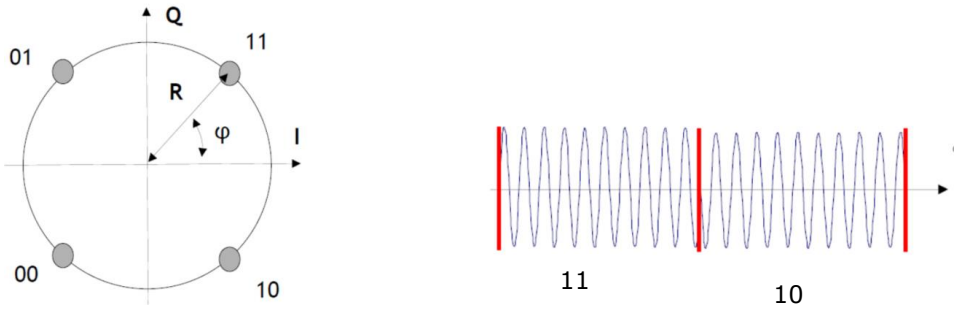

Figure 8: QPSK constellation and example of QPSK signal

16QAM Modulation - can modulate 4 bits per symbol and can generate symbols using 12 phases and 3 amplitudes. It is used in good radio conditions. It can be represented by the constellation below:

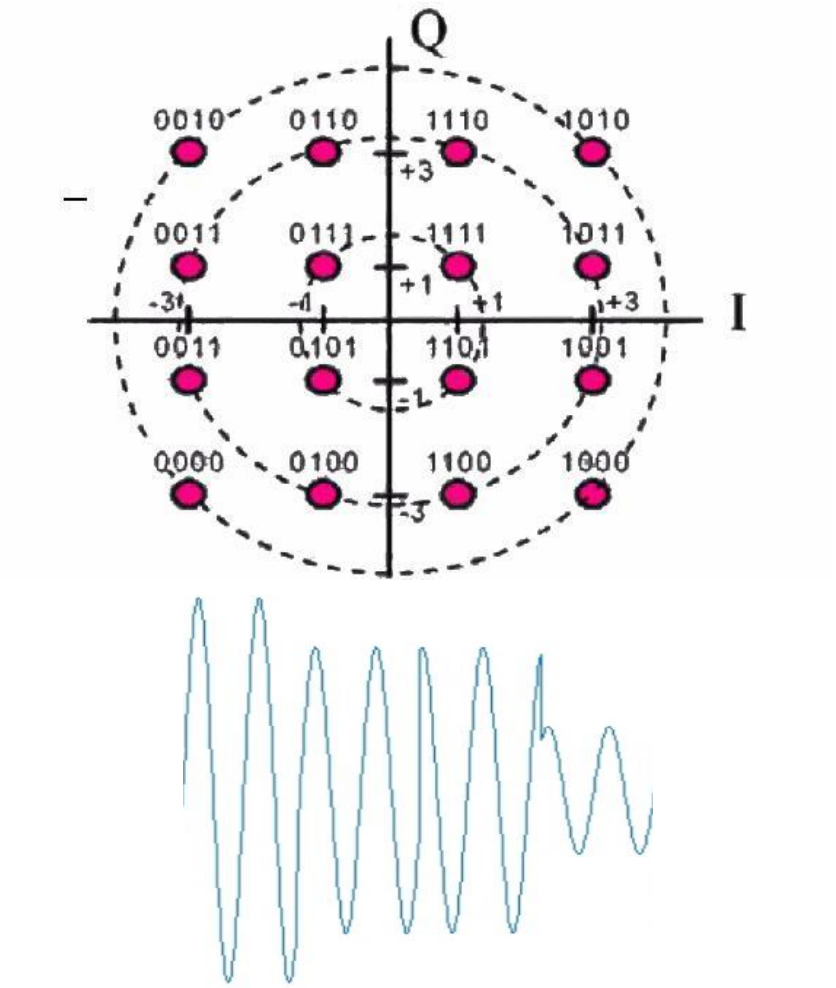

Figure 9: 16 QAM constellation

64QAM Modulation: can map 6 bits per symbol and used for this 64 different constellation points disposed as in Figure 10.

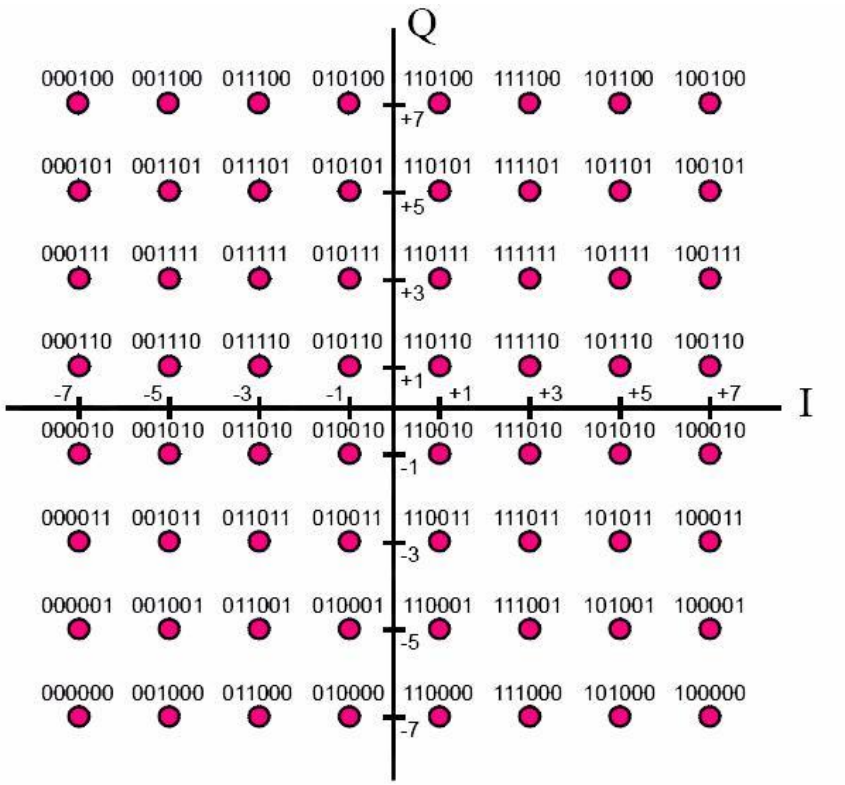

Figure 10: 64QAM constellation

2.2.5 Multiple Access Techniques: OFDMA and SC-FDMA

One of the main changes in LTE with respect to UMTS is the use of different transmission schemes in the air interface.

LTE downlink air interface is based on OFDMA (Orthogonal Frequency Division Multiple Access) whereas the uplink air interface is based on SC-FDMA (Single Carrier-Frequency Division Multiple Access) [12].

The eNodeB can communicate with multiple UEs at the same time by using the multiple access technique called Orthogonal Frequency Division Multiple Access. The advantages of OFDMA include robustness against narrow-band co-channel interference, robustness against Inter-Symbol Interference (ISI), fading and high spectral efficiency.

In OFDM the user data is transmitted in parallel across multiple orthogonal narrowband subcarriers. Each subcarrier only transports a part of the whole transmission.

The spacing between subcarriers is fixed in LTE and equivalent to 15 kHz in the frequency domain.

Figure 11 represents a subcarrier in time and frequency domain.

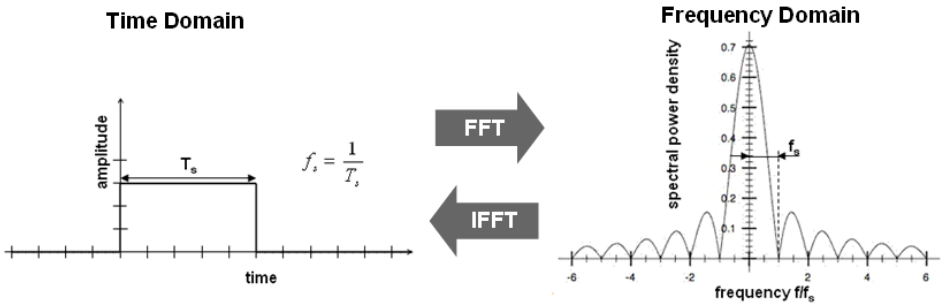

Figure 11: OFDM subcarrier - Time and Frequency Domain representation

The orthogonal subcarriers are generated with IFFT (Inverse Fast Fourier Transform) processing. The number of subcarriers depends on the available bandwidth as shown in Figure 12.

In LTE, they range from less than one hundred to more than one thousand [12].

The bandwidths are: 1.4, 3, 5, 10, 15 and 20 MHz.

The symbol duration is always the same whatever the bandwidth.

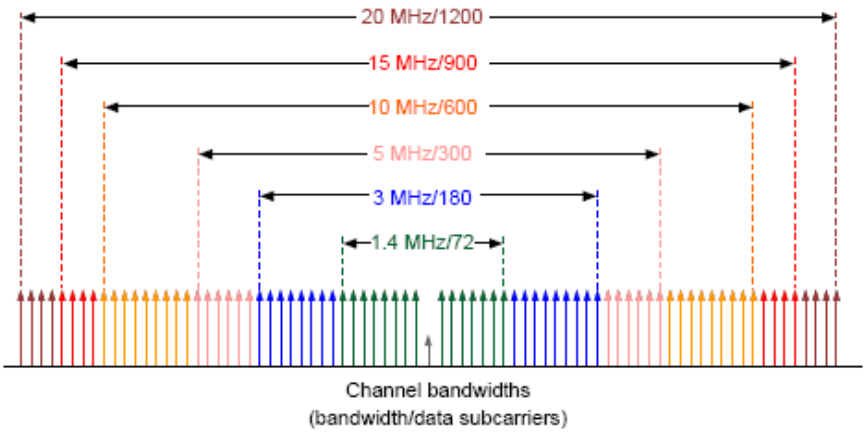

Figure 12: Number of subcarriers for the different bandwidths in LTE

There are 2 times more sub-carriers in 10 MHz than in 5 MHz, 2 times more symbols can be sent or received at the same time. This means that the capacity is multiplied by 2 [10].

On the transmitter side, the modulated symbols are interpreted as frequency domain signal and fed into the IFFT (Inverse Fast Fourier Transform) algorithm that transforms them into the corresponding time sequence. The number of time symbols is equal to the number of carriers. Then, the cyclic prefix (CP) is inserted (see in Figure 13).

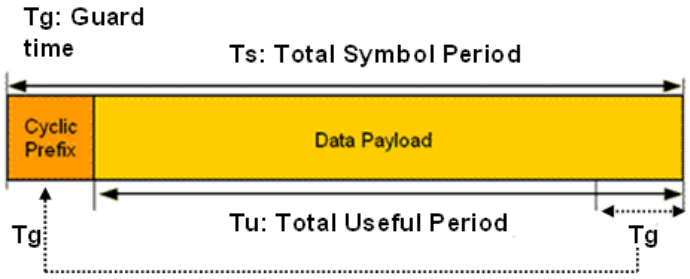

Figure 13: Cyclic Prefix

The length of the CP is expressed in the basic time unit Ts and its duration varies for the normal and the extended cyclic prefix. The bits that define the CP are taken from the end of the symbol and placed as cyclic prefix in front of the symbol (see Figure 7).

Figure 14 summarizes at high level the OFDM operation at the transmitter's and receiver's end. The user data is modulated according to the different modulation schemes (depending on the radio link conditions) [13] .

In the end, the signal is modulated on the radio carrier and transmitted over the air interface. Inverse operations are carried out on the receiver side i.e., removal of cyclic prefix, FFT to bring the signal back to the frequency domain representation and finally, the symbol de-mapping where the original bit sequence is recovered.

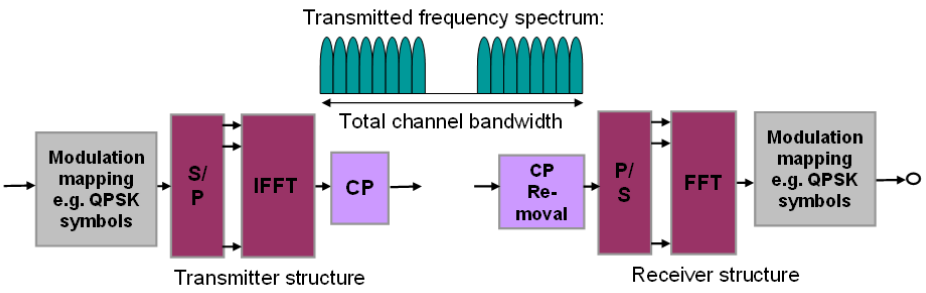

Figure 14: OFDM operations at the transmitter and receiver

Cyclic prefixes are used by all modern OFDM systems as a way of fighting against the Inter Symbol Interference (ISI) that may happen in multipath environments where transmitted signals arrive at the receiver with different delays.

The Cyclic Prefix consists of a copy of the last part of a symbol shape for the duration of a guard time and adding it to the beginning of the symbol. This guard time needs to be long enough to capture all the delayed multipath signals and avoid ISI at the receiver. Besides, the CP is used by the receiver to detect the start of symbol due to the high correlation between the CP and the last part of the symbol that precedes so the receiver can start with the decoding.

Using the CP to manage the effects of ISI is possible due to the long symbol duration in OFDM based systems. LTE's typical symbol duration including the CP is around 71.64 μsec. That is considerably longer when compared with GSM 3.69 μsec or 0.26 μsec for WCDMA. Therefore, LTE does not require complex ISI management techniques like other systems.

There are two cyclic prefix options for LTE:

- *Normal cyclic prefix:* Used in small cells or cells with short multipath delay spread. Its length depends on the symbol position within the slot being 5.21 μsec for the CP in symbol 0 and 4.6 μsec for the rest of symbols. The reason for these two different lengths is so that the slot duration is 0.5ms, facilitating at the same time, that the terminal finds the starting point of the slot.
- *Extended cyclic prefix:* Used with larger cells or those with long delay profiles. Its length is 16.67μs and it is constant for all symbols in the slot. Extended cyclic prefix appeared at RL15A as part of MBMS feature only. It seems there is not strong will to be implemented for regular implementation of extended CP except MBMS solutions in cellular industry at all.

The eNodeB can dynamically assign a different number of channels to different users during a radio frame. It is also possible to change the number of channels given to a user from one frame to the next. The band is divided into several narrow bands called Sub-carriers. It is a multiplexing technique that uses different frequencies to combine multiple streams of data for transmission over a communications medium. It assigns a discrete carrier frequency to each data stream. This can be observed in Figure 15.

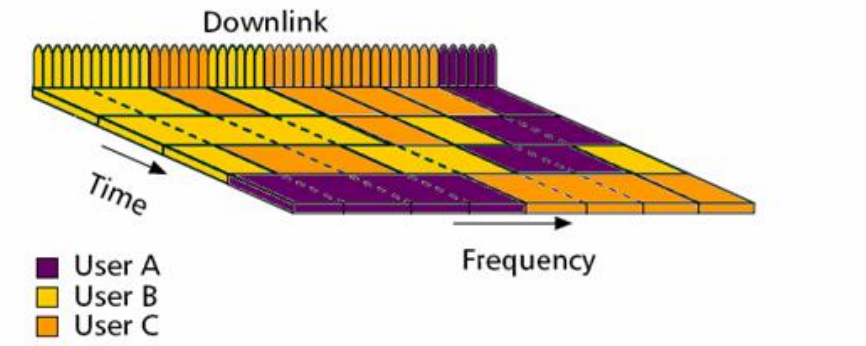

Figure 15: Downlink resource allocation

The inter-channel (or inter sub-carrier) interferences are cancelled because they are located in such a way that when there is the peak for a given sub-carrier, the adjacent subcarriers are null. OFDM allows high density of carriers, without generating Inter-Channel Interference (ICI) [10].

For example, in Figure 16, the red and the blue sub-carriers are crossing the zero point when the green one is at its maximum:

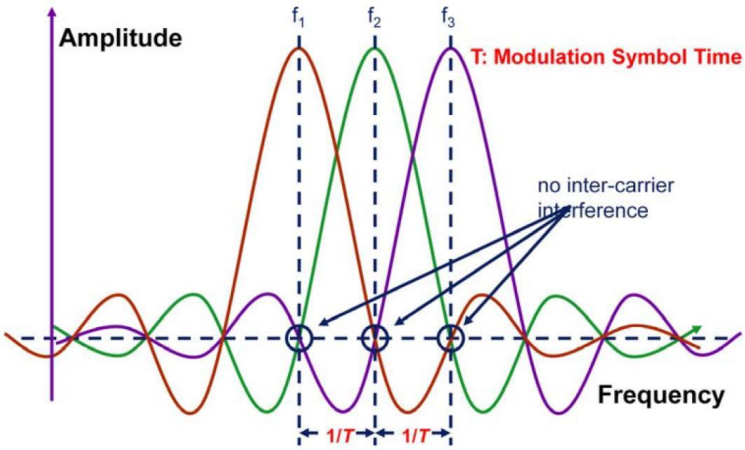

Figure 16: Orthogonal subcarriers in OFDMA

A summary of the main OFDMA parameters is presented in the table below:

Table 1 Main OFDMA parameters

	1.4MHz	3 MHz	5 MHz	10 MHz	15 MHz	20 MHz
Frame Duration	10ms					
Subcarrier Spacing	15 kHz					
Sampling Rate (MHz)	1.92	3.84	7.68	15.36	23.04	30.72
Data Subcarriers	72	180	300	600	900	1200
Symbols/slot	Normal CP=7, extended CP=6					
CP length	Normal CP=4.69/5.12 μsec., extended CP= 16.67μsec.					
Number of RB	6	15	25	50	75	100

Along with benefits brought by OFDMA that have been presented earlier there is also a major disadvantage using this technique and that is represented by a large

value of the PAPR. Peak-to-Average Ratio (PAPR) is a typical problem in the multicarrier modulation technique due to the summation of large number of independent data symbols for transmission [14] .

For the UL part the LTE uses a variation of OFDMA, called Single Carrier FDMA (SC-FDMA).

SC-FDMA improves the peak-to-average power ratio (PAPR) with DFT – Discrete Fourier Transform spreading of modulation symbols.

The distinguishing feature of SC-FDMA is that it leads to a single-carrier transmit signal, in contrast to OFDMA which is a multi-carrier transmission scheme. Subcarrier mapping can be classified into two types: localized mapping and distributed mapping. In localized mapping, the DFT outputs are mapped to a subset of consecutive subcarriers, thereby confining them to only a fraction of the system bandwidth. In distributed mapping, the DFT outputs of the input data are assigned to subcarriers over the entire bandwidth non-continuously, resulting in zero amplitude for the remaining subcarriers.

In OFDM, each modulation symbols "sees" a single 15 kHz subcarrier (flat channel). In SC-FDMA, each modulation symbol "sees" a wider bandwidth (i.e. m x 180 KHz). Equalization is required in the SC-FDMA receiver. This difference between OFDMA and SC-FDMA way of caring information from different users can be observed in Figure 17.

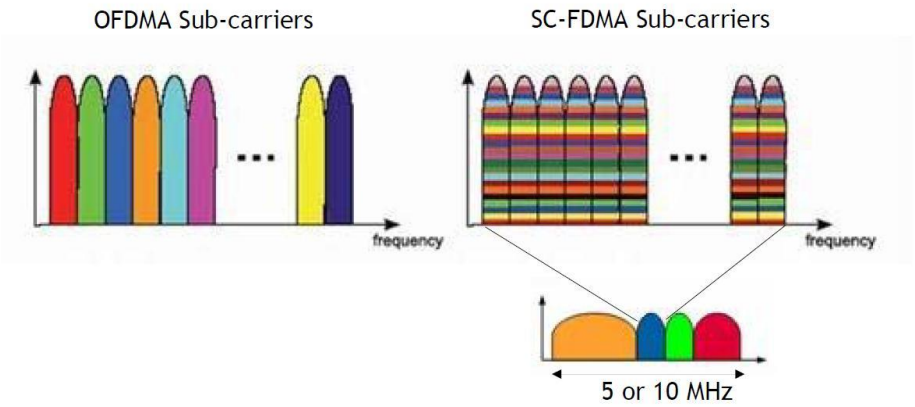

Figure 17: Differences in representation between OFDMA and SC-FDMA

PAPR reduction justifies the selection of the SC-FDMA scheme in the uplink. Since the signal is transmitted over a single band, PAPR can be minimized. This is the most important reason for choosing SC-FDMA in the UL. This leads to the following benefits:

- Supports larger cells due to increased link budget for a given maximum UE power – Enables higher throughput at the cell-edge for a given fixed cell size
- Lower cost of the UE for a given fixed link budget as a lower rating power amplifier may suffice.

2.2.6 FDD Frame Structure

In FDD, the DL and UL Radio Frames (RFs) are not on the same carrier. For FDD, 10 subframes are available for downlink transmission and 10 subframes are available for uplink transmissions in each 10 ms interval. Uplink and downlink transmissions are separated in the frequency domain. The RF frame is called Type 1 by the 3GPP. A frame structure type 2 is also defined and is applicable to TDD.

The RF length is 10 ms.

The radio frame is made up of 10 sub-frames of 1 ms. Each sub-frame is made up of 2 slots of 0.5ms, as can be seen in Figure 18.

Each slot is made up of 7 symbols in case of normal CP (guard time between symbols)

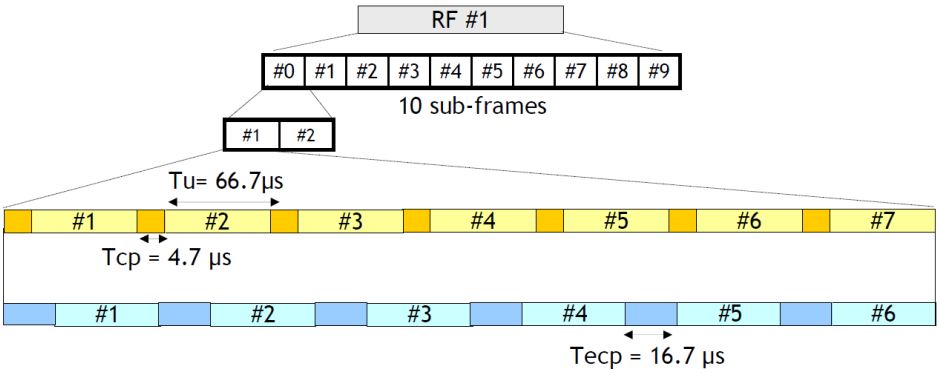

Figure 18: Frame structure in FDD

Where:

T_u = Useful Symbol Duration

T_{cp} = Cyclic Prefix duration

T_{ecp} = Extended Cyclic Prefix duration

The diagram presented in Figure 19 explains the concept of a resource element and resource block. Each timeslot has N OFDM symbols, where N depend of the used bandwidth. One resource element is one OFDM symbol duration for one subcarrier. A resource block can be defined in terms of the number of OFDM symbols and subcarriers. The size of the resource blocks is determined by the scheduler. The resource block consist of is the number of consecutive subcarriers and number of consecutive OFDM symbols.

Physical Resource Block, PRB is the minimum unit of allocation in LTE.

PRB=14 OFDM symbols (2 slots) x 12 Subcarrier.

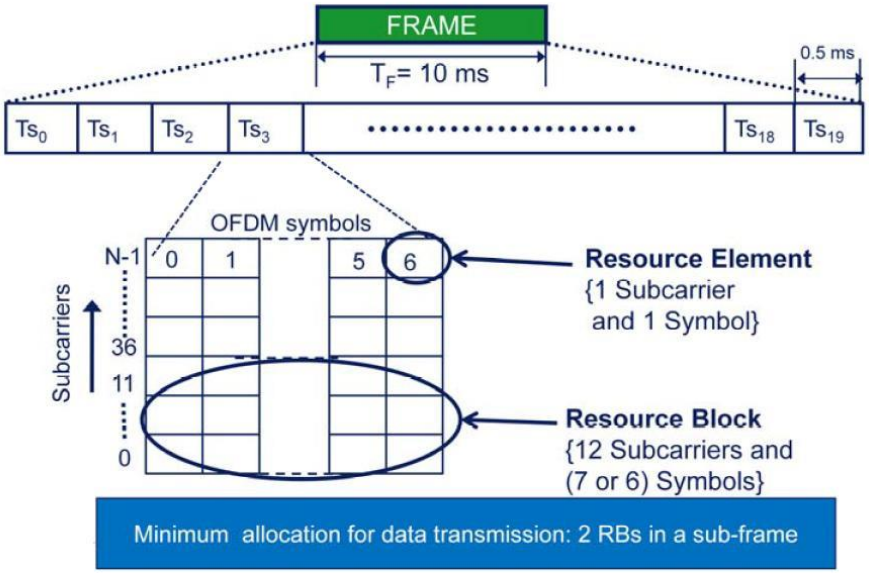

Figure 19: Resource Element and Resource Block

2.2.7 Handover procedure in LTE

Mobility procedures are essential to maintain connections when the users are moving. LTE defines UE-assisted network controlled hard handover procedures in ECM CONNECTED mode. LTE supports two types of mobility procedures:

1**. RAN Mobility**: As the UE moves from one eNodeB to another eNodeB within the same S- GW, radio mobility procedures are performed to transfer connections. RAN Mobility Hard Handover (HHO) procedures can occur with intra-eNodeB, intra-frequency and inter-frequency conditions [15].

2. **CN Mobility:** When the mobile moves between S-GWs, two options are possible. One option is an Intra-MME/Inter-S-GW HHO without changing the anchor P-GW. The other option is an Inter-MME HHO where both the serving MME and S-GW change. The P-GW remains the same during the HHO for both options.

The measurements performed by the UE during the handover procedure include the following:

RSRP - Reference signal received power, is defined as the linear average over the power contributions (in [W]) of the resource elements that carry cell-specific reference signals within the considered measurement frequency bandwidth.

RSRQ - Reference Signal Received Quality is defined as the ratio N×RSRP/RSSI,

where N is the number of RB's of the E-UTRA carrier RSSI measurement bandwidth. The measurements in the numerator and denominator shall be made over the same set of resource blocks.

RSSI - Received Signal Strength Indicator, comprises the linear average of the total received power (in [W]) observed only in certain OFDM symbols of measurement subframes, in the measurement bandwidth, over N number of resource blocks by the UE from all sources, including co-channel serving and non-serving cells, adjacent channel interference, thermal noise etc.

SINR - Signal to Interference plus Noise Ratio. A good SINR value ensures high level of the quality of service for the users and contributes to a more efficient LTE network [16].

Equation 1

$$SINR = \frac{P}{I + N}$$

where *P* is the power of the incoming signal of interest, I is the interference power of the other (interfering) signals in the network, and N is some noise term.

2.3 Heterogeneous networks (HetNet)

The use of mobile devices has been increasing in an exponential fashion in the past few years. The exponential increase in the use of interconnected mobile devices will result in the growth of data traffic [17]

Because there are too many users demanding too much data, the problem currently being faced by the networks operators is not the coverage anymore, which is now quite good, but the network capacity [18].

Since data traffic demand in cellular networks is growing exponentially and bringing with it new challenges on the cellular networks, further improvements in 4G spectral efficiency could be possible by increasing the node densities. However, with current dense deployments, the cell dividing gains are considerably decreased because of severe ICI. Moreover, site acquisition costs can get prohibitively expensive particularly in a space limited dense in urban region [19].

Heterogeneous Network (HetNet) is being considered as a most promising approach to enhance network capacity and increased data throughput, overall performance and to increase coverage in a cost-effective way [20]. A HetNet consists of regular macro cells transmitting typically at high power level, overlaid with low-power small cells such as pico cell, femto cell, metro cell, Remote Radio Head (RRH), etc. The incorporation of such small cells allows offloading traffic from macro cell and providing better network experience by connecting UEs in small cells with low transmission power. In Figure 20 an illustration of a concept with downlink coverage regions in HetNet is depicted where the red dots represent the macro eNodeB's, the green dots represent the Micro Base Stations and the Black dots the femto or pico ones [21].

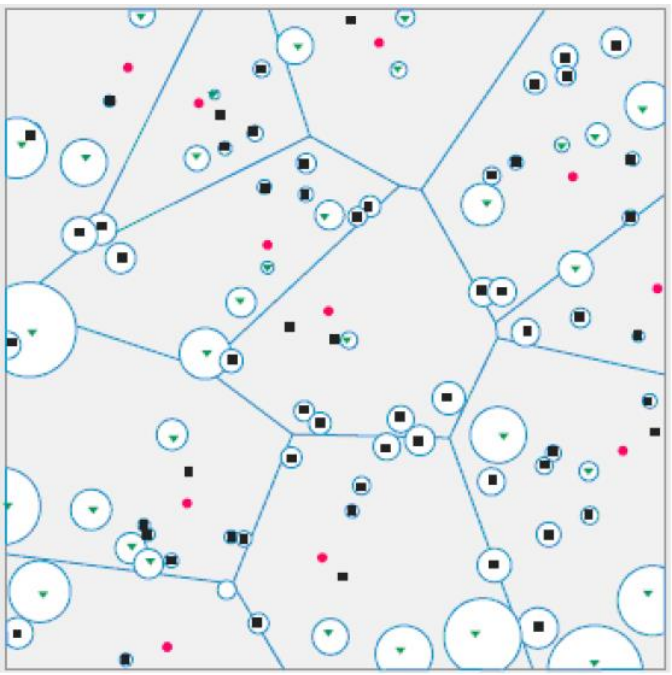

Figure 20: Downlink coverage regions in HetNet

But, this overlaying of macro cell and small cells results severe inter-cell interference in networks, in particular for cell-edge users of small cell [20]. Generally, macro cells are normally placed in a cellular network attending to a prudently network plan, while the placement of low power small cells is typically based on just a knowledge of coverage issues and traffic densities (e.g. hotspots) in the network [22].

Different types of deployment scenarios for HetNet are already available. In multicarrier deployment, small cells utilize different carrier frequency than the macro cell. This process effectively reduces ICI but does not ensure proper spectral utilization. On the other hand, co- channel deployment is utilized by using the same carrier for both of macro cell and small cell in which the spectral efficiency is increased via spatial reuse and popular deployment approach in HetNet. Though co-channel approach ensures effective spectrum utilization but bring high ICI among the macro cell & small cells [23].

A generic HetNet architecture can be seen in Figure 21, where all relevant cell types are presented [24].

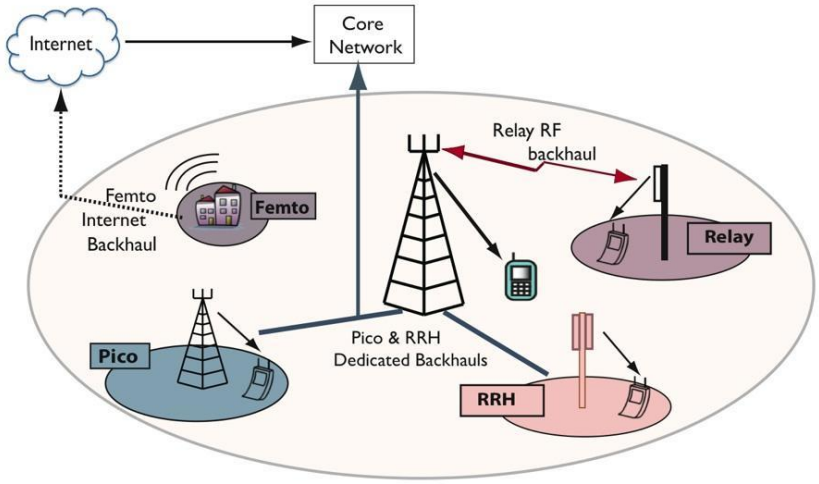

Figure 21: Typical HetNet Architecture

2.4 Inter Cell Interference Cancelation particularities in LTE

ICIC feature was introduced in 3GPP Release 8 [6] in order to mitigate inter – cell interference for cell edge UEs in case of HetNet. The eNodeBs can communicate via the X2 interface. The X2 Application Protocol (X2AP) message is used to "load information" from neighboring cells. The X2AP LOAD INFORMATION message received from a neighboring eNodeB indicates the UL interference level on all of its physical resource blocks (PRBs) and also if the transmission power is high or low for all of the UL PRBs. When the message is received by the other eNodeB, it will make use of the information to schedule the cell edge UEs in the available PRBs. That means, two neighboring eNodeBs will not be using the same set of PRBs at the same time. This scheme is one of the preferred ones in ICIC implementation schemes [25].

This mechanism of ICIC allocating different sub carriers for delivering data channels resulted in a better interference level for the DL data channels or traffic channels, how is showed in Figure 22 [26]. The problem with ICIC is that it requires some of the resource blocks to be reserved resulting in lower throughput for the cells. ICIC also limits the range expansion mechanism. On the other hand, eICIC helps in reducing the interference in both the data channel and control channels [27].

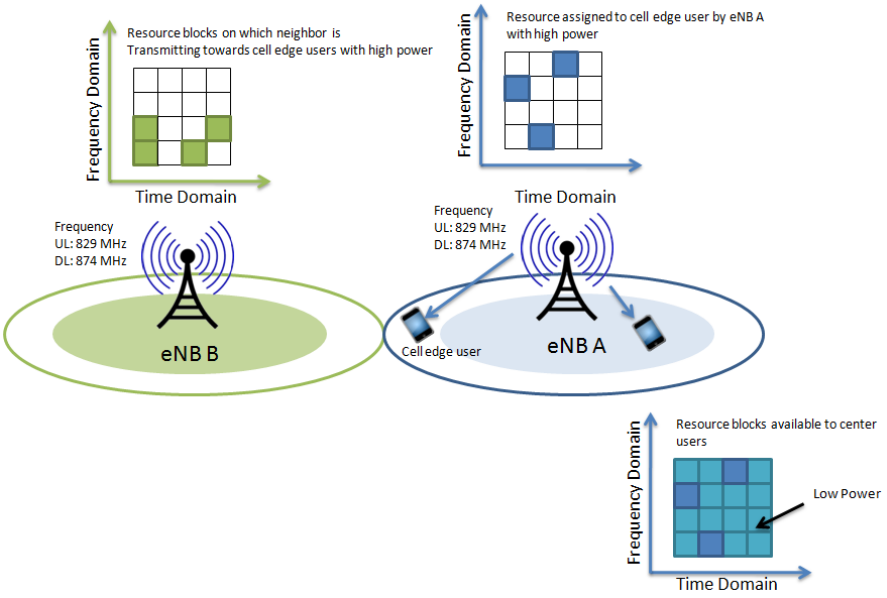

Figure 22: Example of ICIC Implementation – RB assignments

Enhanced ICIC (eICIC), that was introduced in 3GPP release 10 [8] on the other hand, does not require any resource blocks to be reserved for the transmission of either the control or user data. The major shift from ICICs is that eICIC uses time domain. The realization of eICIC is done using ABS (also termed as Almost Blank Subframes). That is, the macro eNodeB almost "silences" some of the Subframes in the DL radio frame. These silenced Subframes contain only control channel and cell – specific reference signals and no data. Thus, cell edge UEs can get both control and user data during ABS. This flexible usage of frames among MeNodeBs and small-cells (like PeNodeBs) makes eICIC easily responsive to load variations. As it was in ICIC, the macro eNodeB will use the X2AP messages to LOAD INFORMATION or send out ABS patterns to the neighboring small cell eNodeBs [28]. Figure 23 shows a cell edge UE for which the resources are scheduled during ABS periods.

Furthermore, enhanced ICIC (FeICIC), has also been introduced in 3GPPs Release 11. [9] The major enhancement from eICIC is that UEs can also participate in the inter-cell interference management by canceling interference signals for their control channel. This capability of UEs' in cancellation of interference for control signals would make even larger cell range expansion possible.

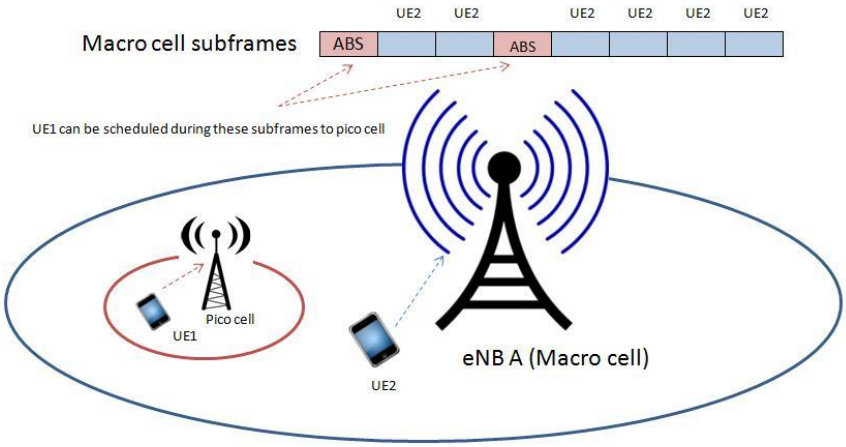

Figure 23: eICIC Implementation – UE1 scheduled during the ABS periods

2.4.1 Cell Range Expansion

Cell selection in LTE is based on terminal measurements of the received power of the downlink signal or more specifically the Common Reference Signals (CRS) downlink signaling. However, in a heterogeneous network we have different types of base stations that have different transmission powers including different powers of CRS. This approach for cell selection would be unfair to the low power nodes (small cell eNodeBs) as most probably the terminal will choose the higher power base stations (macro eNodeBs) even if the pathloss to the small cell eNodeB is smaller and this won't be optimal in terms of:

- Uplink coverage: as the terminal has a lower pathloss to the small cell eNodeB but instead it will select the macro eNodeB.
- Downlink capacity: small cell eNodeBs will be under-utilized as fewer users are connected to them while the macro eNodeBs could be overloaded even if macro eNodeBs and small cell eNodeBs are using the same resources in terms of spectrum, so the cell-splitting gain is not large, and the resources are not well utilized.
- Interference: due to the high transmission power of the macro eNodeBs, the macro eNodeB transmission is associated with a high interference to the small cell eNodeB users which denies them to use the same physical resources.

As a solution for the first two points, cell selection could be dependent on estimates of the uplink pathloss, which in practice can be done by applying a cell-specific offset to the received power measurements used in typical cell selection. This offset would somehow compensate for the transmitting power differences between the macro eNodeB's and small cell eNodeB's; it would also extend the small cell eNodeB coverage area, or in other words extend the area where the small cell eNodeB is selected. This area is called "Range Expansion" and can be seen in Figure 25, where initial small cell area it represented by the pink cell range and the extended area by the hashed ring. [29].

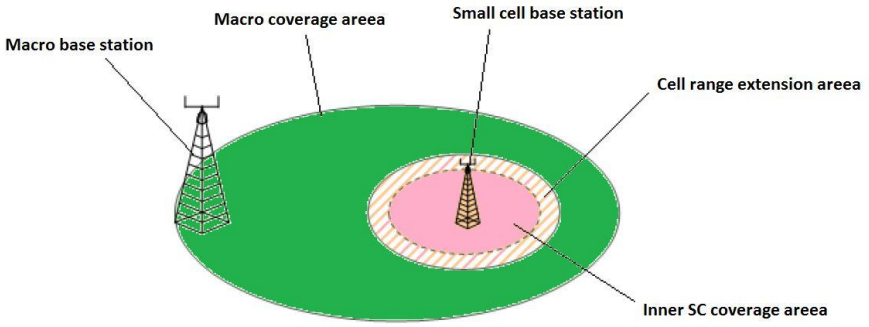

Figure 24: Illustration of small cell range expansion

2.4.2 Almost Blank Subframes (ABS)

An ABS is defined as minimum transmission Subframes, where no data signal will be transmitted from the macro cell but only transmit the most critical information required for the system to provide support to legacy LTE (Release 8/9) UEs. Therefore, during ABS, the signals that are mainly sent are common reference signals (CRS) and other obligatory system information. As a result, during Subframes where the macro cell transmits ABS, the low power small cells are able to schedule UEs from a larger geographical area that otherwise would experience too high interference from the macro layer. This basically implies that using ABS at macro-cell makes possible to increase the offloading of traffic to the small cell. Moreover, this concept allows the use of higher values of CRE for the small cells [20].

ABS patterns are configured semi-statically and signaled between the macro cell and small cell over the X2 interface. The macro cell is supposed to act as the master that decides which subframes are to be set as ABS depending on different information regarding the cluster. Moreover, some improvements for the X2 application protocol are included in the Rellease10 specification, which makes easier the configuration of ABS muting pattern among cells. Regarding the Release 10 specification, the macro cell supports techniques for the configuration of ABS muting patterns, being able to obtain the maximum overall system performance while considering also quality of service (QoS) requirements of individual UEs. [30]

In Figure 25 is showed how, by reserving the ABS subframes we can expand even higher the Small cell area, without to increase the macro interferences

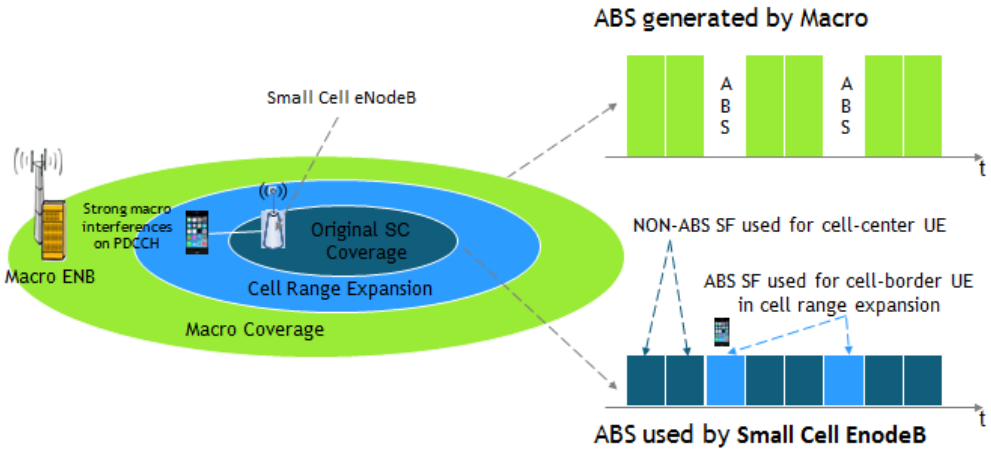

Figure 25: Illustration of ABS implementation

Mixed Sequences of blanked and non-blanked Subframes (Pattern): Blanking pattern, also known as ABS-Pattern defines scheduling restrictions for a sequence of 40 Subframes that controls transmission at Macro as well as at Small cell level. The ABS pattern is repeated continuously over time.

The aggressor cell (mainly macro) is able to define its own ABS-Pattern, where the victim cell (mainly the small cell) is only able to passively use that information. To differentiate both, it is called Own-ABS-Pattern and Received-ABS-Pattern respectively. Each single Received-ABS-Pattern is associated with a unique neighboring cell.

3 In-Building Performance and Feasibility of LTE Small Cells

Small cells are low-cost, low-power base stations designed to improve coverage and capacity of wireless networks. By deploying small cells on top and in complement to the traditional macro cellular networks, operators are in a much better position to provide the end users with a more uniform and improved Quality of Experience (QoE) [4].

3.1 In Building Performance and Feasibility of LTE SC with Beamforming

Small cells deployment is subject to service delivery requirements, as well as to the actual constraints specific to the targeted areas. For a good uniformity of service, in populated areas where presence of buildings is the main reason for significant radio signal attenuation, small cells may need to be closely spaced, e.g. within a couple of hundred meters from each other. Naturally, the performance of small cells is highly dependent on the environment specific characteristics, such as materials used for building construction, their specific propagation properties and surroundings. It is particularly important to have a proper characterization of an environment where small cells are deployed.

The work was focus on in-building performance and feasibility of LTE small cells through measurements, taking as reference both outdoor small cell and indoor pico cell deployments. To evaluate the outdoor and indoor cells feasibilities, we created scenarios where wireless connectivity within a target building is offered either by small cells located on the exterior of other buildings (small cells with outdoor characteristics) or simply by small cells located within the target building (pico cells with indoor characteristics). Those scenarios are analyzed and evaluate from different perspectives, from the coverage perspective, to UL and DL throughput and handover performance [4].

The content of this sub-chapter was also presented in paper [31] and the results are organized in two parts.

In the first part we analyze the measurements results obtained within a building, at 2.6 GHz.

In the second part we show an analytical 3D coverage and capacity prediction framework, which we calibrate and validate against field measurements.

Our framework utilizes the ray tracing tool WiSE [32] for 3D modeling of environments where measurements have been taken. In particular, this framework

can determine detailed performance levels or channel characteristics at any point of interest within a building and allows for fast and easy what-if scenarios testing. It can be used to create rules of thumb for deploying small cells and can be applied to large scale small cell deployments.

3.1.1 LTE Small Cell Field Trials

The goal of the field trials was to investigate the indoor performance and feasibility with LTE small cells placed outdoor and indoor. The measurements are performed at 2.6 GHz over 10 MHz bandwidth, in dedicated small cell carrier (no presence of macro-cell signal at 2.6 GHz) [33]. Measurements are done for a single small cell and a single test mobile or User Equipment (UE) to understand the fundamental aspects of outdoor-to-indoor and indoor-to-indoor propagation. We varied the location of the UE throughout the buildings and measured several Key Performance Indicators (KPIs), as reported by test mobiles. For the analysis in this paper we are addressing the Reference Signal Received Power (RSRP), Signal to Noise Ratio (SNR) and Physical Downlink Shared Channel (PDSCH) data rate at the selected UE locations. In LTE, RSRP is the average of the power of all resource elements which carry cell specific reference signals over the entire bandwidth [33].

The measurements venue is an industrial building with large rooms. It is of size 66 m x 24 m and has three floors as depicted in Figure 26. It has an open floor plan with lots of furniture and equipment on the hallways. We report the measurements taken on the middle floor of this building while using small cells deployed either in outdoor or in indoor. We have conducted trials in many other buildings and found similar results [34].

Services from outdoor small cell: As outdoor equipment we use a beamforming demonstrator, that we will call in this paper "BeamCell" from intellectual propriety reason.

The BeamCell is a high-speed transmissions data overlay designed to give an end user a uniform experience of LTE services over an urban and sub-urban coverage). As most of the active users will be indoor in a position limiting mobility (e.g. seated), this overlay will have the following focus:

- high speed data and video delivery (i.e. designed to limit interference between base stations)
- high capacity (i.e. obtained by a large number of small cells, deployed on urban furniture or building facades)
- fast deployment
- remote energy capability
- high level of indoor coverage (i.e. deep indoor penetration)
- progressive deployment capability
- integration of high-speed backhauling technologies

Each panel can radiate into three directions (three coverage can be created: two symmetrical with regards to the antenna axis, one in the axis). Those directions are constant in azimuth but can be adjusted in site according to the environment. There is a possibility to combine the three beams of a panel to transmit in a half space.

BeamCell panel shall be deployable either on a facade or on urban furniture. A panel with digital unit can be connected, through a CPRI interface with a second panel. The transmission and reception of the two panels shall have the capability to be synchronized.

The operating mode is a combination of re-use 3 and beam-switching. The rationale for these two modes is coming from traffic variation (a small number of simultaneous users is expected) interference avoidance and propagation.

The transmissions of each BeamCell base station is synchronized with the adjacent ones, via X2 interface, in order to minimize the mutual interferences.

Each element of a panel antenna is fed with a small power, typically 50 to 250 mW in average.

The performance simulations have shown that beam switching (or re-use 3) combined with fractional frequency reuse (or carrier coloring) and cooperation between sites allowed in a rich scattering environment significantly high performance. An appropriate level of EIRP or sensitivity is necessary for deep indoor coverage. Compared with other technologies (i.e. pico or large femto, directive pico,etc.) these features permit to achieve coverage (> 95% at high speed versus 5% to 65% for other technologies), capacity (>>x3 the pico one at equivalent coverage), and user rate. X2 interface inter-site coordination permits to deliver much higher user experience than any other technology at lower

For our experiment, the outdoor small cell, with integrated 8x8 antenna, was attached on the exterior of the building on the same level as the middle floor. The arrow in the Figure 26 shows the main direction of the beam formed by the small cell. We refer to this beam orientation as the 0° beam. During measurements, this beam has been also electronically steered by +/-30° in the azimuth plane. For each instance of the beam we have taken independent measurements within the building (only one beam instance was active during measurements).

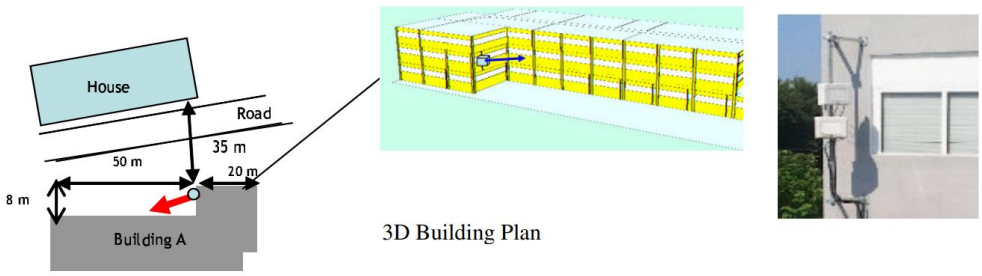

Figure 26: Layout and 3D building plan of the measurement building and its surroundings. The small cell location and antenna orientation is marked with an arrow towards the middle of the long edge of the building. Outdoor small cells are attached to the exterior of the building at the height of the floor where measurements have been taken (right).

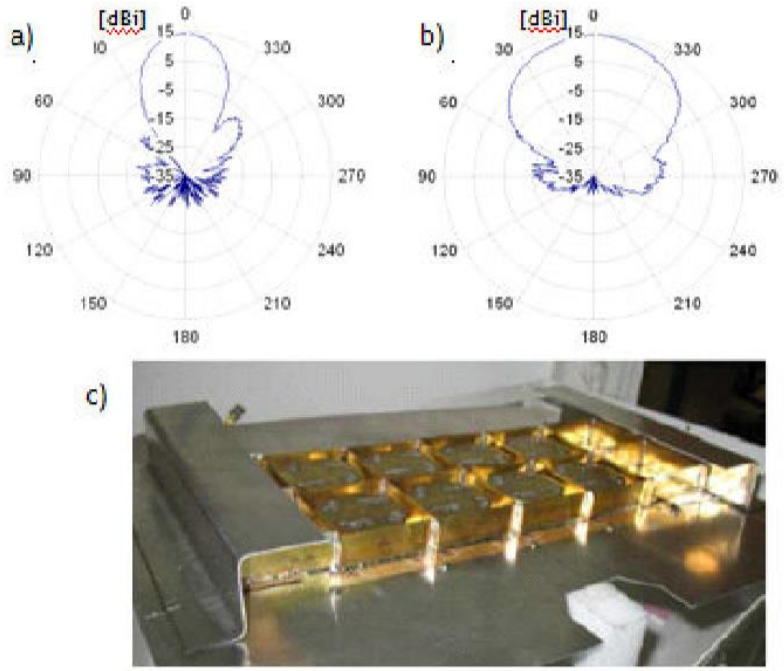

Figure 27: Directive Antenna pattern for the outdoor small cell a) Horizontal plane (14.2 dBi gain, 25° horizontal half power beamwidth); b) Vertical plane (14.2 dBi gain, 49.6° vertical half power bandwidth); c) 8-element smart prototype antenna panel for outdoor deployment to improve the indoor antenna coverage.

For outdoor to indoor coverage we used a directive beam with 14.2 dBi gain. The beam is formed with an eight-element smart antenna panel showed in Figure 27. Its horizontal and vertical patterns corresponding to the 0° beam direction are illustrated in Figure 27a and Figure 27b, respectively. The antenna pattern has 25° horizontal half power beamwidth (-3dB power) and 49.6° vertical half power beamwidth. The narrow horizontal beamwidth is designed with the purpose to reduce the interference with any potential adjacent transmitters, while larger vertical beamwidth enables coverage across several floors of a building. All measurements using the outdoor small cell were made with the LTE Transmit Diversity Mode or Transmission Mode 2 (TM 2) [33], which can yield a maximum measurable throughput over-the-air around 30 Mbps (single data stream) over a 10 MHz channel.

Services from indoor small cells: We show results also for the cases where two indoor small cells are used for coverage.

For indoor-to-indoor measurements we used a less directive pico-cell pattern as shown in Figure 28. The antenna pattern has a directivity of 7 dBi and has a 60° horizontal and 62° vertical half power beamwidth. All measurements with the pico cells were made using the LTE Closed Loop Spatial Multiplexing Mode or Transmission Mode 4 (TM 4) [33], which can yield a maximum measurable throughput over-the-air around 60 Mbps (two data streams) over a 10 MHz channel.

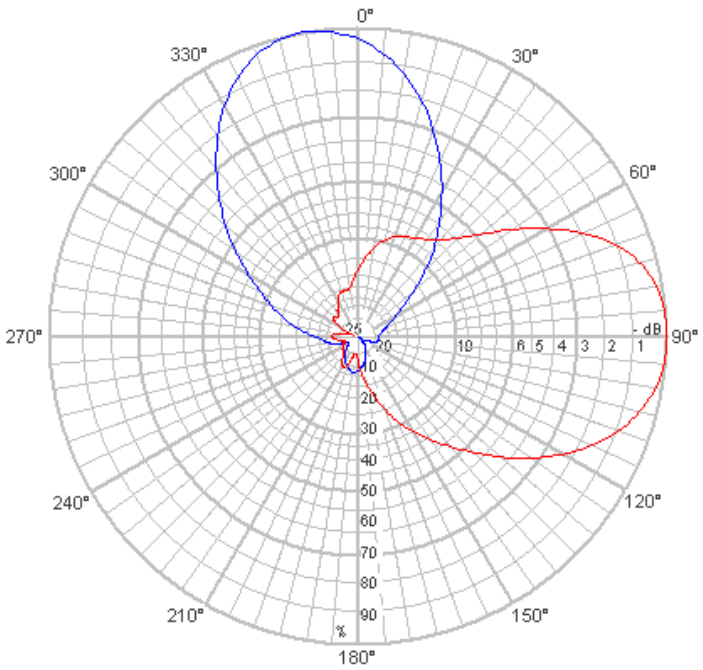

Figure 28: Indoor small cell antenna pattern: a) Blue: Horizontal plane; b) Red: Vertical plane.

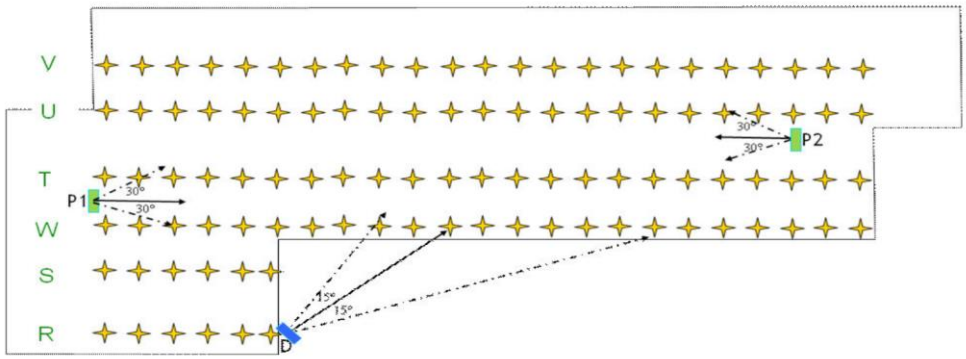

Figure 29: Grid of measurement points and small cell locations. The outdoor small cell is located at D. The pico cells are located at P1 and P2 in indoor.

A. Outdoor-to-indoor and indoor-to-indoor LTE small cell trials

Figure 29 shows the grid of measurement points in the building, where KPIs are collected along with the small cell locations on the middle floor. We grouped the measurement points as rows labeled with the letters R, S, W, T, U and V. The lines are not alphabetically arranged, the measurement row W being located at window side. The rows R and S are close to the outdoor small cell located at the point labeled

with D, though they are not in the main beam direction. The rows V and U are the furthest away in the interior of the building. There are up to 23 measurement points on each row. The straight line at point D shows the 0◦ beam direction of the small cell. The directions of the beams resulting from electronic beam-steering by +/-30◦ of the 0◦ beam in the azimuth plane are also represented by the dashed lines coming out of the location D. Only one beam is activated at one time, but the measurements are taken for all tree beams, one by one.

The indoor pico cells are located at the points P1 and P2, attached to the ceiling, with antenna orientation pointing at each other. The corresponding arrows indicate the main directions of the pico cells antennas.

Two dimensional (2D) maps visualize the variation of KPIs of interest over an entire area and help identifying potential zones of a building which need improvement in terms of coverage and data rates.

The analyzed KPIs are: RSRP, SNR and PDSCH data rate.

The 2D maps are obtained by interpolating the KPIs collected at the measurement points shown in Figure 29 .

1) Coverage and data rates using the outdoor BeamCell: Figure 30 shows the 2D maps for RSRP, SNR and PDSCH data rate for the 0° beam of the outdoor small cell. The total transmit power was set to 125 mW. Although the transmit power is quite small, the significant small cell antenna gain enables penetration of the signals into the building and yields good coverage over a large area of the building. We measured RSRP values up to -68 dBm near windows (measurements points form line "w") as can be seen in Figure 30A. The maximum possible downlink (DL) data rate of 30 Mbps was achieved at measurement points falling within the span of 0° beam. Further, we were able to ensure data rates higher than 15 Mbps for 85% of receiver locations. The lowest measured data rate was 7.4 Mbps, corresponding to the right uppermost corner of the building, highlighted in Figure 30C (between lines U and V and columns 22 and 23). Higher data rates would be possible through spatial Multiple Input Multiple Output (MIMO), which allow for multiple data streams to be delivered simultaneously.

The SNR shown in the 2D map is capped at 29 dB. The SNR was above 20 dB at 52% of the locations. Only 5% of measured locations have a SNR below 7 dB.

Outdoor-to-indoor penetration depends highly on the type of the windows and exterior wall. The building has regular windows without any metallic shielding, which was favorable for outdoor-to-indoor propagation. On the other hand, its exterior wall is made of thick concrete layer and the floors were filled with lossy office furniture and metallic equipment's on the shelves. To quantify the effective losses through the exterior we have placed the UEs in outdoor, 30 cm away from the window at 140 cm height (this is the level which corresponds to the base of the window on this floor). In addition, we have also placed UEs in indoor, 20 cm away from the exterior wall, on a table at 80 cm height (40 cm below the base of the window).

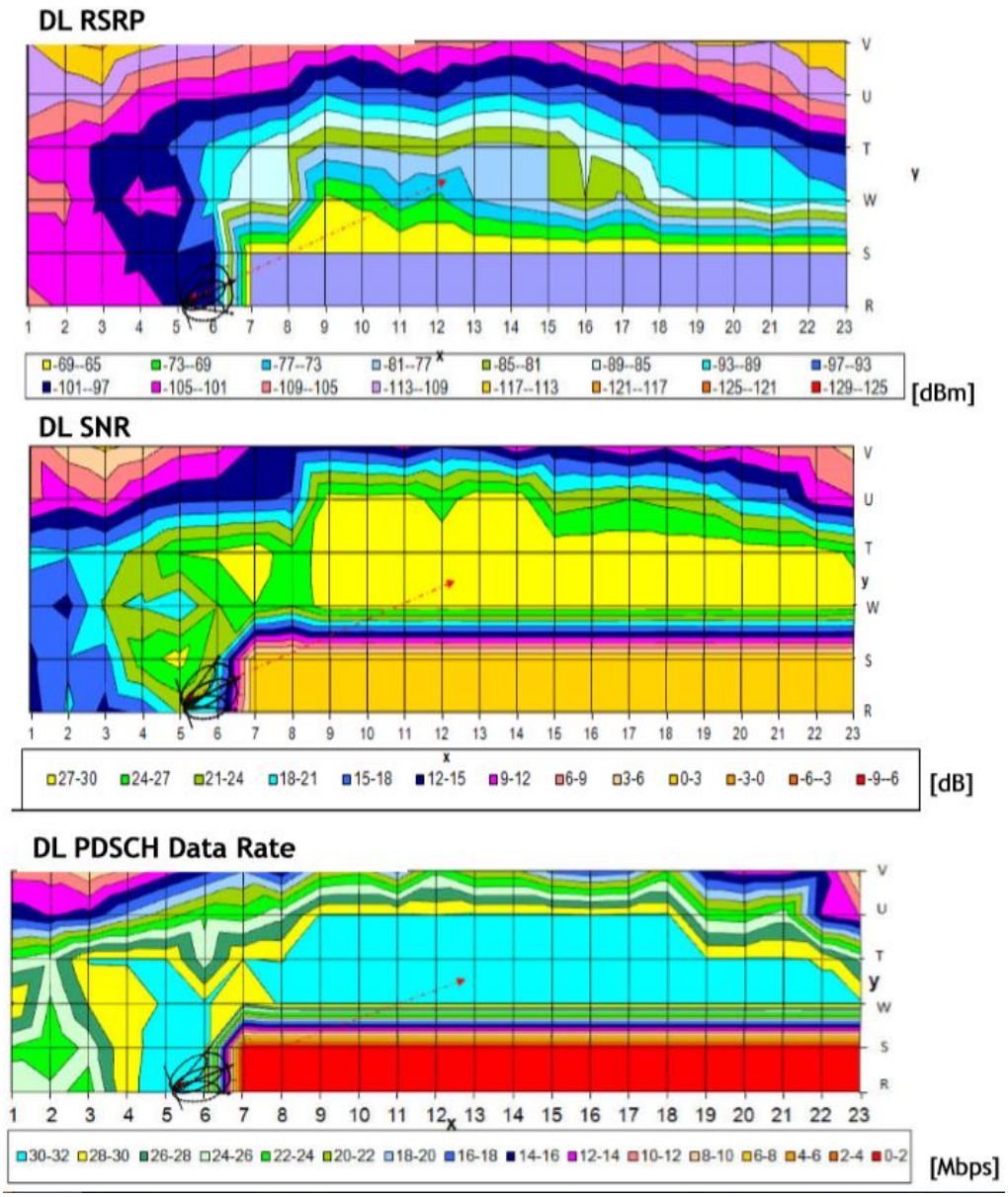

Figure 30: Building A: 2-D RSRP, SNR and measured PDSCH data rate maps using the outdoor small cell (0◦ beam).

The SNR shown in the 2D Map is capped at 29 dB. Analyzing the results obtained for all the measurements points we observed that for the SNR measurements we obtain values above 20 dB at 52% of the locations. Only 5% of measured locations have a SNR below 7 dB.

Outdoor-to-indoor penetration depends highly on the type of the windows and exterior wall. The building has regular windows without any metallic shielding, which was favorable for outdoor-to-indoor propagation. On the other hand, its exterior wall is made of thick concrete layer and the floors were filled with lossy office furniture and metallic equipment's on the shelves. To quantify the effective losses through the exterior we have placed the UEs in outdoor, 30 cm away from the window at 140 cm height (this is the level which corresponds to the base of the window on this floor), we have also placed UEs in indoor, 20 cm away from the exterior wall, on a table at 80 cm height (40 cm below the base of the window). We repeated this experiment at measurement points parallel to row W in Figure 29, which are associated with six adjacent windows within the span of the 0◦ beam. The windows are around 6 m apart from each other. The difference between measured outdoor and indoor RSRP values in these experiments varied between 10 dB and 21 dB. This corresponds to the penetration loss caused by the front wall of this building. The obtained values are in line with normal attenuation patterns considering the same materials and the same working frequency. Also, these results, allow us to calibrate our propagation model inside the WISE tool.

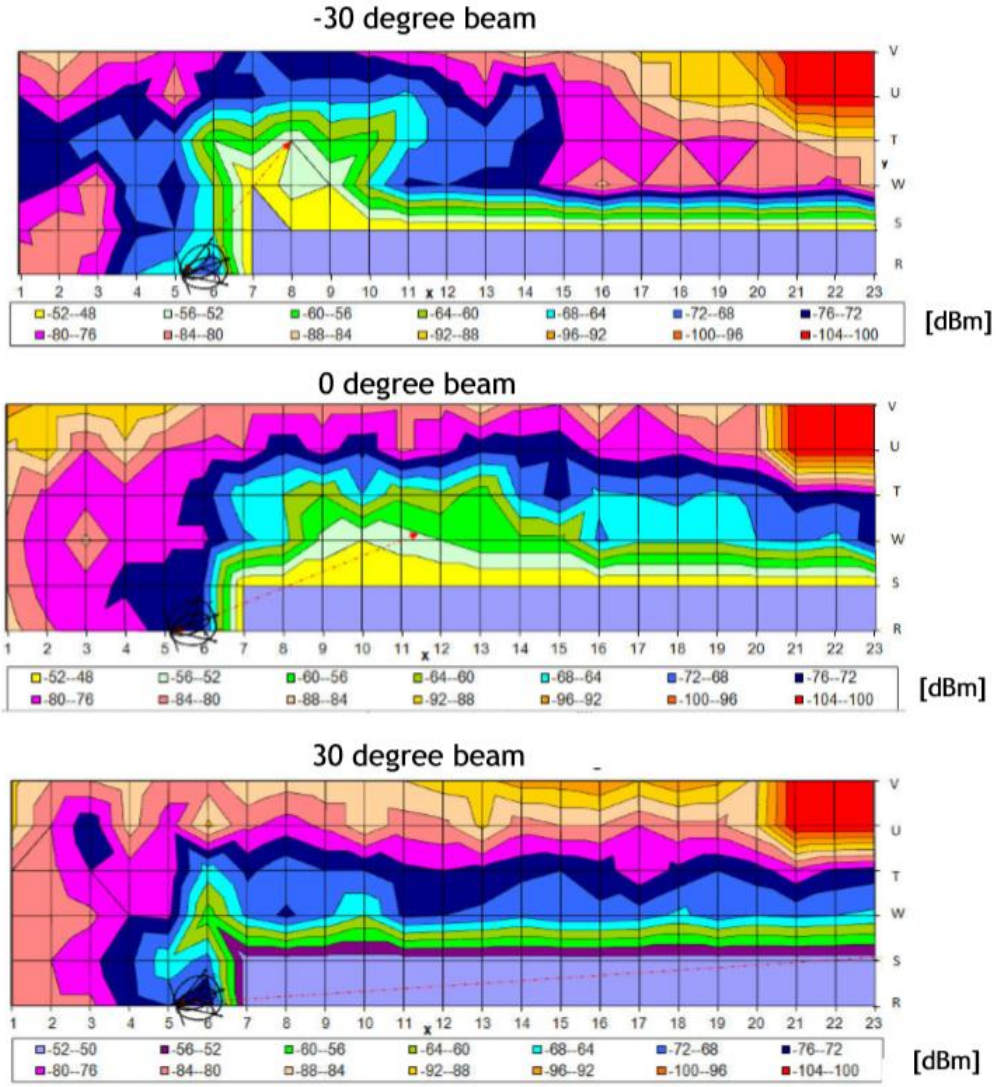

Figure 31: Measured RSSI with 0, 30 and -30 degree beams

2) Small cell footprint within the building: Figure 31 displays the measured received signal strength indicator (RSSI) values for the beams directed at three beam orientations (azimuth values: 30◦, 0◦, -30◦), each active one at a time. For each azimuth value, we see that the coverage footprint within the building, is consistent with the orientation and directivity characteristics of the antenna, yielding the low angular spread at the transmitter side. This is an important result, which can be further exploited by enabling multiple simultaneous active beams with narrow horizontal beamwidth, without causing severe interference to each other.

3) Indoor mounted Small Cell: Pico cell transmit power was set to 250 mW for these experiments with the indoor small cells. Figure 32 shows the RSRP, SNR and PDSCH data rate for the scenario where only the pico cell at P1 marked in Figure 29 is active. With a single pico cell the transmitted, only P1 located pico from Figure 29, signals penetrate well up to the measurement column 16. The cell edge forms on the opposite side of the building. In Figure 33, both pico cells located at P1 and P2 are active. This improves the RSRP on the side of the building close to P2 but reduces the SNR and PDSCH data rates in the middle of the building.

Figure 34 shows the comparison of the Cumulative Distribution Function (CDF) of PDSCH data rates between one pico cell (only P1 active) and two pico cell deployments (both P1 and P2 are active) in Building A. Although RSRP distribution is improved by adding the second small cell at P2, as shown in Figure 29, there are no data rate gains in comparison to the single pico cell scenario due to the reduced SNR in the middle of the building. On the other hand, each small cell is an access point, serving users in its proximity. Through these experiments, one can interpret that the small cells densification is possible but need to be made considering the particularities of each building and each traffic model. When we analyze the indoor coverage is always a discussion about the compromise between level of signal and the quality of signal. The performance is significantly improved when we use a higher range of frequency reuse, using different frequency bands for indoor neighbor cells.

Considering the tree analyzed scenarios for building coverage: using one outdoor BeamCell - Figure 30, using one indoor pico cell - Figure 32 and using two indoor pico cells - Figure 33 we can conclude that the beam forming demonstrator enable us to obtain better indoor coverage using low power base stations, mounted outdoor, with possibility to adjust the beam electrically, remote, without OPEX costs. Of course, for the situations when we can’t mount outside the BeamCell, from different reasons, the indoor pico cell remain the only available option. Also, the number of indoor stations will be choosing based on several criteria’s: number of users that will need to be deserved, level of existing indoor interferences, available frequencies and imposed safety norms [35]

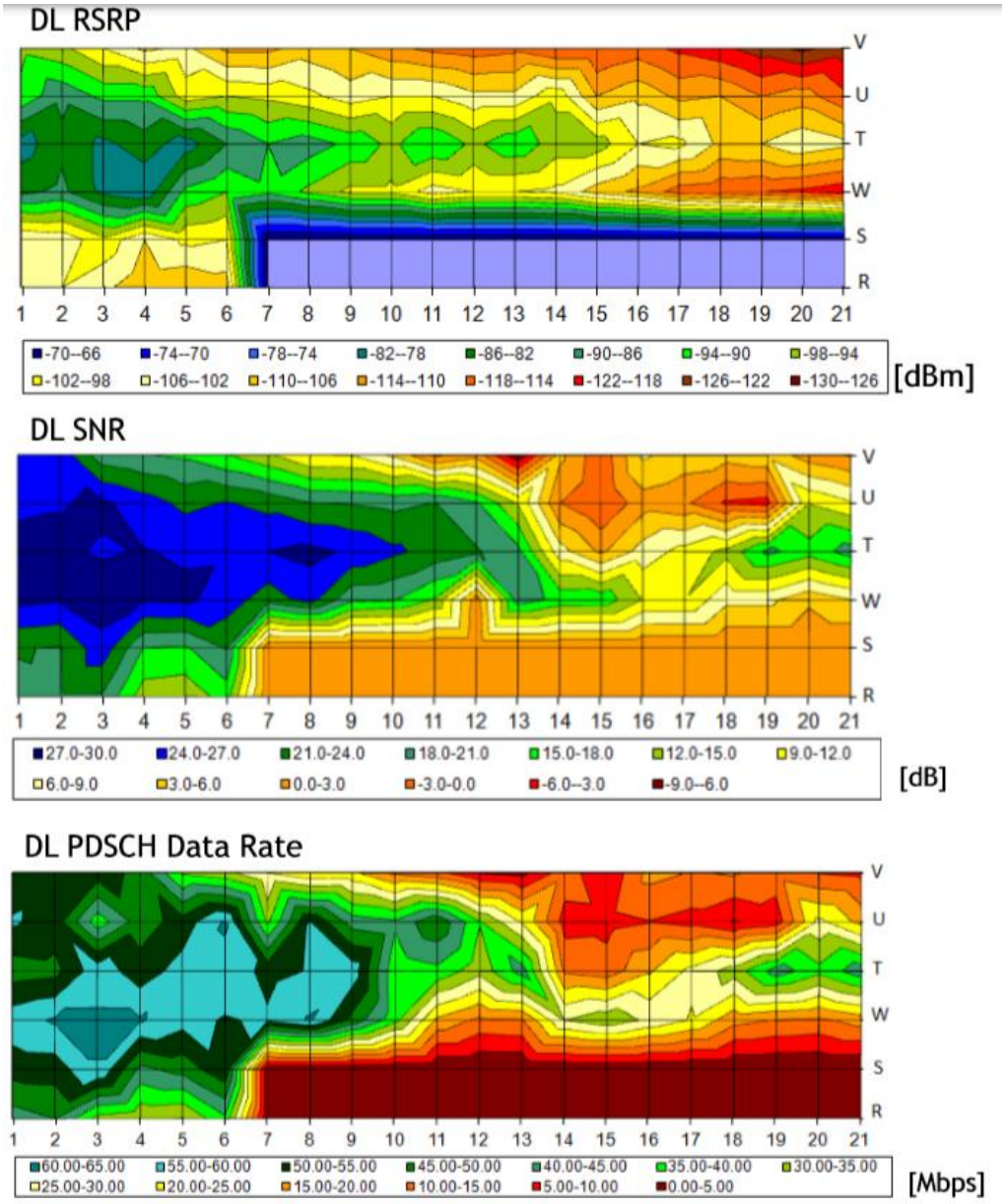

Figure 32: 2-D RSRP, SNR and measured PDSCH data rate maps with only the pico cell at P1 active

Analyzing the SNR values from Figure 32 and Figure 33 we observed a interference area in proximity of windows, at that point where the reflection of electromagnetic waves are maximum. This area with high interference can be determinate in both ways: empiric and theoretical.

The empiric determination we done by analyzing the measurement graph and in particular for one radiating source the area is at column 1. In case of two radiating sources the interfered area become significant bigger (the effect induced by P1 and P2 small cells are combined) and affect the area between columns 10 and 16. Theoretically these observations can be validated by reflection and refraction laws (Snell's law), considering the refractive indices for air n1=1 and for windows a normal-index glass n2= 1.5. [36]

Considering these values, the critical angle is computed as:

Equation 2

$$\theta_c = \sin^{-1}\frac{n_2}{n_1}\sin\theta_2,$$

where θ_2 is π/2, and $\sin\theta_2 = 1$

the critical angle is 41.8°, that means for incidence angles higher than 41.8°, the waves are reflected integrally.

These observations are very important especially in case of offices buildings, where a significant number of users are located near windows to take benefits of natural light. Basically, for those types of buildings, the solution to mount outside the cell is cleaner from interference point of view and radiation in proximity of human body. The outdoor placement of cells is also suitable for buildings with access restrictions from security and/or intellectual propriety reasons.

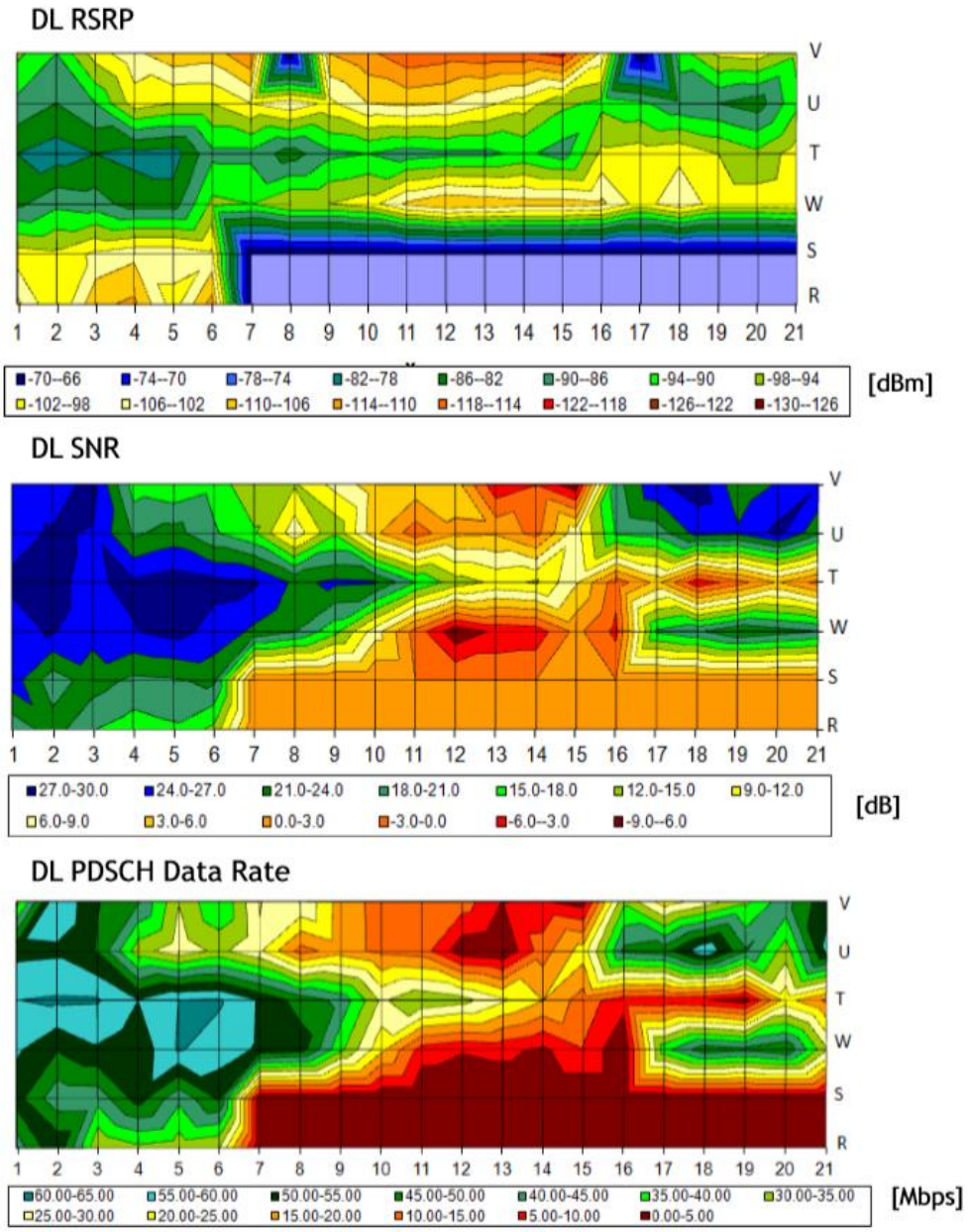

Figure 33: 2-D RSRP, SNR and measured PDSCH data rate maps with both of pico cells at P1 and P2 active

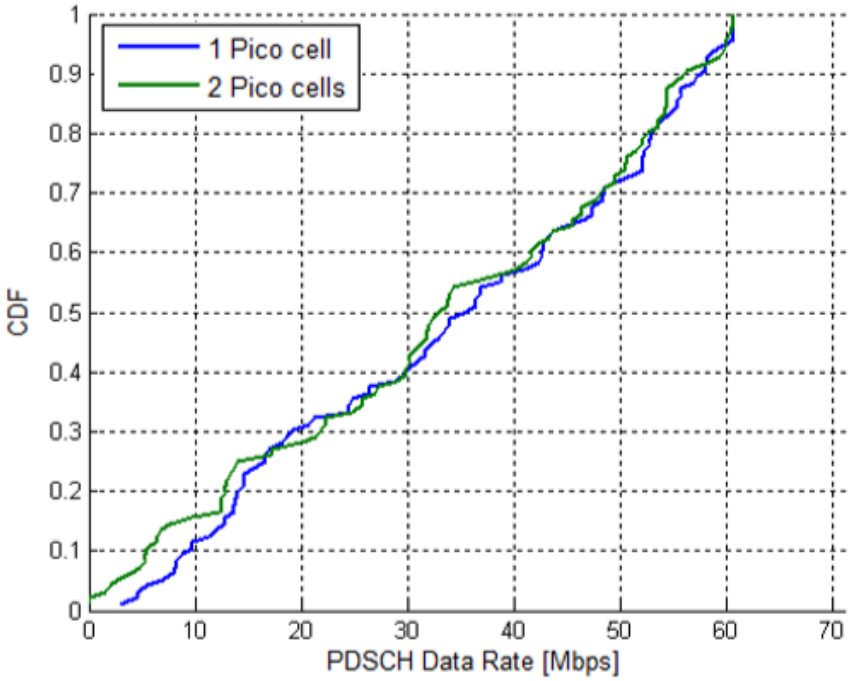

Figure 34: Measured PDSCH data rate comparison between single pico cell and two pico cell deployments

3.1.2 LTE Performance Prediction Framework Validation with Measurements

3D ray-tracing based techniques simulate the physical environment and use wave propagation theory to predict the radio signal level received at any point. They also account for transmission through walls and diffraction around walls. When the physical environment is well-specified, such as the layouts and materials of walls, floors and ceilings are known, 3D environment simulations can be deployed on a very large scale and with limited effort.

Our experience has indicated that after an initial training and calibration phase with measurements, 3D environment simulations can be used with a high degree of confidence in complement of measurements, which are known to be labor-intensive and costly, [34]. When measurements are not available for whatever reason, 3D environment simulations can be used instead, as an efficient tool to understand performance of wireless technologies, and in particular to get a good sense of how some specific product features, such as power levels and/or antenna characteristics would impact product performance [37], [38]. They can be also used to assist RF network design, and to derive rules of thumb for wireless products deployment in real environments. Their prediction accuracy can be only as good as the environment modeling assumptions are.

Ray-tracing is a method for calculating the path of waves or particles through a system with regions of varying propagation velocity, absorption characteristics, and reflecting surfaces. Under these circumstances, wave fronts may bend, change direction, or reflect off surfaces, complicating analysis. Ray tracing solves the problem by repeatedly advancing idealized narrow beams called rays through the medium by discrete amounts [39]. Ray-tracing techniques are already established as a promising environment emulator for studying channel characteristics in urban environments. There are several studies confirming ray-tracing predictions with experimental results. Ray tracing predictions in urban environments have been favorably compared to field measurements for received power, RMS delay spread, crosspol antenna behavior, angle of arrival, and link performance in many studies conducted by independent research groups e.g., [40], [41], [42], [43], [44]. The ray-tracing tool we use is WiSE, an environment simulator developed by Bell Labs for wireless system engineering [32]. WiSE tool takes into account the geometry of buildings, type of materials, angle of incidence, dielectric coefficients, wall thickness, and frequency and 3D antenna patterns. It has been validated for both indoor and outdoor environments in previous studies [44], [45], [46], [47]. The distributions of arrival times and angular spreads generated with WiSE agree quite well with those of an empirical model based on measurements in [47].

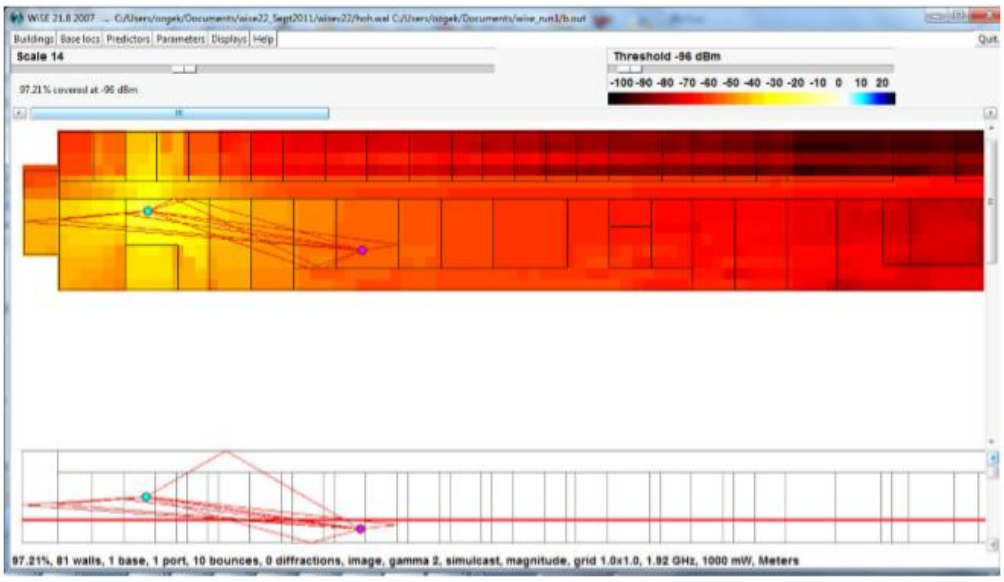

Figure 35: WiSE ray tracing tool. WiSE simulates rays between a transmitter-pair. Rays shown are projections onto the azimuth and elevation plain. It can predict the received power for any given location in the building.

We are aware of other ray tracing emulators for indoor-to-indoor or outdoor-to-indoor simulations (e.g., [48]) available commercially but we did not compare their performance with WiSE, as our main goal did not consist in a cross-ray tracing tools performance comparison. The main goal for us was to optimize the prediction tool in

a such a way to be able to prove the similarity of results obtained using our tool with empirical results determined by measurements.

Given a building plan and transmitter and receiver locations, WiSE compute the radio-signal level at any point in the building. The reflection and transmission coefficients are determined based on the angle of incidence and layer properties at each interaction with a wall. WiSE simulates the ray traces at the receiver both in elevation and azimuth plane in Figure 35. In order to determinate the signal level in every point of the interest area (target building), for each received ray in a specific point, WiSE computes the angle of arrival (AOA), the delay and the power. The power of a particular ray is given by the following formula:

Equation 3

$$P_R = G_R G_t (\lambda|2\pi d)^2 \prod_{m=1}^{M} t_m \prod_{m=1}^{M} r_{mk} P_T$$

where d is the unwrapped distance traveled by the ray, G_t is the transmit antenna gain, G_r is the received antenna gain, P_t is the transmit power, λ is the wavelength. We assume the ray undergoes M transmissions and K reflections before reaching the receiver; t_m denotes the transmission coefficient for the *m-th* transmission; and r_k denotes the reflection coefficient for the *k-th* reflection. The reflection and transmission coefficients are computed by each interaction with a wall taking into account the frequency and angle of incidence. We forgo in the scope of the paper explaining further details of WiSE ray tracing tool. For more details on WiSE ray tracing algorithm we refer the readers to the reference [32].

We modeled the building where the field trials have been held. We had the exact detailed information on geometry of the buildings, and some prior information on electromagnetic properties of materials. We set these parameters after some trial-error-steps, where the simulations are compared against the field measurements and adequate tuning of in-building propagation losses was made to match experimental results.

For prediction we used the same 3D antenna patterns and power levels as in the field trial experiments. During measurements we recorded the measured metrics at specific locations. We exported these locations to WiSE and predicted the corresponding RSRP. The validation consists in comparing the measured RSRP against corresponding predicted values, through a point by point comparison.

Figure 36 shows the predicted versus measured RSRP on the rows denoted by: R, S, W, T and U in Figure 29. The measurement points and drive test rows are presented in Figure 29. The red line corresponds to the predicted RSRP without any losses through the building, which corresponds to the free space propagation. We determined it by removing the building from the simulation setup but keeping all other parameters unchanged. Comparing the free space with the measured RSRP we observe that the measurement pattern follows the antenna directivity characteristics.

This is an indicator of low angular spread, which encourages the use of directive antennas for outdoor small cell deployments.

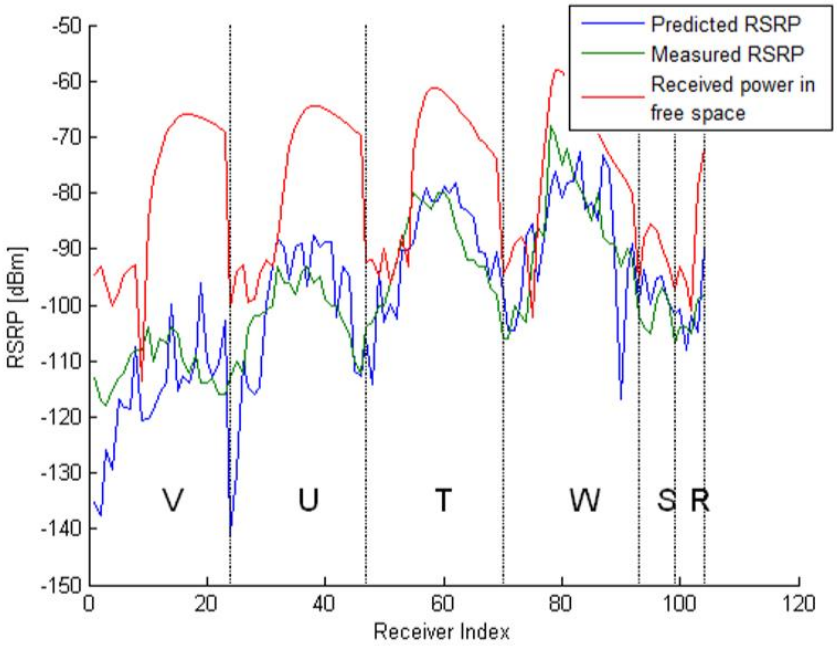

Figure 36 Building A: Comparison between measured/predicted RSRP and the received power in free space.

When we perform a detailed comparison between measured values and compute values graphs, we observed two anomalies: beginning of U line and at the end of W line. The explanation for this difference is: the tool considers these measurement points being located nearby wall (0 cm distance). In reality these measurements were taken at list 50 centimeters far from the wall from practical considerations (the laptop use for measurements was hosted on top of a mobile table that have approximatively this size).

One of the applications of this framework is extracting the channel parameters for specific environments of interest. After calibrating with the available information, we extracted the parameters that largely characterize the behavior of the wireless channel in this office building. Relative angles along with RMS angular spread indicate the severity of the dispersion in the angular domain therefore the applicability of the beamforming algorithms. It shows the deviation of the multipath signals from a mean angle of arrival (angle of departure).

To analyze the behavior of multi antenna systems, we need to consider several signal sources. For each of the N transmitter-receiver pairs, we determine the relative angles (deviation from the mean angle of arrival (AOA) and angle of

departure (AOD). We aggregate relative angles data from all of N links and compute the percentage of occurrence for each angle bin. We use 1-degree equally spaced bins between -180° and 180°. In [47], it is shown that the Laplacian distribution is a good fit for distributions of relative angles in indoor to indoor channels. The Laplacian distribution is given by:

Equation 4

$$f_L(\omega) = \frac{1}{\sqrt{2}\sigma}\, e^{-\frac{\sqrt{2}}{\sigma}|\omega-\mu|}$$

where w is the deviation of the angle from the mean AOA and σ is the standard deviation and μ is the mean. Similarly, we apply the Laplacian fit to the relative angles in outdoor to indoor channels. Figure 37 shows the Laplacian fits for the predicted AOD relative angles. The theoretical Laplacian fit for AOD has σ = 18° and the theoretical Laplacian fit for AOA has σ = 72°.

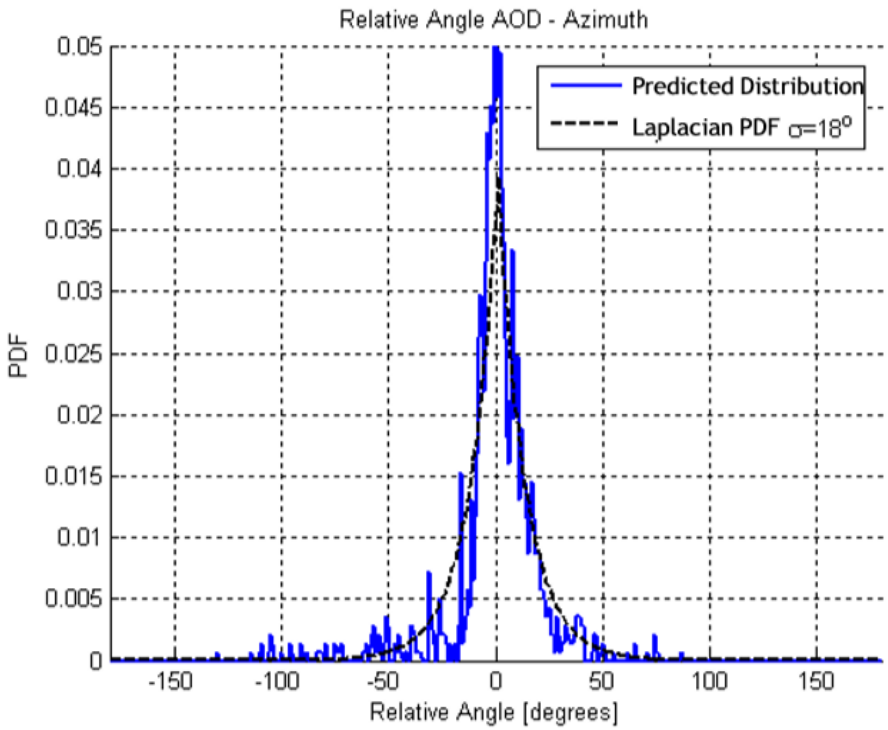

Figure 37: Laplacian fit to relative angles (AOD, azimuth plane)

RMS angular spread gives the width of the sector from which most signal power is received (sent). RMS angular spread is defined as the second central moment

of the power angle profile. The predicted RMS angular spread at the transmitter side is less than 5 degrees at the median. At the receiver side the angular spread in azimuth plane is close to 40 degrees at the median.

Both measurements and predictions encourage the use of directive antennas for outdoor small cell deployments indicating low angular spread at the transmitter side.

3.1.3 Discussions

Experimental results run in related work showed the feasibility of beamforming for LTE small cell deployments in outdoor for covering indoor environments through measurements. With a single small cell employing directive antennas and using low power we were able to establish good indoor coverage (Only 5% of measured locations have a SNR below 7 dB) delivering high data rates for large parts of an office building (for a theoretical max throughput of 30 Mbps, we obtained 15 Mbps for more than 85% of the measurements points). These results are in line with our other LTE measurement campaigns associated with other buildings (the framework was used in commercial networks, having different types of target building, and the predictions obtained was validated after implementation trough drive tests). The measurement campaigns mentioned above was performed in the customer's premises and are subject of a Not Disclosure Agreement contract, as a consequence the results can't be listed here.

For each azimuth value we showed that the antenna footprint is well preserved within the building. This result encourages the simultaneous use of multiple narrow beams with high gains to cover indoor environments. The scattering within the building contributes to coverage of locations which are not in line-of-sight of the transmit antenna, yielding service continuity throughout a building. Our measurement results indicate low angular spread at the transmitter side and high angular spread at the receiver side.

Furthermore, we showed an analytical 3D performance prediction framework, which we calibrated and validated against available field measurements. The framework provides detailed performance levels at any point of interest within a building; it allows to determine the minimum number of small cells required to deliver desirable coverage and capacity levels, their most desirable location subject to deployment constraints, transmission power levels, antenna characteristics (beam shapes) and antenna orientation (azimuth, tilt) to serve a targeted geographical area. The good match between measurements and predictions encourages the use of the 3D performance prediction framework, in complement to field measurements, to support small cell deployments [4].

The WiSE tool, with prediction algorithm optimized using our results, can be easily used in LTE network deployment, from the phase of planning up to network optimization phase, in two different ways: when we have constrains related to performance, we can determine the minimum number of small cells that are able to fulfill our requirements, or when we have already the cells installed we can optimize the parameters (azimuth, elevation, Tx power, beam direction,..) in order to maximize the coverage and/or the overall throughput.

3.2 Improved LTE Macro Layer Indoor Coverage Using SC Technologies

The most important asset of a mobile network provider is the ability to cover in an efficient way the territorial area. From quantitative perspective, the Regulators impose for a commercial network two requirements: percentage of territorial coverage and percentage of population. The qualitative perspective analyzes aspects from Quality of Experience area as: call success rate, call block rate, drop call rate and speech quality (MOS- Mean Opinion Score). [49].

In the qualitative approach, the in-building segment become an important component. A cost effective and low power solution to meet the indoor requirements is offered by small cells solution. 3GPP defines small cells as low-cost, low-power base stations designed to improve coverage and capacity of wireless networks. By introducing small cells on top and in complement to the traditional macro cellular networks, operators are in a much better position to provide the end users with a more uniform and improved Quality of Experience (QoE). Small cells deployment is subject to service delivery requirements, as well as to the actual constraints specific to the targeted areas. Small cells need to be closely spaced, e.g. within a couple of hundred meters from each other, for a good uniformity of service, in populated areas where presence of buildings is the main reason for significant radio signal attenuation [4].

As expected, the performance of small cells is highly dependent on the environment specific characteristics, such as materials used for building construction, their specific propagation properties and surroundings. For example, a building with concrete walls and anti-fire doors will have low outdoor cell signal penetration and a high room to room indoor attenuation, in opposite with an office building with glass walls and open-space office. Obviously, it is particularly important to have a proper characterization of an environment where small cells are deployed. This is based on in-building performance and feasibility of LTE small cells through measurements and takes as reference both outdoor macro and indoor metro cell deployments.

Particularly metro cells (part of small cells) are 100% percent aligned with macro protocols and architecture using the same interfaces.

In this sub-chapter we analyze how to improve the indoor coverage offered by an existing macro cell based network. The proposed solution is based on introducing low-power equipment into the network to create a metro cell. The low-power profile is needed for the new introduced cell from two reasons: safety norms imposed by authorities and macro layer interference mitigation.

3.2.1 Environment and System Test Definition

The goal of experiments was to optimize the LTE network architecture by introducing the metro layer on top of existing macro layer to improve the indoor coverage and service accessibility (the service accessibility is indirectly increased by macro layer decongestion and higher network capacity). The targeted building was an

office building with: small and medium offices. All these aspects perform to increasing the end user experience, especially in indoor environment.

The measurements were performed at 2.6 GHz using the LTE Closed Loop Spatial Multiplexing Mode or Transmission Mode 4 (TM 4) [50], which can reach a maximum measurable throughput over-the-air around 60 Mbps (two data streams) over a 10 MHz channel. Measurements are done using a single test mobile or User Equipment (UE) to highlight the fundamental aspects of outdoor-to-indoor and indoor-to-indoor propagation.

In our experiments we address the following KPI (Key Performance Indicators):

- Reference Signal Received Power (RSRP)
- Received Signal Strength Indicator (RSSI)
- Signal to Noise Ratio (SNR)
- Data rate at the selected UE locations

The RSRP parameter provides cell-specific signal strength metric. RSRP is defined as the linear average of the power contributions of the REs which carry cell-specific reference signals within the considered measurement frequency bandwidth [51]; [52]. This measurement is used mainly to rank different LTE candidate cells according to their signal strength and is used as an input for handover and cell reselection decisions.

RSRQ measurement is intended to provide a cell-specific signal quality metric. This measurement is used as an input for handover and cell reselection decisions, for example in scenarios for which RSRP measurements do not provide sufficient information to perform reliable mobility decisions. The RSRQ is defined as the ratio:

Equation 5

$$RSRQ = N * RSRP/LTE\ carrier\ RSSI$$

, where N is the number of Resource Blocks (RBs) of the LTE carrier RSSI measurement bandwidth [51]; [52].

The measurements in the numerator and denominator are made over the same set of resource blocks. While RSRP is an indicator of the wanted signal strength, RSRQ additionally takes the interference level into account due to the inclusion of RSSI. RSRQ therefore enables the combined effect of signal strength and interference to be reported in an efficient way. Similarly, to RSRP, this metric is used mainly to rank different LTE candidate cells according to their signal quality.

For experiments we used 3 LTE Base Stations (eNodeB) located P1, P2 and P3 as can be seen in Figure 39 (2 of them are considered useful - P1&P2 and the third one is used as interferer- P3) having the following characteristics:

- The first eNodeB is a macro eNodeB having a default transmission power equal to 2x40W is and connected to a Xpol antenna (typical combination for Macro layer in LTE B7). The antenna pattern has a directivity of 18 dBi and has a half power beamwidth of 58◦ horizontal and 5◦ vertical as can be seen in Figure 38 [5].

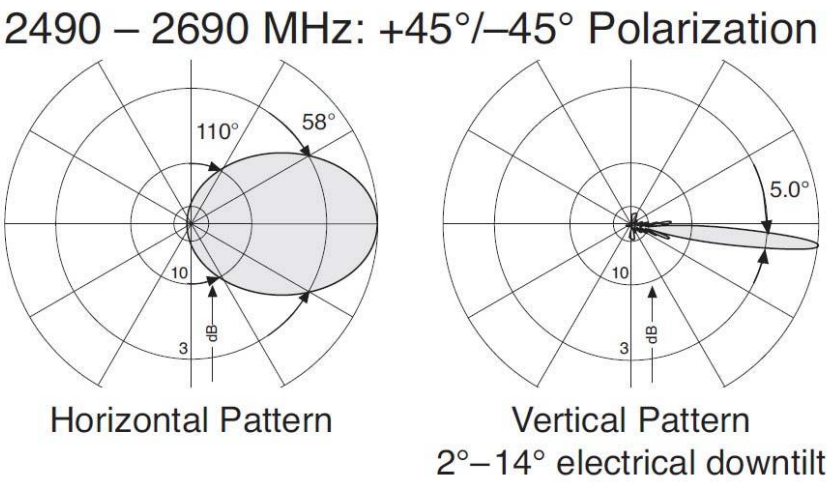

Figure 38: Antenna pattern for macro cell

- The second eNodeB is a metro eNodeB (called "metro cell") with 2x1W transmission power connected to a less directivity antenna as showed in Figure 28. The antenna pattern has a directivity of 7 dBi and has a 60° horizontal and 62° vertical half power beamwidth [33].

- The third metro eNodeB (called "interferer metro cell") was used only to introduce interference over the radio channel. It was connected to an omnidirectional antenna having a 2dBi gain [53].

The subscribers are not accepted on the interferer metro cell because the interferer cell is barred in the database.

3.2.2 LTE Small Cell Field Trials

We considered the indoor area covered by one "useful" metro eNodeB and one external macro eNodeB. We used a second metro eNodeB ("interferer") emitting on the same bandwidth as macro to degrade the quality on macro layer (to reach typical macro layer radio conditions in the field).

In this way one METRO acts as an interferer for our call being on the same frequency as the macro eNodeB, proving in this configuration UE is capable at this limit conditions to perform inter - frequency handover (HO) between macro eNodeB (stronger signal but lower quality) and Metro eNodeB (indoor power settings so lower signal but good radio quality).

In Figure 40 the DL RSRP is displayed to highlight the building coverage obtained using a single outdoor macro eNodeB emitting in 20 MHz bandwidth on a dedicated carrier (without any interferer).

Even if the macro eNodeB is located in the building proximity and have a straight forward orientation the coverage is poor (for less than half of the buildings we measured PSRP higher than -130 dBm).

The macro eNodeB is mount in building proximity how can be seen in Figure 39 in location named P1. The useful metro is located in P2 location and the main beams for the useful cells have opposite orientation. The interferer metro is located nearby macro cell and have the same beam orientation.

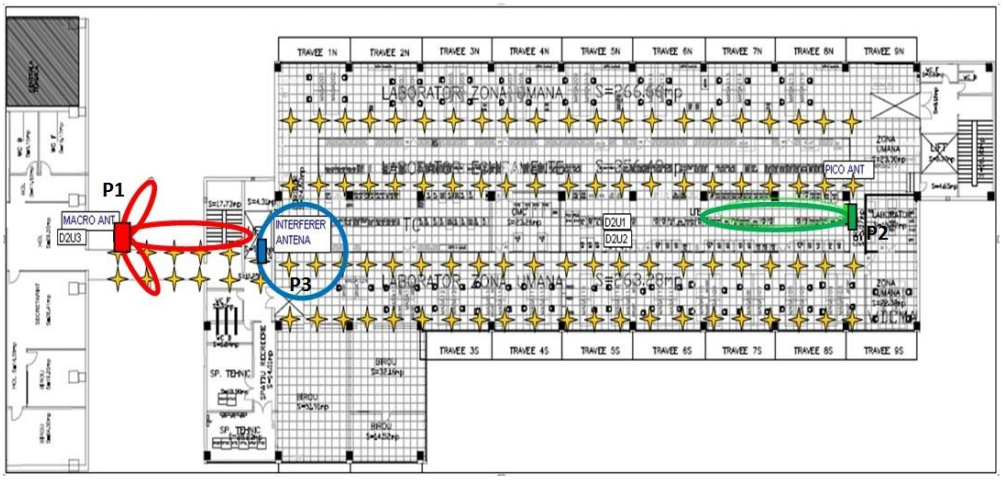

Figure 39: Building top view measurement points and cell locations. The macro cell is located at P1. The metro cell is located at P2 and interferer metro at P3

The stars in figure represent the measurement points. In every point we measure all the KPIs related to power of signal and quality of signal. Two dimensional (2D) maps visualize the variation of KPIs of interest over an entire area and help identifying potential zones of a building which need improvement in terms of coverage and data rates. The 2D maps are obtained by interpolating the KPIs collected at the measurement points shown in Figure 39. To determinate initial condition for coverage offered only by the macro eNodeB, in Figure 40 is display the DL RSRP values to highlight the building coverage obtained using a single outdoor macro eNodeB emitting in 20 MHz bandwidth on a dedicated carrier (without any interferer).

In the second scenario, on top of the existing macro cell we introduce one indoor metro cell transmitting on 10MHz adjacent bandwidth located in P2. The transmitting power for metro is 250mW. The 2D map of RSRP distribution for the second scenario is represented in Figure 41.

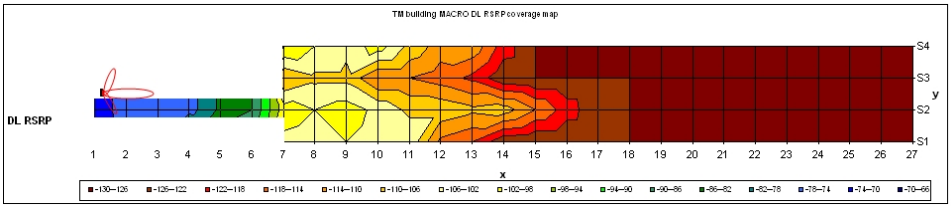

Figure 40: DL RSRP map for a single macro emitting on dedicated 20 MHz channel with 2x40W transmitting power

After coverage determination we measured an end user KPI, throughput in all three cases. Considering the poor indoor coverage in macro cell only case, for these specific scenario, the throughput was not represented due to the fact that is no service availability for more than 70% of the focus area.

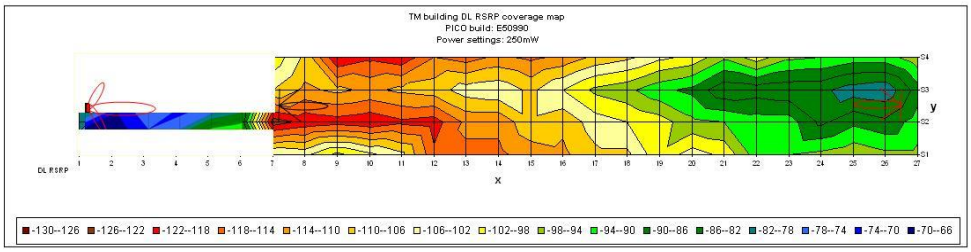

Figure 41: DL RSRP map for two eNodeBs Macro on dedicated 20MHz channel with 2x40W and metro on adjacent 10 MHz channel with 2x250 mW power

The third scenario with two eNodeBs Macro on dedicated 20MHz channel with 2x40W and metro on adjacent 10 MHz channel with 2x250 mW power is represented in Figure 42.

In Figure 43 we highlight the traffic restoration when the mobile switch to metro cell. The difference between maximum throughput on macro (~100Mbps) and metro (~60Mbps) derives from the different transmit bandwidth (20MHz and 10MHz respectively). In this scenario the mobile moves from P1 outside the building (macro coverage only) inside the building to P2, following a linear trajectory between macro and metro cells. The mobile switch the cell performing an inter-cell handover intra/inter-bandwidth.

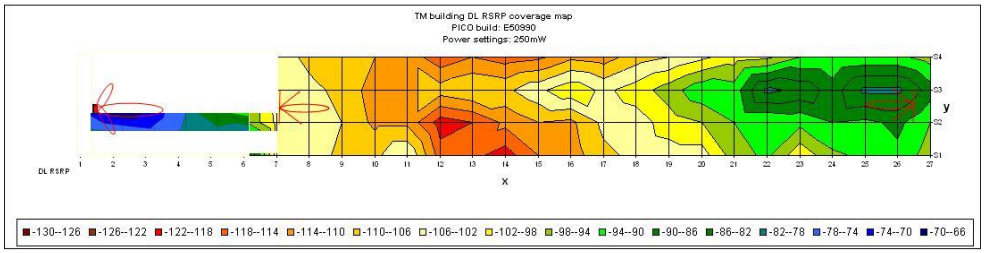

Figure 42: DL RSRP map for two eNodeBs Macro on 20MHz with 2x40W power and metro on overlapping 10 MHz channel with 2x250mW power

From Figure 40 it is evident that, in current conditions, the Macro layer didn't succeed to provide a decent signal level inside the building, that why, the network densification become mandatory to deserve indoor users. Analyzing the results obtained in Figure 41 and Figure 42, we can conclude that even using the same radio resources (overlapping bandwidth) the Metro cell located in P2 succeed to provide a good indoor coverage and service availability for target building.

In this scenario the mobile moves from P1 outside the building (macro coverage only) inside the building to P2, following a linear trajectory between macro and metro cells. The mobile switch the cell performing an inter-cell handover intra/inter-bandwidth.

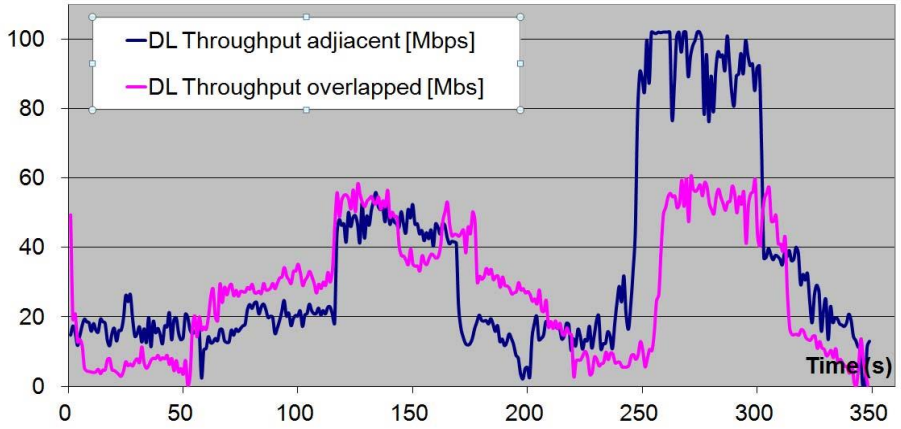

Figure 43: DL throughput for moving user

Figure 44 represents the RSRP and RSSI parameters in both cases (adjacent and overlapping bandwidth) for the same moving scenario as considered for throughput. The graphic highlights the RSRP and RSSI degradation inside the building.

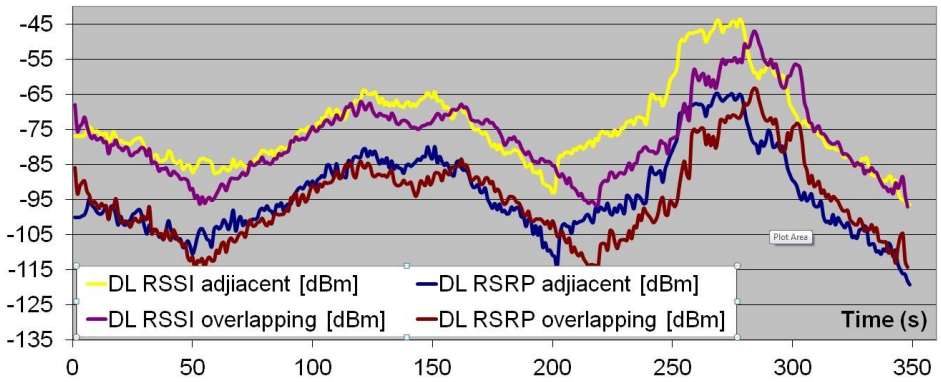

Figure 44: DL RSSI and DL RSRP for moving user

In the absence of metro cell, the degradation introduced by the building wall attenuation leads faster to service release at mobile level. Metro cell improves the RSSP and RSSI level and provide better coverage in indoor area.

3.2.3 Discussions

In this sub-chapter we presented a set of results about Heterogeneous Network field trial experiments conducted in an LTE network at 2.6 GHz and focused on coverage within an office building. This results we disseminate in paper [54].

Two LTE metro cells deployed in indoor as well as LTE macro cells deployed in outdoor are considered. The later rely on small transmission power levels combined with easiest deployment of small cells. We considered an indoor area covered by one useful metro eNodeB and one external macro eNodeB. The second metro cell eNodeB emit on the same frequency as macro cell to degrade the quality on macro layer to reach typical macro layer radio conditions in the field. Analyzing radio parameters for different configuration we highlight the benefits of using small cells to increase the indoor coverage and the end-user experience. We showed the feasibility of small cell deployments to develop LTE network, covering indoor environments, through measurements. With a single small cell employing directive antennas and using low power we were able to establish good indoor coverage delivering high data rates for large parts of an office building. In the same environment we performed a set of handover test where we highlight the capacity of metro cells to accept the mobiles coming from macro cells offering to users a continuality of services inside the buildings.

4 Heterogeneous networks improvements and optimizations

Wireless communications traffic continues to grow rapidly due to wide spread adoption of smart phones devices and the subsequent fast extension of mobile applications. To carry on the traffic, grow and in the same time to improve user experience and network coverage constant, technology innovations are required. The 3rd Generation Partnership Project (3GPP) started in 1998 plays a leading role in this area and develops a family of technologies (from GSM-EDGE up to LTE-Advanced) enabling diverse data applications and enhanced user experience [16]. The performant LTE system, based on Orthogonal Frequency Division Multiple Access (OFDMA) in downlink and Single-Carrier Frequency Division Multiple Access in uplink (SC-FDMA) with high Quality of Services (QoS) and evolved system architecture, is now faced with the challenges added by the new services: high data rates and increased user density [16]; [4]. The development efforts in LTE are oriented to increase spectrum efficiency and reduce the "price per bit". All these are reached by using edge hardware technologies and avant-garde features. HetNet architecture with the overlay of macro cells and small cells of the same air interface is a promising direction for evolution. It authorizes integration of diverse technologies and network architectures in achieving high spectrum efficiency and quality of service (QoS) [4]; [55]. The solution adopted by network operators for dense urban environments consists in combining a macro cell layer equipped with large bandwidth and high power Base Station (BS) with a second layer deploying small cells technology such as pico cells, metro cells and femto cells equipped with low power base stations. In this way the network architecture evolves to HetNet [4]; [55]; [56].

Small cells or small cellular base stations contain several different technologies but could describe them as anything other than a typical macro site. These are implemented to address network capacity issues in a relatively small area, as a hot spot or an important area that is a subset of the macro cell coverage. Small cells typically have a range from 10 meters (femto) to several hundred meters (metro) [54].

Femto cells or femtocells are small basic telecommunication stations that can be installed in residential or business environments, either as independent individual elements or in clusters to provide and/or improve cellular coverage within a building.

A picocell is a small cellular base station that usually covers a small area such as in-building (offices, shopping centers, railway stations, stock exchanges, etc.) or, more recently, in aircraft. In cellular networks picocells are typically used to extend coverage to indoor areas where outdoor signals do not go well or to add network capacity to areas with very dense phone use such as stations or stadiums. Picocells

offers coverage and capacity in hard or expensive areas using the more traditional macrocell approach [57].

Metrocells are compact and discrete mobile phone base stations, located in urban areas. They can be mounted on lampposts, positioned on the sides of buildings or found indoors in stadiums, transport hubs and other public areas. They provide excellent mobile phone service, delivering very high data speeds and capacity, solving the problem of growing data traffic demand cost effectively. These small cells are usually owned and installed by the mobile network operator themselves, who plan, manage and maintain them in the same way as their larger macrocell cousins. However, the large numbers of metrocells change the way in which the industry operates. [58]

4.1 Uplink performance improvements in LTE Heterogeneous Networks

In this sub-chapter we explore uplink connection performances in a LTE Heterogeneous Network (HetNet). Based on experiments we analyze the system performance in different LTE HetNet configurations and emphasize the advantage of small cells utilization. We perform a set of experiments in two different LTE HetNet configurations and focus on uplink coverage and capacity within an office building. The current results are obtained in single user equipment (UE) environment but the network optimization recommendations are valid also for multi-UE scenario, with or without mobility [59]. The analysis is based on two of the most important indicators for end user experience:

- UE data throughput
- UE power consumption

As we presented in chapter 3.1, a HetNet consists of a series of low-power BS (metro cells) distributed throughout the existing macro cell network. This arrangement allows improving the spectral efficiency per unit area, since low-power BS fill holes in the existing network coverage and increase the capacity in areas with high traffic volume (hotspot). In LTE HetNet arrangement there are eNodeBs (eNodeBs) with different transmission power. The high power eNodeB provides the macro cell and the low power eNodeB serve the small cells located within the coverage area of the high power eNodeB. Macro cell and most small cells are connected via S1/X2 interface and are implemented by the operator, in a planned manner.

4.1.1 Theoretical Uplink throughput computation

Depending of radio resource availability, two types of deployments can be used in HetNet: co-channel deployment and dedicated channel deployment. In a co-channel scenario, the macro cell as well as the small cells uses the same frequency band, which is an advantage if the available spectrum is limited. In this case, the main design problem is the interference management. In a dedicated (adjacent) channel deployment there is no interference between the macro and the small cells, and the

spectrum is segmented between the tiers. In a HetNet architecture the power received by the UE plays a critical role to provide a suitable SINR at the eNodeB and an acceptable level of interferences for the neighboring cells [59].

In a model with no interference management the UE receives a power according to:

Equation 6

$$P_{r,down} = P_i h_{x_i} ||x_i||^{-\alpha}$$

where P_i is the transmit power of the serving eNodeB, h_{xi} is the fading, and $\|x_i\|^{-\alpha}$ is the pathloss at distance x_i considering the pathloss exponent α.

The mobile on the first tier experiences total downlink interference, including the noise, as indicated by:

Equation 7

$$I_{down} = \sum_{x \in \Phi_1 \setminus x_i} P_1 \, h_x ||x||^{-\alpha} + \sum_{x \in \Phi_2} P_2 \, h_x ||x||^{-\alpha} + \sigma^2$$

Where Φ_1, Φ_2 refer to all the interfering eNodeB in the corresponding tier and σ^2 is the noise.

Based on Equation 6 and Equation 7 the SINR in downlink can be evaluated as:

Equation 8

$$SINR_{down} = P_j h_{x_j} \left| x_j \right|^{-\alpha} / I_{down}$$

Due to traffic asymmetry, downlink transmission is critical and is extensive considered in literature [54]; [56]. Uplink traffic analysis is important in different applications that require symmetric traffic such as real-time video calls. On the other hand, uplink traffic problem is even more important due to LTE standard specifications that introduce an asymmetric traffic rate. In uplink we consider for each UE the same nominal transmit power P_j, weighted with the inverse of pathloss $\|x_j\|^{\alpha\varepsilon}$.

The eNodeB receives the signal transmitted by the j_{th} UE located at distance x_j :

Equation 9

$$P_{r,up} = P_j g_{x_j} ||x_j||^{\alpha\varepsilon} ||x_j||^{-\alpha} = P_j g_{x_j} ||x_j||^{\alpha(\varepsilon-1)}$$

Where g represents the uplink fading and $\varepsilon \in [0, 1]$ is the fractional power control factor [53].

The total interference plus noise in uplink can be expressed as:

Equation 10

$$I_{up} = \sum_{y \in Y} x^{\alpha\varepsilon} g_y y_y{}^{-\alpha} + \sigma^2$$

where x generically refers the distance between the interfering UE and their serving eNodeB, and y is the distance between the same UE and the interfered eNodeB [59].

The SINR in uplink can be evaluated as:

Equation 11

$$SINR_{up} = P_j g_{x_j} ||x_j||^{-\alpha(\varepsilon-1)} / I_{up}$$

The data rate in bps/Hz defined by Equation 12 is another important parameter for practical applications:

Equation 12

$$R_{down,up} = \log(1 + SINR_{down,up})$$

This parameter is computed in the next section and confirms the accuracy of experimental results regarding the spectral efficiency in the trial network.

4.1.2 Trial network and experimental results

The study is focused on the UL performance analysis in a Heterogeneous Network and compares the network behavior in two different spectrum allocation configurations. The advantage of small cells utilization from UL performance perspectives is highlighted. The experiments are conducted in a LTE FDD system emitting in band 7 (2600 MHz) that illustrate a LTE HetNet. For test bench we use 3 eNodeBs: two useful eNodeBs are considered: one macro cell and one metro cell and a third metro eNodeB is used as interferer in order to emulate real field conditions.

The measurement area is a small office building (66m×24m) with three floors and large rooms as showed in Figure 45. A detailed presentation of the focus area was made in Chapter 3.1.1. It has an open floor plan with lot of furniture and equipment on the hallways. To this building compared to other office buildings is the increased level of interference and multipath signal propagation resulted from high density concrete walls and multiple metallic equipment racks distributed throughout it [59].

The measurements are performed on the middle floor of this building at an average pedestrian speed of 5 km/h and at an average UE height of 1.5 m while crossing the main hallway from West to East [60].

The UE route is indicated in Figure 45 with dotted line starting with a circle marked point and ending with a triangle marked point. For experiments and analysis, the focus area is covered with signal from the macro eNodeB placed outdoor, as first tier of the network, in conjunction with a metro eNodeB placed indoor, as a second tier. In our experiments we also introduce an interferer metro eNodeB that uses the same bandwidth as macro eNodeB to corrupt the quality on macro tier and to achieve typical radio conditions meet in the field.

Using this configuration is relatively easy to highlight the UE behavior when indoor environment meets better signal quality in comparison with serving macro eNodeB. Basically, the network asks UE to perform inter-frequency handover (HO) between macro eNodeB (stronger signal but lower quality) and metro eNodeB (indoor power settings so lower signal but good radio quality).

The macro eNodeB is mounted in building proximity in location named P1 as can be seen in Figure 45. The useful metro eNodeB is located in P2 and its main beam has opposite orientation to the macro eNodeB. The metro interferer is located nearby macro cell in P3 and has the same orientation.

The stars in Figure 45 indicate the measurement points. In every point we measure pathloss, uplink SINR, UETx power, and throughput meaning the Key Performance Indicators (KPIs) related to power and quality of the signal [54].

In order to collect the wanted parameters, we use a prototype Qualcomm LTE device customized for R&D activities, in conjunction with a decoding tool, called Sherpa [61].

Based on the variation of KPIs of interest over the entire area we can identify potential zones of the building that need improvement in terms of coverage and data rates [54]; [31].

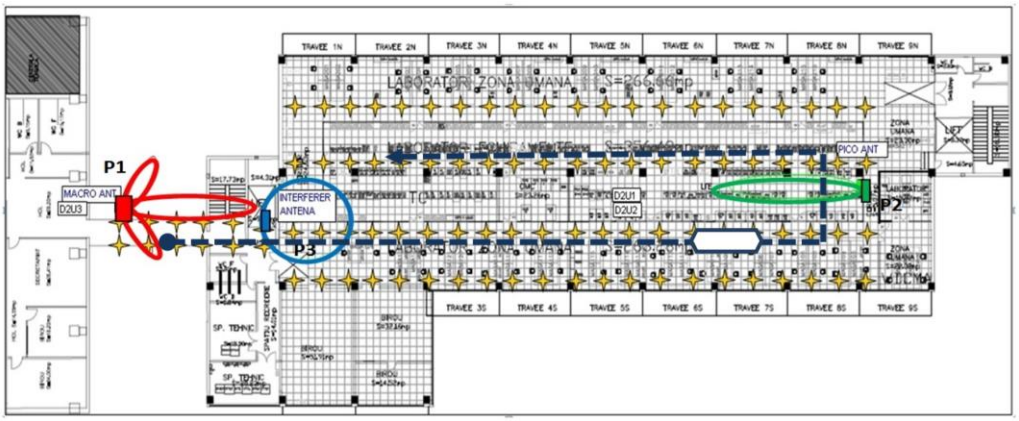

Figure 45: Building top view measurement points and cell locations

For experiments the available bandwidth of the HetNet is 20 MHz There are 2 ways to allocate the available bandwidth:

- The total bandwidth is shared equally by the useful eNodeB: macro cell uses 10 MHz bandwidth and metro cell uses the remaining adjacent 10 MHz bandwidth;
- The macro cell uses entirely 20 MHz bandwidth and the metro cell uses 10 MHz from the total of 20 MHz in an overlapping bandwidth allocation (the upper 10MHz bandwidth is used by both eNodeBs).

We compared the two cases to analyze the pros and cons for sharing the same bandwidth.

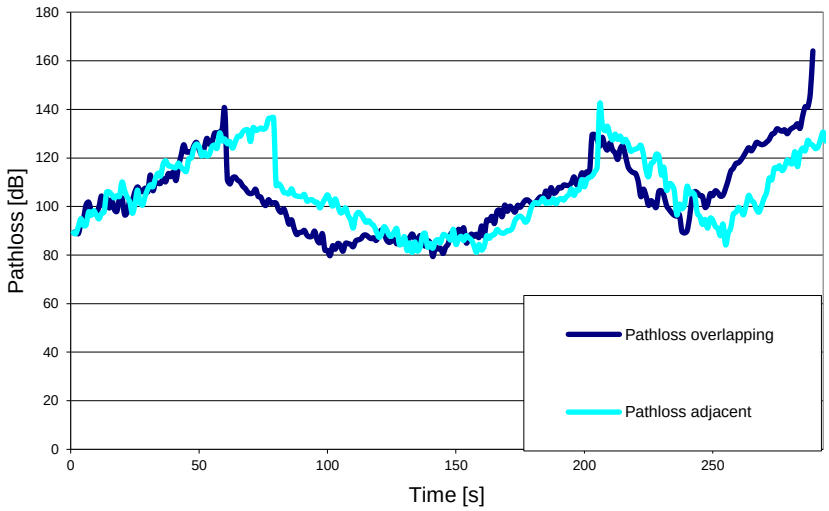

Figure 46: Uplink pathloss for adjacent and overlapping bandwidth

In Figure 46 is shown the UL pathloss for a mobile moving from outside the building, under macro coverage, inside the building, under metro coverage, and back as drawn with dotted line in Figure 45. The pathloss values presented in Figure 46 are computed at eNodeB side using the measured UL RSSI and the UE transmit power reported by UE through power headroom report. These values are used to set target SINR.

Power headroom report also indicates the power budget of UE. In other words, it is the difference between the UE transmit power and the maximum UE transmit power [62]. Analyzing the curves in Figure 46 we observe that the pathloss increases slowly when using overlapping bandwidth allocation in the area where the influence of interferer eNodeB is consistent (before timestamp 50 and after 250), what was expecting due to the higher interferences.

Between the two charts there is a slight slip that is due to the different moments of triggering the handover, the handover is triggered earlier in case of overlapping allocation.

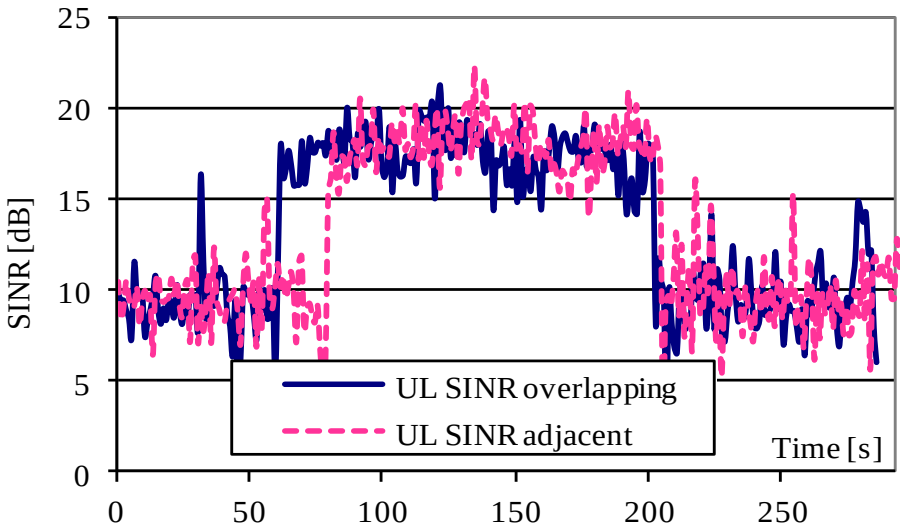

Figure 47: Uplink SINR for adjacent and overlapping bandwidth

The uplink SINR (SINRup) in both cases is depicted Figure 47. What is surprising in these results is the fact that on metro cell the SINRup is bigger even when the used bandwidth is overlapping. We can adopt overlapping bandwidth on HeTNet equipment's that transmit in the same geographical area, sharing the same radio resources. For a larger area we can go forward with this approach considering for macro a 20 MHz bandwidth and two overlapping metro, using each 10 MHz adjacent bands.

In order to increase the efficiency of spectrum utilization, the LTE system is designed to work properly even with frequency reuse factor 1 when data and control

channels become more sensitive to inter-cell interference, that limits cell edge performance and cell capacity.

Therefore, Power control mechanism plays a critical role to provide a suitable SINR at the eNodeB and an acceptable level of interferences for the neighboring cells [62].

In a homogeneous LTE network with reuse factor 1, at the cell edge the interference level is high requesting a more robust modulation and coding, leading to a lower throughput and poor end-user experience. This drawback is mitigated by HetNet architecture as our experimental results prove.

The UE power consumption has two main components: the power required for data processing and the power used on radio part as transmit power. Figure 48 shows how UE transmit power is reduced when the mobile switch to metro cell. This aspect represents a major advantage of using HetNet.

From the user point of view, the power consumption is another critical parameter. Today the smartphones producers and mobile operators attempt to reach as much as possible the market share by satisfying the end user needs: high data rates and UE power consumption.

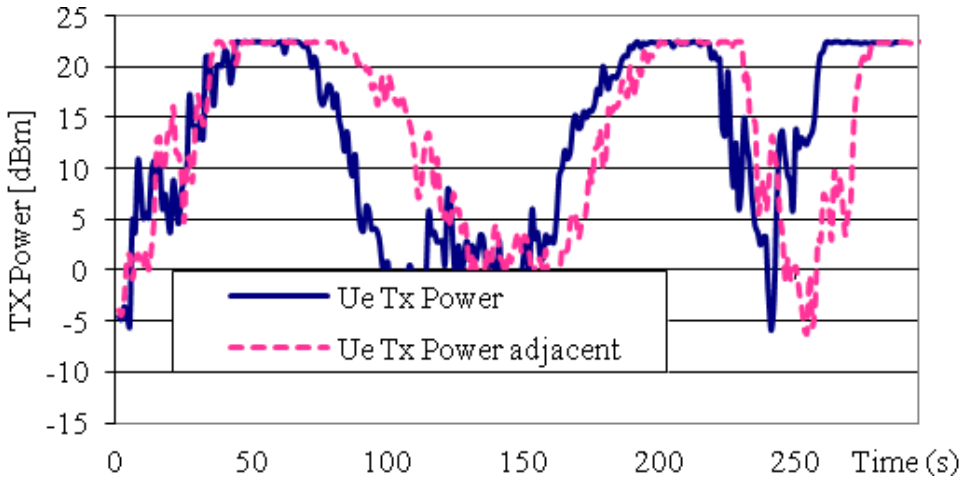

Figure 48: UE transmit power

For the two analyzed scenarios the firs HO is triggered around timestamp 60 for overlapping and around 70 for adjacent. After these times, when mobile switch to Metro cell, the Tx power will drop, which will have the effect of reducing uplink interference and power consumption by the mobile station. For cells with small radius, the power budget in uplink and downlink is almost equal, since UE is located all the time in proximity of eNodeB and transmits with reduced power.

All the aspects and benefits exposed before are relevant for network optimization, but the decisive indicator is the end user experience expressed by

throughput as shown in Figure 49. The red line graph corresponds to the computed throughput based on measured uplink SINR values using Equation 12.

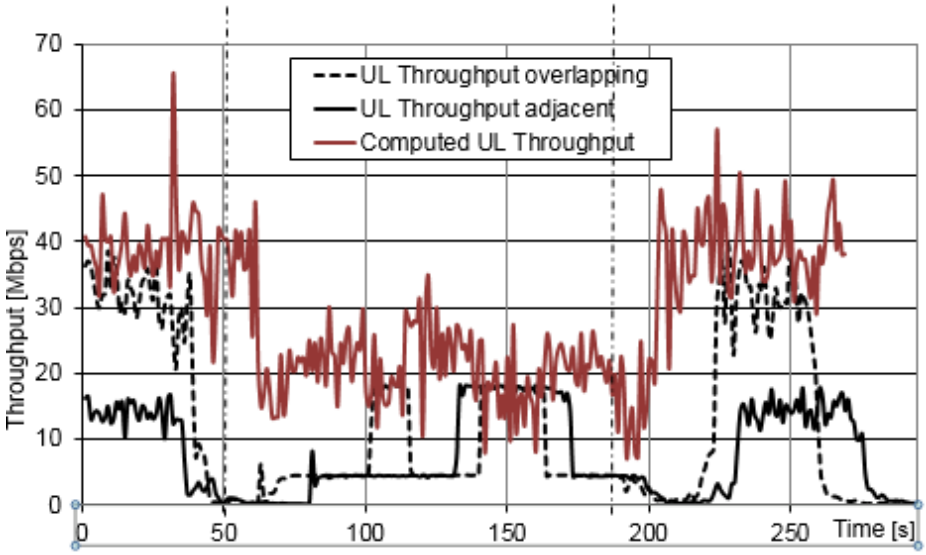

Figure 49: Uplink throughput for adjacent and overlapping bandwidth

The experimental results suggest that a network densification using small cells technology is highly recommended for indoor coverage. Additionally, the small cell eNodeB is suitable for network densification in small areas with high user density.

In Figure 49 the traffic gap between the 120th and the 140th seconds is generated by a handover event. During that time the UE passes a "blind" area marked with a white hexagon in Figure 45. In this area the UE switches back to macro eNodeB for a short period of time due to a higher signal level (RSSI) even if the signal quality RSRQ is better on metro cell.

This specific behavior claims to be analyzed in future studies based on different test scenarios where the RSRQ will act as a main handover trigger in HetNet. In Figure 49 we also compare the measured throughput with the calculated one according to Equation 9. The uplink SINR values in Equation 9 are measured and reported by the UE during the experiments. The measured values match the computed values for both macro and small cells. The differences around the handover events in Figure 49 are due to the fact that handover is triggered by RSRP.

The experimental results suggest that a network densification using small cells technology is highly recommended for indoor coverage. Additionally, the small cell eNodeB is suitable for network densification in small areas with high user density. The reported measurements were done without activating DL enhanced Inter Cell Interference Coordination (eICIC) feature in the experimental network due to low number of small cells in the cluster, but activating maximal ratio combining (MRC) algorithm in UL. An extensive analysis regarding the eICIC opportunity is given in [57], where is proved that the cluster capacity gain increases proportionally with the

number of small cells in the cluster. Each experiment presented in this paper was iterated at least 50 times and the results were averaged.

4.2 HetNet Handover optimization using RSRQ as trigger

The edge features offered by the modern terminals such as smart phones and tablets, challenge the network operators to provide new services and network capabilities to support the corresponding data traffic. The video streaming, the on-line games and the social networks are the main data rate intensive applications that represent a constant challenge for mobile operators [63].

The LTE system based on Orthogonal Frequency Division Multiple Access (OFDMA) in downlink and Single-Carrier Orthogonal Frequency Division Multiple Access in uplink (SC-OFDMA) with high Quality of Services (QoS) and evolved system architecture is now confronted with the requirements introduced by the new services: high data rates and increased user density [64].

A HetNet consists of a series of low-power BS distributed throughout the existing macro cell network. This arrangement of multiple tiers (layers) of networks of different cell sizes allows improving the spectral efficiency per unit area, as the low-power BS make possible to fill coverage holes in the macro only network and increase the capacity in areas with high traffic volume [55]; [65].

LTE system handover (HO) procedure is based on UE measurements and reports regarding the downlink signal level and quality. These reports are sent periodically or when triggered by an event to the serving BS – eNodeB (eNodeB) in LTE technology [66]; [67]. In HetNet architecture a moving UE has to perform more handovers due to the high number of small cells. The measured parameters defined by 3GPP specifications that could be used are: Reference Signal Received Power (RSRP), Received Signal Strength Indicator (RSSI) and Reference Signal Received Quality (RSRQ) [66].

The parameter used in HO procedure in LTE is usually RSRP, but different practical scenarios, especially in HetNet, suggest that HO based on RSRQ is a better solution. When we consider as trigger the RSRQ, basically we just rely on the quality of connection (in a high interference environment, the power of reference signal received it's misleading, and can give us a false information about the connection itself). In HetNet co-channel and/or adjacent channel interference might cause poor downlink quality although the signal level and RSRP are still good. In this situation RSRQ based HO can trigger a handover to prevent service degradation [68].

The purpose of this thesis section is to investigate the HO procedure in a HetNet environment based on RSRP and RSRQ triggers. The focus point of our analysis is the improvement of user experience measured by two highly critical factors: throughput and UE power consumption.

All the measurements are performed in a cabled environment. We emulate HO procedure using high precision multipath variable attenuators [69]. The attenuation is modified using a command script develop by us, and dynamic set in such a manner to correspond to a movement speed of 5 km/h for the user (we chose this speed due to pedestrian mobility specific to indoor environments).

4.2.1 Handover procedure

User mobility in LTE is ensured using UE-assisted HO procedure [64]. The UE reports measurement information for a set of cells consisting in serving cell and active cells set, according to the measurement configuration as provided by the network by means of dedicated signaling messages [65].

A cell is included in the active cell set if the measured cell received level exceeds a given threshold. Cell ranking according to received level is used for cell selection/reselection and for handover procedure. Before the UE can add a cell to the active cell set and to perform a measurement, the target cell must be identified using synchronizations signals (primary and secondary synchronization signals). The UE can be requested to perform the following types of measurements: intra-frequency measurements (measurements at the downlink carrier frequency of the serving cell); inter-frequency measurements (measurements at frequencies that differ from any of the downlink carrier frequencies of the serving cell); inter-Radio Access Technology (RAT) measurements for inter-system handover. For some measurements the UE does require measurement gaps accorded by the network.

The UE and the eNodeB execute physical layer measurements of the radio parameters according to the 3GPP specifications and the results are reported to the higher layers and are used for a variety of purposes including intra- and inter-frequency handover, inter-RAT handover, timing measurements, and other purposes in support of Radio Resources Management (RRM) [66].

The reported F_n values are obtained by filtering several last individual measured values according to:

Equation 13

$$F_n = (1 - \alpha) * F_{n-1} + \alpha * M_n$$

Where M_n is the last measured value, F_{n-1} is the old filtered result, $a=1/2^{k/4}$, and k is the filter coefficient provided by the network [67].

According to 3GPP standard [67] a handover can be triggered by the following events:

- Event A1 (Serving becomes better than threshold)
- Event A2 (Serving becomes worse than threshold)
- Event A3 (Neighbor becomes offset better than PCell)
- Event A4 (Neighbor becomes better than threshold)
- Event A5 (PCell becomes worse than threshold1 and neighbor becomes better than threshold2)
- Event A6 (Neighbor becomes offset better than SCell)

PCell and SCell denotes primary and secondary serving cell for UE supporting carrier aggregation (CA), i.e. use one or more SCells, aggregated with the PCell, for increased bandwidth. Similar events denoted B1 and B2 are defined for inter RAT handover.

The reference signal received power used for handover procedure is defined as the linear average over the power contributions in [W] of the resource elements

carrying cell-specific reference signals within the considered measurement frequency bandwidth. For RSRP measurement the cell-specific reference signal R0 shall be used [70]. If the UE can detect that cell-specific reference signal R1 is available, it may use R1 in addition to R0 to find out RSRP. It is not necessary for the UE to measure every Resource Symbol on the relevant subcarriers.

RSRP can be expressed as:

Equation 14

$$RSRP = \frac{1}{K}\sum_{k=0}^{K}(\frac{1}{M}\sum_{m=0}^{M}P(k,m))$$

where *P (k,m)* represents the signal power of the Resource Element (RE) *m* of the Resource Block (RB) *k*, *K* is the total number of RB and *M* is the number of RE that transport reference signal in a RB. RSRP formula can be simplified considering a flat channel for each RB, i.e. all RE within a RB have the same power.

Absolute RSRP value is essential information about the strength of cells and allows the UE to estimate the pathloss that can be used in the appropriate algorithms for computing the optimum power settings for both UE and eNodeB. RSRP is used both in idle and connected states. The relative RSRP for different cells is used as a parameter in multi-cell scenarios, including HO procedures [67].

Although RSRP is an important measure, RSRP alone gives no indication of signal quality. Reference signal received quality parameter provides this measure. Measuring RSRQ becomes particularly important near the cell edge when decisions need to be made, regardless of absolute RSRP, to perform a handover to the next cell and is used during connected states [68].

Reference signal received quality is defined based on the measured RSRP as:

Equation 15

$$RSRQ = \frac{N * RSRP}{RSSI}$$

where *N* is the total number of the RB over the entire bandwidth. The measurements for RSRQ shall be made over the same set of RBs.

Received Signal Strength Indicator (RSSI) in Equation 15 comprises the linear average of the total received power in [W] measured only in OFDM symbols containing reference symbols for antenna port 0, in the measurement bandwidth, over *N* number of resource blocks from all sources, including co-channel serving and neighboring cells, adjacent channel interference, thermal noise etc. If higher-layer signaling indicates certain Subframes for performing RSRQ measurements, then RSSI is measured over all OFDM symbols in the indicated Subframes [33].

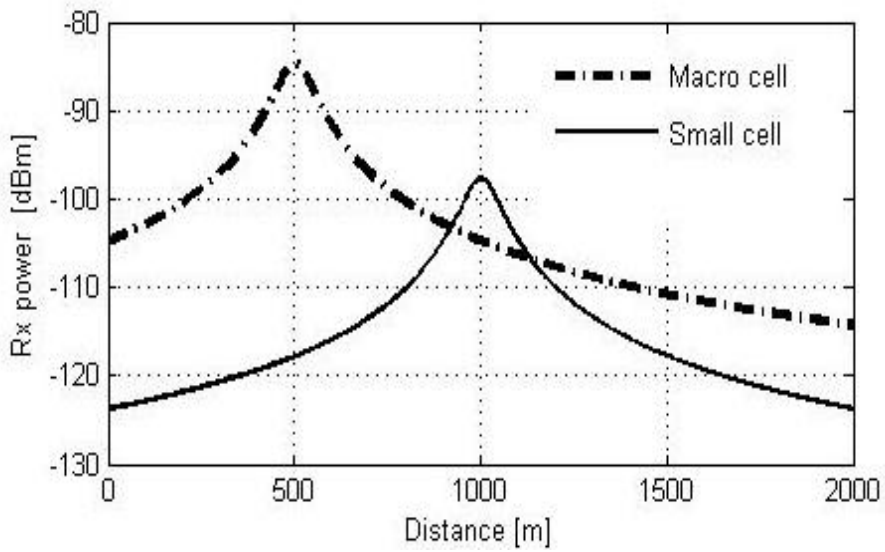

Figure 50: Received power for macro and small cells

The reference point for the RSRP and RSRQ shall be the antenna port of the UE. Figure 50 shows the received signal power for a simple HetNet configuration consisting in one macro cell and one small cell. For all the measurements we rely on measurements reported by the real mobile station, and on channel estimations made by the LTE base-station. In the previous figure, it can be seen that for small cell inbound and outbound mobility, handover will be demanding due to rapid change of small cell signal.

4.2.2 Experiments and results

For the experiments reported in this section we use a HetNet LTE cabled test bench. The RF configuration is complex and involves several components creating a controllable environment. In the test scenario two eNodeB are considered: one macro and one small cell eNodeB both transmitting in 1900 MHz (B2 band) each using adjacent 10 MHz bandwidth of the total 20 MHz bandwidth.

We develop this test bench according to Figure 51 trying to emulate a real dense urban environment, with a macro cell placed outdoor as an umbrella cell affected by AWGN noise and fading added by a channel emulator, and a small cell placed inside the building [54]. To add impairments for the macro, cell the uplink and downlink signals are separated using circulators/duplexers and splitters/combiners how can be seen in Figure 51.

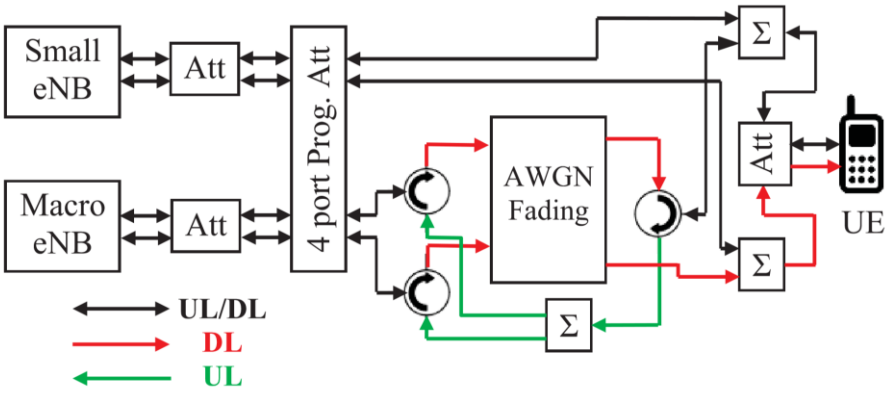

Figure 51: Experimental cabled test bench

The radio conditions are dynamically modified using programmable attenuators (Att) that simulates the movement of UE from outdoor to indoor and back. The attenuation step and speed are selected to simulate a UE movement speed of 5 km/h corresponding to a pedestrian model. The eNodeB are customized as in a real network from transmit power point of view. To become suitable for cable environment we add additional fix attenuation at antenna ports: 40 dB attenuator per each macro antenna port and 20 dB attenuator per each small cell antenna port. The UE used in experiments is a Qualcomm 9630 Engineering UE – CAT4 mobile device placed in a shielded box in order to avoid any uncontrolled noise or interference from mobile commercial networks. When the UE goes into the building, significant macro cell signal degradation occurs, and a HO procedure is triggered.

The test scenario is according to Table 2. In our experiments we consider for HO trigger only the A3 event as a good balanced between analyze complexity and available information usage.

Event A3 presentation: Neighbor becomes amount of offset better than serving

First of all, the user equipment uses either RSRP or RSRQ measurements to determine whether to enter the EventA3 condition. The triggerQuantityA3 parameter is used to configure whether RSRP or RSRQ values are used to trigger EventA3 [12].

Measurements of RSRP and RSRQ are performed on the serving and detected neighboring cells. The measured values of RSRP and RSRQ can then be filtered based upon the settings of the parameter filterCoefficientEUtraRsrp and filterCoefficientEUtraRsrq parameters. The filter averages a number of measurements in order to filter out the impact of large scale fast fading.

The user equipment then uses an offset value, a3offset, and a hysteresis value, hysteresisA3, to determine whether to trigger the EventA3. Non default offset relationships use the value cellIndividualOffsetEUtran instead of a3offset for the particular cell relationship.

The formula used by the user equipment for evaluating entry to EventA3 is shown below:

Equation 16

$$Mn - HysteresisA3 > Ms + a3offset$$

Where,

Mn = measured value of the neighboring cell (either RSRP or RSRQ)

Ms = measured value of the serving cell (either RSRP or RSRQ)

Once EventA3 is triggered, the user equipment will wait a predetermined time (timeToTriggerA3) before it commences sending measurement reports to the serving RBS. These measurement reports contain measurements for the serving cells and up to three detected intra frequency neighbor cells. The reportQuantityA3 parameter indicates whether RSRP or RSRQ measurements, or both, are to be included in the measurement reports.

Measurement reports are sent periodically whilst the EventA3 condition is active. The parameter reportIntervalA3 determines the time interval between measurement reports. The parameter reportAmountA3 indicates how many reports to send; a value of 0 indicates that the reports should be sent indefinitely whilst the EventA3 condition is active [12].

The user equipment uses the same offset and hysteresis values to determine when to leave EventA3 when the serving cell improves in RSRP or RSRQ relative to the neighboring cells. The formula used by the UE is shown below:

Equation 17

$$Mn + HysteresisA3 < Ms + a3offset$$

Table 2 Simulation Scenario

Parameter	**Macro eNodeB**	**Small cell eNodeB**
Carrier frequency	1900 MHz	1900 MHz
Bandwidth	10 MHz	10 MHz
Transmit power	40 W/46 dBm	2 W/33 dBm
HO event	A3	A3
HO trigger	RSRP/RSRQ	RSRP/RSRQ
HO time-to-trigger	40 ms	40 ms
Environment	outdoor	indoor

In order to prepare the tests, we perform the test bench setup, configuring the eNodeBs based on the parameters showed in the Table 2. Initially the entire ensemble is calibrated and the automated scripts for attenuation command are developed in a way that allows repeating the experiment using different HO events and different HO triggers in the same radio condition. For each iteration of the test, the UE is attached to the macro eNodeB in the same good radio condition, the UL and DL traffic is started followed by the movement emulation (outdoor to indoor and back)

until UE performs HO on small cell and back to macro cell. In order to emulate the movement, we modify the attenuation on both eNodeB with a granularity of 0.5 dB.

During the HO scenario simulation, the macro eNodeB starts from good radio condition, expressed by an initial value for pathloss of about 110 dB, computed according to macro eNodeB transmit power. The pathloss for macro eNodeB linearly increases in order to emulate the UE movement from the macro eNodeB toward the small cell. The metro cell starts in the experiment in bad radio condition, with an initial pathloss according to the eNodeB transmit power. The pathloss for metro cell decreases to emulate the UE movement. After the first HO the UE remains connected to the small cell for approximately 60 second and after that UE starts to move back to macro cell through HO procedure.

HO parameters are set according to Table 3. For each experiment we collect the traces from UE side and plot the most relevant information.

Each experiment was run using both triggers RSRQ and RSRP and the focus was on the throughput performance in different cases. In both graphics the HO moment is marked by black stars.

In the first experimental scenario the macro to small cell HO is triggered almost in the same time independently what trigger is used: RSRP or RSRQ. The measured downlink throughput during the HO according to the first scenario is show in Figure 52. The 3 dB threshold for RSRP is a relatively small value and is suitable only for clean environment, without multipath propagation and noise. In a dense urban environment, the macro cell is affected by multipath propagation, fading and noise and the RSRP can easily fluctuates with more than 3 dB on a short distance. This fact produces a ping–pong effect and the UE performs repetitive HO between eNodeB very fast in an unproductive way.

In order to avoid the ping–pong behavior we need to increase the RSRP offset or to add hysteresis margin. The tests using new values for HO offset and hysteresis according to experimental scenario 2 show a significant improvement in case of RSRQ threshold usage. Due to the low dynamic of RSRQ we can keep a small threshold for this parameter.

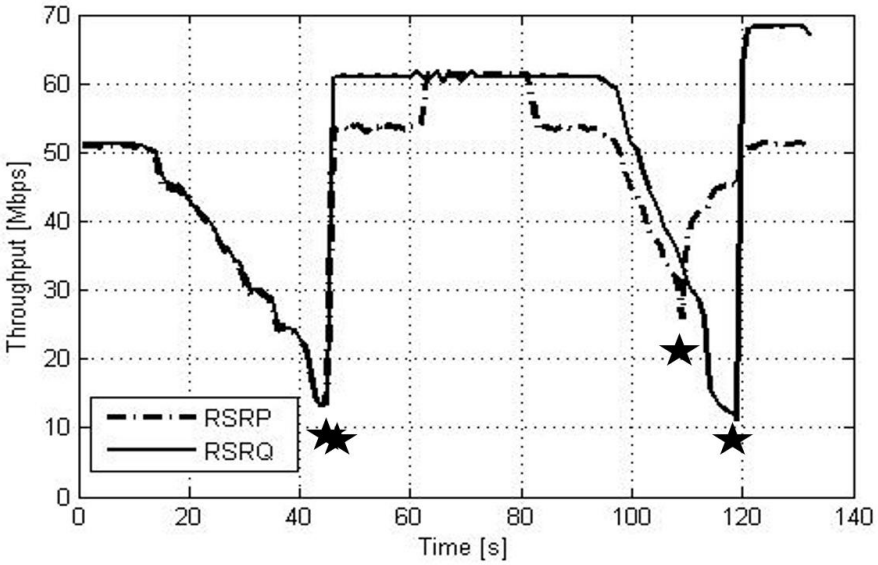

Figure 52: Handover – Scenario 1

Downlink throughput for scenario 2 is illustrated in Figure 53. Throughput evolution around HO event reveals that for a period of few seconds RSRQ triggered HO performs better, and the throughput difference achieves about 20 Mbps. Indeed, the duration is not long, but essentially is the moment when it happens: around HO point.

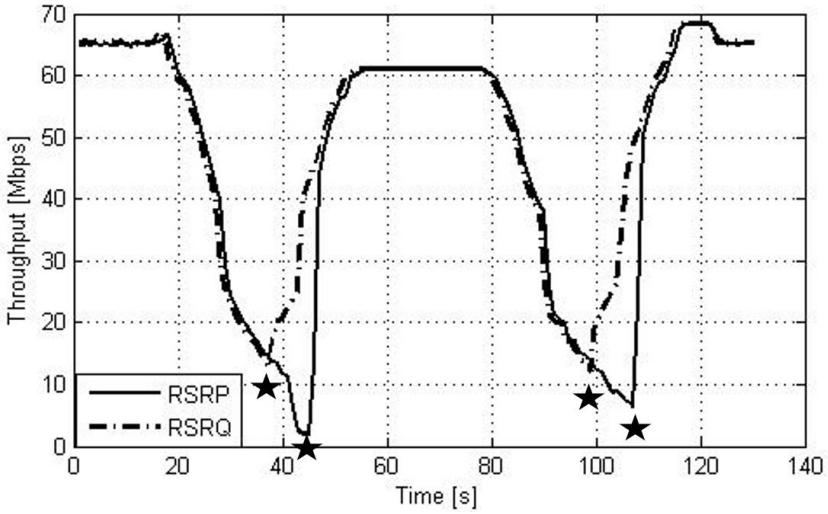

Figure 53: Handover – Scenario 2

In the dense urban environment, a significant part of the services requires a guaranteed bit rate and the network Key Performance Indicators (KPI) are very demanding for real time services.

Table 3 Handover Parameters

Parameter	Scenario 1	Scenario 2
EventA3Offset RSRP	3	4
Hysteresis RSRP	0	3
EventA3Offset RSRQ	1	1
Hysteresis RSRQ	0	0
HO triggers	RSRQ/RSRP	RSRQ/RSRP

In Figure 54 it is shown that RSRQ trigger for HO in a HetNet scenario leads to transmit power reduction for UE. Mobile devices obtain the energy required for their operation from batteries. The modern smart phones integrate various functionalities as voice communication, audio and video playback, web browsing, short-message and email communication, media downloads, gaming and more. These new functions increase the pressure on battery lifetime, and deepen the need for effective energy management.

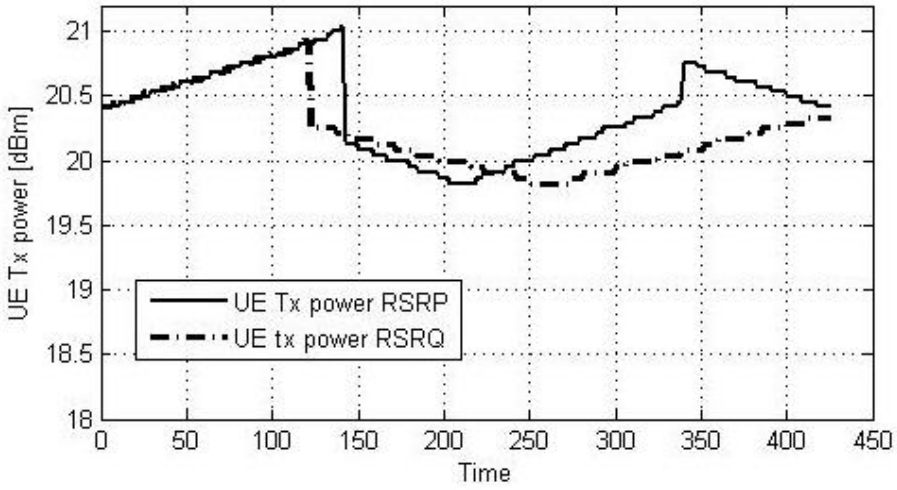

Figure 54: UE Tx power for RSRP and RSRQ triggered HO

According to literature a significant part of the total energy consumption of the UE is used by RF module. The main component of power consumption is RF transmit power [71]; [72]. Reducing Tx power improves the power budget, increases significantly the UE autonomy reducing in the same time the interference level produced by UE and the radiation exposure of the users.

4.2.3 Discussions

In LTE networks handover performance are of high importance. In this chapter are presented the results obtained during several handover experiments in LTE HetNet considering for handover trigger the A3 event and different parameters: RSSP and RSRQ. We also provide some recommendation for parameter tuning for different scenarios. All the measurements are performed in a cabled environment under the conditions characteristic for dense urban settings. Our results show the improvement of two important indicators for end user experience: data throughput and User Equipment (UE) power consumption. [73]

Analyzing the results, we can assert that the widespread use of RSRP as a handover trigger, even in the indoor environment, results in a much diminished transfer rate for moving mobiles that pass from a macro cell to a cell metro. For several iterations of the experiment, using different power settings (at list 50 iterations for each configuration), we obtained similar results, that allow us to generalize the recommendation of using the RSRQ as HO trigger for HetNet environment, with the observation that an individual analysis and optimization of handover parameters for each indoor environment is needed.

The propagation model and the test environment on which these experiments were run are characteristic for a dense urban environment. Although it requires more parameter tuning and involves more effort in network optimization phase, the RSRQ trigger HO procedure shows a great potential due to the end user throughput improvement and the increasing of spectral efficiency.

Additional to the throughput improvement the reduction of power consumption is another important factor which improves the overall user experience.

4.3 Interference effect mitigation in Heterogeneous Networks

The increased demand for mobile broadband services with higher data rates recently became a challenge for the mobile telecommunications networks. Researches dedicated to increase the capacity and data rates in parallel has lead the spectral efficiency (bps/Hz) to reach a value close to the theoretical limits as implied by the Shannon's bound. Since the radio link spectral efficiency approached its fundamental limits researches address new network techniques which suggest transforming the conventional homogeneous network topology into multi-tier architecture- HetNet [74].

Integrated in the LTE – Advanced standard heterogeneous networks refer the limitations implied by channel capacity to transport information by improving the spectral efficiency per unit area and provide a uniform broadband experience to users irrespective of their location in the network [67].

A HetNet consists of a set of Base Stations (BSs), also called eNodeBs in LTE, of different sizes and transmit powers distributed throughout the network in a roughly planned manner. The system involves the co-existence of a wide range of cell sizes ranging from Macro Cells (MC) to Small Cells (SC). This arrangement of multiple tiers of networks of different cell sizes allows improving the spectral efficiency per unit

area, as the low-power BS make possible to fill coverage holes in the macro only network and increase the capacity in areas with high traffic volume [67].

The heterogeneous architecture also introduces several concerns regarding the complicate cell access and mobility procedures. Besides, incorporation and co-existence of macro and small cells introduce several new interference scenarios which can degrade the overall system performance.

The new architecture also shows some impairment:

- The high level of interferences at the edge of SC;
- Inefficient resources utilization inside SC due to the reduced number of User Equipment's (UEs) connected to SC compared to MC.

In LTE Rel-10, 3GPP introduces two approaches to coordinate inter-layer interferences in HetNet deployment scenarios [67].

In one approach, interferences avoidance is addressed by means of Inter Cell Interference Coordination (ICIC) in frequency domain and relies on carrier-aggregation (CA) technique. In the other approach, interferences avoidance and inefficient resources utilization inside SC are addressed by means of ICIC in time domain. The eICIC new technique overcomes these two problems by extending the SC radius by adding the so called Cell Range Extension (CRE) and by reserving for this area a part of MC resources through Almost Blank Subframes (ABS) approach [75]; [76].

4.3.1 eICIC in LTE

The eICIC concept was developed in order to reduce the interferences in a HetNet clusters operating with reuse factor 1. The cluster assures LTE services for a specific geographical area and consists of one Macro cell and several small cells. These small cells are used for densification and capacity increase. There are two mechanisms that are activated in the network when the eICIC is implemented, that are presented in **Error! Reference source not found. Error! Reference source not found.**. [77] ; [78]On the small cells side the cell coverage is extended using CRE to allow macro layer decongestion and more efficient resources utilization in SC. The extension is made by adding a handover offset parameter *p* to the SC reference signal received power (RSRP) that triggers handover for UE located nearby SC edge area preferentially toward the SC even when it is not the strongest cell [57]; [79] Although CRE enables higher user offloading from MC on to SC, the UE connected to SC with large CRE offset can suffer severe interference from the MC. In the CRE area the received signal power from MC is higher than the received signal from SC. On the Macro cell side the resources allocation algorithm is modified in order to reserve a percentage of the radio resources for SC [57] [80].

This resources reservation is called ABS and according to standard can be between 0-70% from total amount of MS radio resources. In this way MC creates protected sub-frames for SC by turning off its downlink transmission (or just reducing the power of some downlink signals) in certain sub-frames. [81] The information regarding ABS sub-frames are known a priori at all SC in the cluster via X2 interface. Consequently, these resources can be used by all small cells inside the cluster, in

order to avoid the interferences and to extend the initial coverage area for each small cell. During ABS sub-frames, the MC does not transmit UE data (Physical Dedicated Control/Data Channels PDCCH/PDSCH) but may transmit cell reference signals (CRS), control channels, as well as broadcast and paging information to ensures legacy UE support. [82] In Figure 55 we show a typical HetNet cluster in a dense urban area. Before eICIC activation, the users from the dotted area are served by Macro cell and they have poor signal quality due to high level of interferences [57].

After eICIC activation the small cells radius is proportionally increased with the offset parameter, drown in Figure 55 as dotted rings. Small cells eNodeBs will allocate reserved resources for users located in dotted zones. The same resources will be reused by every small cell from the cluster; as consequence the overall end user throughput per cluster is increased proportionally by the number of small cells from the cluster [80].

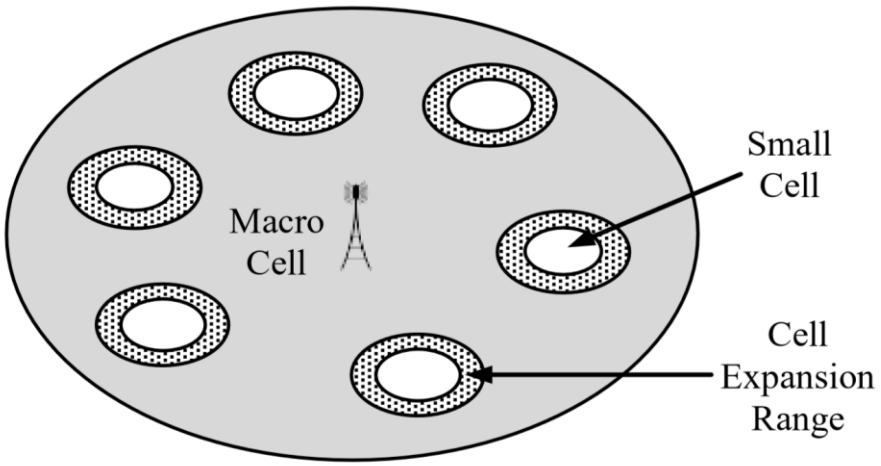

Figure 55: HetNet cluster using CRE

The small cell limit corresponds to the handover trigger point, where is satisfied the handover condition expressed as follows:

Equation 18

$$R_{MC} > R_{SC} + HOM + O_{CRE}$$

where R_{MC} and R_{SC} are the RSRP value for macro and small cell respectively, *HOM* is the handover margin and O_{CRE} is the offset that determine the CRE area.

Figure 56 shows the received power from small cell and macro cell and the CRE area for a given offset according to Equation 18

The benefits of eICIC feature can be summarized below:

• Increase the spectral efficiency by reducing the level of interferences in the most affected areas (at the border of small cells). This gain is evident even when the cluster consists of a single small cell;

• Increase the overall cluster throughput. This increase is mostly visible in networks consisting of a reduced number of small cells.

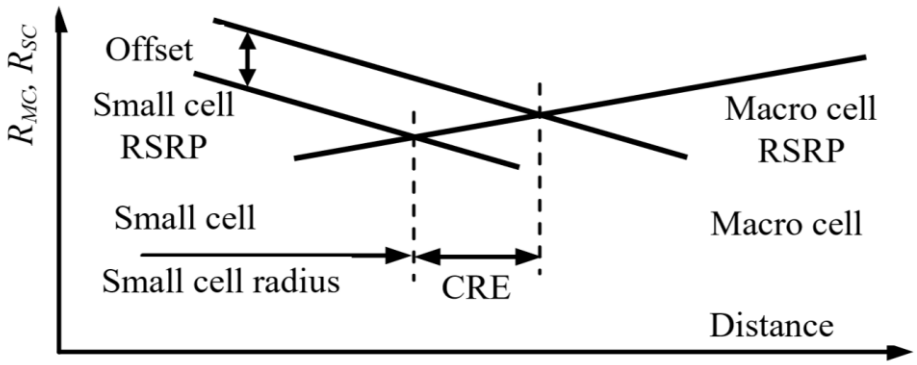

Figure 56: Small cell offset and CRE

4.3.2 Experimental analysis and results

The experiments are conducted on a cabled test branch environment using a basic cluster, operating in 2.6 GHz. The cluster consists of two eNodeB: one macro cell and one small cell eNodeB that transmit both in 20MHz bandwidth. The User Equipment (UE) is connected using a channel emulator, that simulates a real channel with noise and fading. Programmable attenuation equipment simulates the UE movement with 5km/h constant speed, corresponding to a pedestrian channel [73]. Inside the cluster a user equipment (CAT4 UE) is able to use all available resources allocated by eNodeB [80].

The aim of the experiments is to analyze the eICIC functionality in specific network architecture. In all the experimental scenarios we consider the same 30% ratio for ABS resources reservation and different range expansion offset values. In the experiments initially, the UE is attached to the small cell and has ongoing DL transfer, reaching the maximum cell capacity of about 100 Mbps. From this point UE starts moving with constant speed towards the Macro cell. The UE performs HO and changes the serving cell to macro cell, continuing to move inside Macro area until reaching the best signal quality. After that the UE returns back to the small cell through HO moving with the same speed until he reaches again the best signal quality also on small cell [57].

For each experiment we report averaged values computed based on 300 iterations. The first scenario for eICIC analysis corresponds to the simplest case when we have only one small cell in the cluster, that uses in CRE area the resources reserved by macro cell (30% in our experiments). In the first experiment we measure and plot in Figure 57 the Channel Quality Indicator (CQI).

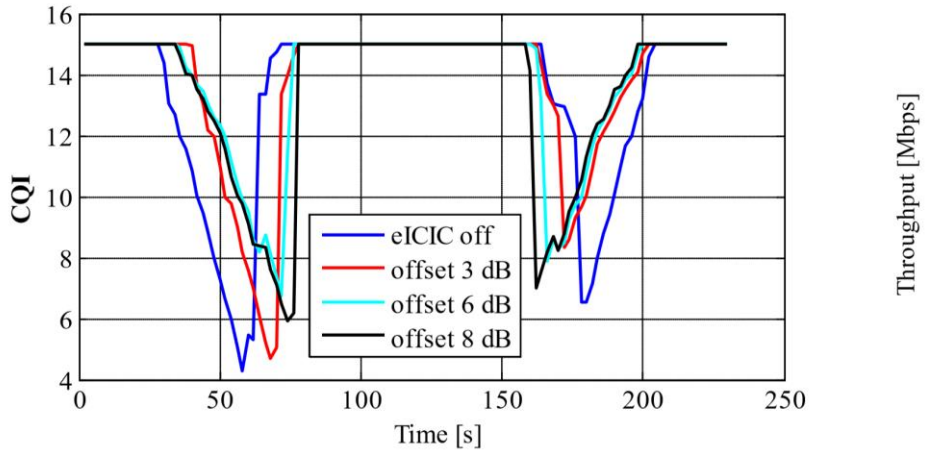

Figure 57: CQI reported by the UE for different offset values

The CQI values in Figure 57 are reported by the UE for 3 different CRE offset values (3, 6 and 8 dB) and for eICIC off as reference. CQI values are measured each 2 s, corresponding to around 2.75 m travel distance at the considered UE speed. The handover points in Figure 57 shows the CRE dependency according to the offset values. The spectral efficiency analysis through CQI reflects the eICIC benefits even for one single small cell in the cluster.

To find out the best offset value for eICIC we repeat the experiment for different offset values between 1 and 10 dB. For a more relevant analysis of the spectral efficiency of CRE, we compute the mean CQI for each offset value. The results are plotted in Figure 58 for particular offset values 3, 6 and 8 dB and compared to eICIC off. The optimum offset value is 6dB and corresponds to the maximum CQI and therefore to the maximum of spectral efficiency. For large offset values the eICIC efficiency decreases, due to the poor radio conditions for the UE at small cell edge, as the small cell radius increases. In the second experiment we analyze the cluster capacity by measuring the total UE throughput. We consider first the simplest case of a cluster with a single small cell. Based on this result we analyze the cluster behavior when the number of small cells increases. For this analysis all small cells are considered to be located approximately at the same distance from the Macro eNodeB, without coverage overlapping between neighbor's small cells.

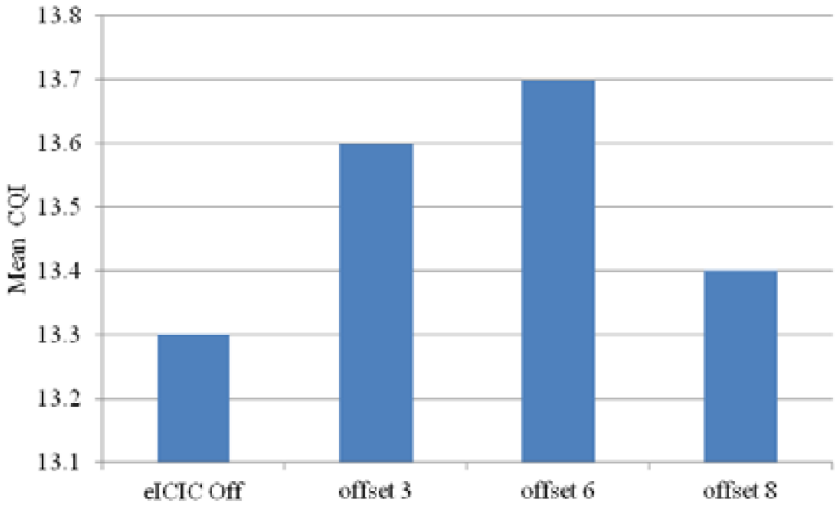

Figure 58: Mean CQI for different offset values

In Figure 58 we report the throughput evolution during the tests for 4 different scenarios: without eICIC, with eICIC and corresponding offset values 3, 6 and 8 dB. From the graph it is obvious that the overall transfer per cycle is correspondingly reduced in the macro cell area when the eICIC is activated, regardless the offset value, due to ABS reserved resources for small cells (30% in our experiments).

The cluster capacity evaluated as the overall DL traffic during the UE round-trip movement is presented in Table 2. The presented scenario corresponds to the worst case, since we have only one small cell in the cluster that reuse ABS resources reserved by macro cell for CRE. Based on this scenario we compute a minimum capacity gain for eICIC cluster as function of the number of small cells in the cluster. We define a gain G based on the capacity of the small cell using CRE, denoted C_{SC}, and small cell capacity without CRE and eICIC, denoted $C_{SC|eICICoff}$, according to:

Equation 19

$$G = C_{SC} - C_{CSC|eICICoff}$$

Based on the gain G, computed in Table 2, we can estimate for each offset value the minimum number of SC from a cluster for which the overall cluster capacity is higher than the cluster capacity in case of eICIC disabled. The global capacity C of the non-eICIC cluster can be expressed as:

Equation 20

$$C = C_M + \sum_i C_{SC_i}$$

where C_M is the macro cell capacity and C_{SCi} the capacity of the i-th small cell For a cluster that uses eICIC the capacity becomes:

Equation 21

$$C_{eICIC} = \alpha C_M + \sum_i (C_{SC_i} + G_i)$$

Table 4: Transfer per test cycle [Mbytes]

	eICIC off	offset 3	offset 6	offset 8
C_{SC}	8730	9532	9745	9683
C_M	9391	6510	5993	5784
Total	18121	16042	15738	15467
Gain G	0	802	1015	953

where α is the ratio of the macro cell resources reserved for ABS, and i G is the gain of the i-th small cell. Using Equation 21 and the gain G, we compute the global cluster capacity for different offset values as function of the number of the small cells in the cluster. The results are listed in Table 4 and plotted in Figure 59.

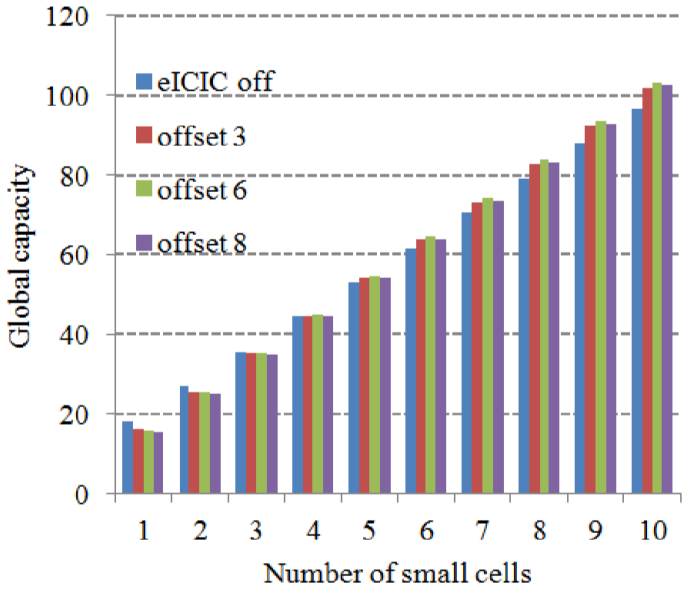

Figure 59: Global Cluster capacity

The results show that for a small number of SC in the cluster, the gain of the eICIC is exceeded by the ABS resource reservation, and the best situation is eICIC off. Figure 59 shows that for clusters with 4 or more SC the capacity is higher with eICIC activated for each offset value. We anticipate that the gain continues to grow by increasing the number of SC in the cluster, as long as there are no interferences between SC. For a very large number of SC in the cluster the inter-SC interferences become dominant and eICIC have to be related with other techniques in order to sustain the HetNet gain [80].

Table 5: Global cluster capacity [Mbytes]

Number of SC	eICIC off	offset 3	offset 6	offset 8
1	18121	16042	15738	15467
2	26850	25574	25484	25149
3	35580	35106	35229	34832
4	44310	44638	44974	44515
5	53040	54170	54719	54198
6	61770	63702	64465	63880
7	70499	73234	74210	73563
8	79229	82766	83955	83246
9	87959	92298	93701	92929
10	96689	101830	103446	102611

4.3.3 Small Cells deployments in LTE and eICIC optimization

The concept of heterogeneous deployments make reference to networks deployments where base stations with different transmission powers and coverage area sharing, fully or partially, the same set of frequencies and having an overlapping geographical coverage. One major problem with heterogeneous networks is associated with inter-cell interference coordination in such areas. 3GPP LTE - Release 10 introduced improved inter-cell interference handling creating HetNet scenarios more robust.

The concept introduced to mitigate the interference caused by the Macro–eNodeB to the Pico–eNodeB users is called enhanced Inter-Cell Interference Coordination (eICIC). Pico–eNodeB have a transmission power of 1W and offer high data rates and capacity where they are deployed by offloading the Macro eNodeB. This allows the Macro–eNodeB to serve better its users, increasing the end user experience. Due to their low transmission power and small physical size they can offer flexible site acquisitions. In LTE, cell selection is based on UE terminal measurements of received power of the downlink signal or more precisely the cell specific reference (CRS) downlink received power signal. Due to the transmitting power differences

between Macro and Pico eNodeB a low number of users are attached to Pico cells and these might be under-utilized. Also due to the Macro–eNodeB high transmission power the Pico–eNodeB users experience a high interference which disallows them to use the same physical resources.

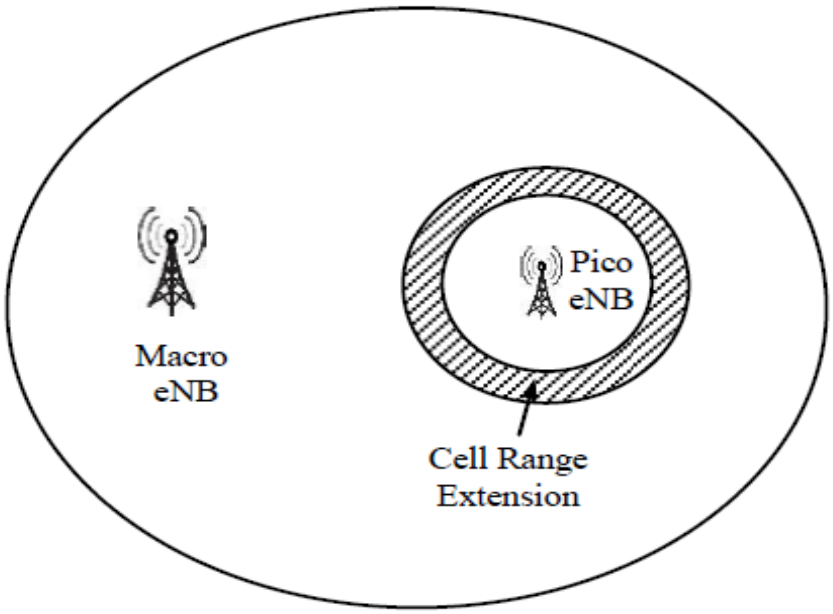

Figure 60: Cell Range Extension in HetNet

The first problem is solved by applying a cell specific offset to the received power measurements used in typical cell selection. Thereby the differences between the Macro and Pico eNodeB transmitting powers are compensated. Therefore, the coverage area of the Pico–eNodeB is extended increasing the number of users served by the small cell. This technique, illustrated in Figure 60, based on small cell radius extension is called Cell Range Extension (CRE) and involves some important advantages:

In downlink: increases the number of users connected to Pico–eNodeB; mitigates the interferences applied on the Pico–eNodeB by Macro–eNodeB because fewer users are served by Macro–eNodeB.

In uplink: reduces the UE transmit power because the user is associated with the Pico–eNodeB. The interference to other cells is also reduced and the uplink system efficiency is improved.

CRE technique also brings some disadvantages:

The user in the extended cell area, where the power received from the Macro–eNodeB is much higher than the power received from Pico–eNodeB, are subject to interferences from the Macro–eNodeB.

The interference effects associated with CRE are addressed in time domain by a multiplexing technique called Inter-Cell Interference Coordination scheme based on Almost Blank Sub-frames. In this approach Macro–eNodeB transmissions are switched off periodically during the frame and interferences produced by Macro–eNodeB do no longer aggress the users attached to Pico–eNodeB Figure 61. This allows range extension for Pico–eNodeB users. The term "Almost Blank" is because Macro transmissions are not completely stopped as certain control signals are still transmitted [67].

Researches in this section are conducted on a system model and are based on simulations scenarios according to [67]. The model addresses a heterogeneous network deployment with the following characteristics:

The network contains 1 Macro–eNodeB and a certain number, NP, of Pico–eNodeB. The Pico–eNodeB are randomly distributed in the network.

We assume open access to network resources which means a user is allowed to access any tier's eNodeB. We consider an eNodeB association based on maximum received power (MRP). The power received by any user, $\{P_{r,j}\}_{j=1,K}$, can be expressed as [83]:

Equation 22

$$P_{r,j} = P_j L_0 (R_j / r_0)^{-\alpha_j} B_j \, , j = 1,..K$$

where L_0 is the pathloss at a reference distance r_0, j indicates the tier to which the user connects and K is the total number of tiers [57].

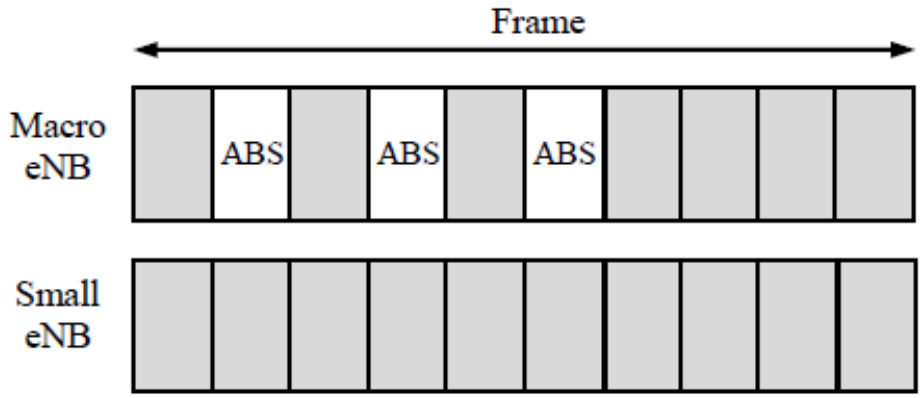

Figure 61: Almost Blank Subframes in HetNet

In our experiments $K = 2$ (1 indicates the Pico cell and 2 the Macro cell).

B_j characterizes the cell range extension offset and is identical for all cells in a specific tier j. Employing $B_j > 1$ extends the cell coverage of the j_{th} tier as shown in Figure 60. This allows the tier selection to be adjusted for cell load balancing.

Consequently, to this criterion a mobile user is associated with the strongest eNodeB in terms of Maximum Received Power (MRP):

Equation 23

$$MRP = \max\{P_{r,j}\}$$

If we consider that users are located inside HetNet according to a homogeneous PPP (Point Poisson Process) with intensity $\lambda^{(u)}$ and the position of eNodeB inside the j_{th} tier is modeled according to a PPP process with intensity λ_j the average number of users associated with an eNodeB in the k_{th} tier is given by [83]:

Equation 24

$$N_k = 2\pi\lambda^{(u)} \int_0^{\infty} r \exp\{-\pi \sum_{j=1}^{K} \lambda_j \left(P_j' B_j'\right)^{\frac{2}{\alpha_j}} r^{\frac{2}{\alpha_j}'}\} dr$$

where $\hat{P}_j, \hat{B}_j, \hat{\alpha}_j$ are respectively the transmit power ratio, the offset power ratio and the pathloss exponent ratio of interfering to serving eNodeB:

Equation 25

$$P_j' = \frac{P_j}{P_k}, B_j' = \frac{B_j}{B_k}, \alpha_j' = \frac{\alpha_j}{\alpha_k}$$

The parameter r represents the distance between the user and the serving eNodeB.

If we assume the same value *a* for all α_j, Equation 24 simplifies become [83]:

Equation 26

$$N_k = \frac{\lambda^{(u)}}{\lambda_k + \sum_{j=1}^{K} \lambda_j (P_j' B_j')^{2/\alpha}}$$

For a HetNet consisting of two tiers (Macro and Pico cell) we evaluate the SINR for a user attached to a specific eNodeB in each tier.

Equation 27

$$SINR_p(r) = \frac{P_{rP}}{\sum_m P_{rM,m} + \sum_{n,n\neq n_0} P_{rP,n} + N_0}$$

$SINR_P$ in Equation 27 characterizes a user located at distance r and served by Pico – eNodeB, m indicates the Macro–eNodeB in the HetNet and n indicates the Pico–eNodeB except the serving cell n0.

We assume that users are only impaired by additive white Gaussian noise (N_0) and interferences produced by users located in the same cloud.

The received power is calculated assuming a pathloss PL_p for users attached to Pico–eNodeB that transmits with a power P_p:

Equation 28

$$P_{rP} = P_P - PL_P$$

and :

Equation 29

$$PL_P = 150.4 + 37.5 \log r$$

In the same way, the SINR for a user attached to Macro–eNodeB that transmits with a power PM is expressed as:

Equation 30

$$SINR_M(r) = \frac{P_{rM}}{\sum_n P_{rP,n} + \sum_{m,m\neq m_0} P_{rM,m} + N_0}$$

where:

Equation 31

$$P_{rM} = P_M - PL_M$$

and the pathloss, PL_M , for user attached to Macro–eNodeB is:

Equation 32

$$PL_M = 141.1 + 42.8 \log r$$

In SINRP and SINRM expressions we neglected the fading associated with transmissions in mobile networks.

4.3.4 Simulation and results

The objective of our research is to analyze eICIC functionality in a HetNet deployment and to draw some conclusions useful for design purposes. The experiments are conducted in a basic cluster that consists of: one Macro–eNodeB and four Pico–eNodeB that share the same bandwidth.

The experiments are aimed at highlighting the throughput per user variation at the cell edge based on CRE offset and ABS allocation ratio (β).

For a user attached to Pico–eNodeB the throughput, in terms of spectral efficiency [bit/Hz], is given by:

Equation 33

$$C_P = (1 + \log_2 SINR_P)(1 - \beta)$$

Similarly, the throughput for a user attached to Macro–eNodeB is:

Equation 34

$$C_M = (1 + \log_2 SINR_M)\beta$$

We develop a MATLAB program to study HetNet performances in terms of user's throughput, based on theoretical approach in II and III. We start with the influence of CRE offset on Pico cell area and on the number of users attached to.

Figure 62 plots the received power from Macro–eNodeB and Pico–eNodeB versus distance, for different offset values applied to the pico cell. It can be observed that the pico cell expands from a radius of about 100m without offset to a radius of about 170m for an offset of 10dB. Correspondingly the area occupied by the pico cell varies between 4% and 14% related on macro cell area which will lead to change in the number of users. We plot in Figure 63 the throughput per user in Macro and Pico cell accordingly to Equation 33 and Equation 34 as function of ABS allocation ratio β for different CRE offset values.

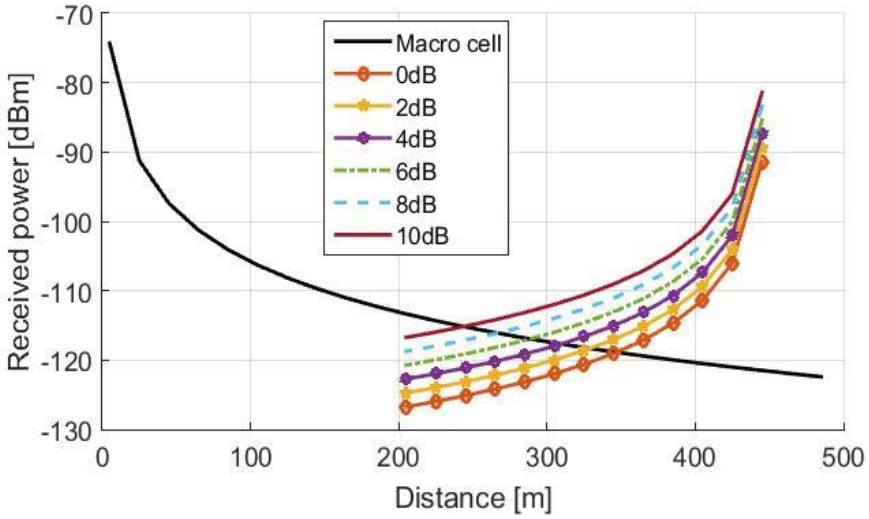

Figure 62: Received power from Macro and Pico–eNodeB for different offset values

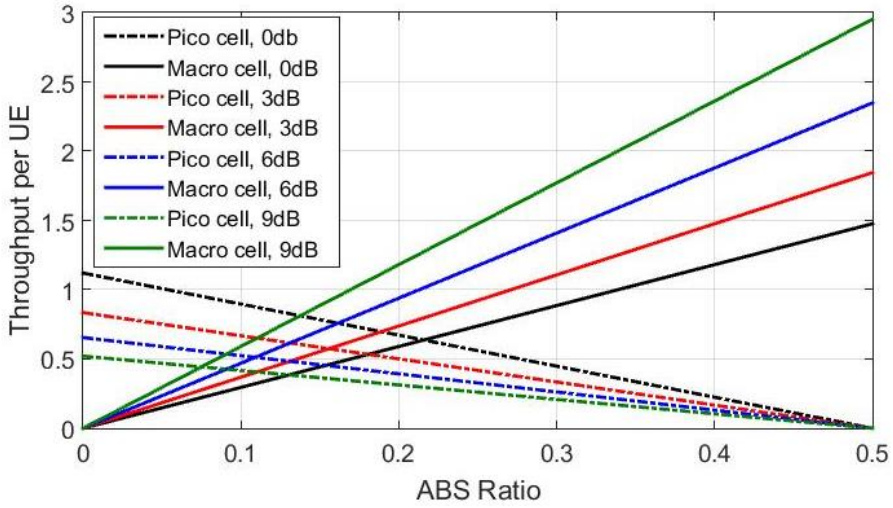

Figure 63: Throughput per user against ABS ratio and CRE

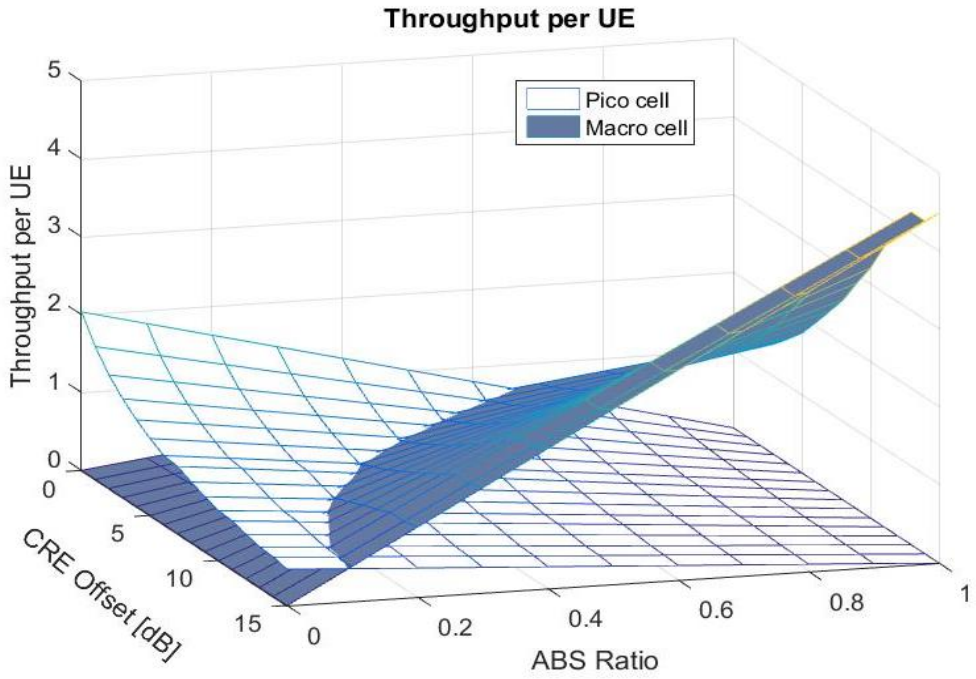

Figure 64: 3D plot of throughput per user

Figure 64 represents the 3D plot of throughput values against CRE offset and ABS ratio. For Macro cell the throughput variation is linear in term of ABS ratio and increases with the CRE offset because the number of users decreases in the Macro coverage area. The number of users attached to Pico cell grows and therefore Pico cell resources are more efficiently used. For users attached to Pico cell the throughput decreases but resources inside the Pico cell are enough to sustain the desired throughput. This behavior leads to an efficient load balance between Macro and Pico cells. The maximum throughput per user as in Figure 64 is reached for ABS values in the range 0.35 – 0.4 and CRE value approximately 5dB. In both figures presented behind, the Throughput per UE is represented in [Mbps].

4.3.5 Discussions

The mitigation of interferences between cells is one of the hardest challenges in a heterogeneous network developing and optimization.

From the experimental results analysis, we can conclude that even for the worst case scenario, when the cluster contains only one small cell located in the area covered by Macro, the eICIC mechanism activation increases the spectral efficiently of the cluster. Considering a specific value for ABS and testing several values for eICIC CRE

offset we find the optimal offset value equal with 6 dB. When the analyses are capacity driven in the eICIC, a gain exists only for clusters with more than 3 small cells. The cluster capacity gain increases proportionally with the number of small cells in the cluster. The number of small cells in the cluster can be increased until the distance between two neighbor small cells become critical in terms of interferences between them. For future studies on the current topic we intend to perform a joint optimization of the eICIC parameters: the ABS ratio, the CRE offset and the number of small cells in the cluster [57].

CRE technique aims to balance the Macro and Pico cell loads by enlarging the Pico cells size and increasing the number of users attached to Pico cell. To combat the large interference in the Range Extension area ABS scheme is introduced in eICIC. Through this paper we developed a simulation tool to analyze the throughput per user inside a two tiers HetNet. Essentially, the throughput per user dependencies on CRE and ABS are investigated in order to emphasize optimum values for these parameters. We conclude that the influence of these parameters on the throughput per user depends on the current system load and suggest that the network should dynamically adjust the CRE and ABS values leading to Self-Optimizing Networks [80].

5 User experience in mobile networks

Based on new 3G and 4G technologies wireless networks become more and more complex and due to advanced operating capabilities of smart phones, offer support for implementing complex multimedia applications besides the classical voice applications. These new services involve high bandwidth and have severe requirements for both network and user equipment [60].

From the network perspective, performance can be measured by collecting and investigating technical indicators known as Quality of Service (QoS) parameters. These relevant indicators collected at network layer are: bandwidth, delay, jitter, and packet loss rate and at UE level: signal level, noise and interference level, connection establishment time, drop rate, etc.

Quality of Experience is the overall performance of a system from the end-user point of view and is affected by various technical, business and contextual factors. QoE can be appreciated as a measure of the end-to-end performance level from the user perspective and as an indicator of how well this system meets the user needs.

Actually, QoE provides an assessment of human perceptions, feelings, emotions, and intentions with respect to a particular product, service and application [84]; [85]. In this context it is critical to identify requirements for mobile multimedia applications that are associated to the wireless 3G/4G network QoS as well as to the UE context and UE feedback.

Today there are a variety of methods of network planning and optimization, but these methods do not always provide results that express the real end-user experience [86].

The most important planning and optimization methods are presented below [60]; [87]:

- Pathloss Prediction, Automatic Frequency Planning (AFP) and Automatic Cell Planning (ACP)
- Field Drive Test using scanners and call placement equipment
- User device measurement collection
- Operation Support System (OSS) Key Performance Indicators (KPI) statistics
- Heuristic data analysis

The first method is used during the network planning phase, before the network to become operational, giving a first estimation of the network structure which needs to be improved later using more accurate methods.

Field drive testing is an essential part of the network deployment starting on the early stage of network operation and provides true real world measurements of

the RF environment. On the other hand, drive testing is a time-consuming technique and requires very expensive equipment's. For these reasons LTE release 10 and 11 propose the minimization of drive tests by introducing new UE measurements capabilities.

The third method collects measures made by the user equipment: these can be regular measurements (for power control, handover, timing advance) sent by the user to eNodeB (eNodeB) or measurements provided by special applications installed on UE. These applications are developed based on new capabilities offered by smart-phones.

Compared to drive test technique, the technique based on UE measurements is less expensive, but the results can be less accurate and might depend on UE model. The fact that users are randomly distributed in the network can be an advantage by collecting measurements from a wider area than that covered by a field drive test. Since the UE processing capacity is still limited, techniques based on measurements taken by the UE and stored in a database and subsequently processed centrally have been developed.

OSS KPI statistics technique relies on statistics provided by eNodeB and OSS. But these statistics are not specified by 3GPP and are based on equipment vendor implementations. The performance averages afforded by KPIs give information about a specific cell, in general, and little information about the entire network.

Heuristic data analysis is based on algorithms developed to extract useful information regarding the network planning and management. Although based on large amounts of data collected by the techniques mentioned above heuristic algorithms provides information relating only to restricted areas and not on the entire network [60].

In our study we use a technique in the third category based on DATUM application provided by SPIRENT Technologies [88]. Datum is an application that can be downloaded and installed on smart UE. This application connects to cloud-based servers including: the call server, used to initiate tests, the media server containing media files and the data base server where the UE measurement results are stored. Representative tests include: web browsing, file transfer, streaming data, multiservice (voice call and data) and latency. Centralized test scenarios are developed, and tasks can be combined in any desired order of preference for tests purposes.

5.1 Environment preparation

We conduct a set of measurements in real environment (a 2G/3G/4G commercial network is considered for this analysis), using as a measurement tool the user equipment (UE), in order to evaluate and analyze end user experience. We transform the real UE in to a measurement equipment by using the client functionalities of the DATUM platform. In the complex equation of end user experience are involved several factors as: voice quality, call performance, data performance, web browsing, video performance, location accuracy and application performance and battery life. Analyzing all these parameters we estimate an important but also subjective parameter related to end user experience: user perception. We propose a solution for

increasing Quality of Experience (QoE) that consists in network densification with Small Cells equipment's customized for targeted building.

5.1.1 Experiment implementation

For tests and analysis, we configure the DATUM platform to work as a client-server application; the UE plays the client role and all processing effort is moved to the remote DATUM server. The Spirent Datum system provides device-based data testing, including configurable test scenarios and local and centralized results analysis. For the experiments we use a set of commercial UE having data and voice subscription with 2G, 3G and/or 4G capabilities. All the mobiles involved in experiments have Android Operation System (OS), but the mobile application for the client, DATUM, is available and can be installed on all mobile OS types.

The test scenarios are developed on the Datum server, available on the cloud. Once the test cases are created and the UE are registered to the test project, each test scenario can be run on any individual client. To avoid unwanted interactions between our test results and regular user traffic, each test case needs to be run by the end user, preferably when no other applications at UE level generate traffic (no ongoing video/voice calls or data traffic) [60].

The aspects that we set out for our research are:

- Analysis the feasibility of commercial UE usage as a measurement tool.
- Evaluation of service quality ensured by two different service providers (in the analysis we considered 3G and 4G networks) inside a typical office building.
- Proposal of the network densification in the target area, based on the experimental measurements.

The measurements were performed in an office building with large rooms. The building dimensions are roughly 104 m x 24 m and it has three floors including an open floor plan with lots of office furniture and equipment's. To this building compared to other office buildings is the increased level of interference and multipath signal propagation resulted from high density concrete walls and multiple metallic equipment racks distributed throughout it. The measurements were performed on the middle floor of this building at an average pedestrian speed of 5 km/h and at an average UE height of 1.5 m while crossing the main hallway from West to East.

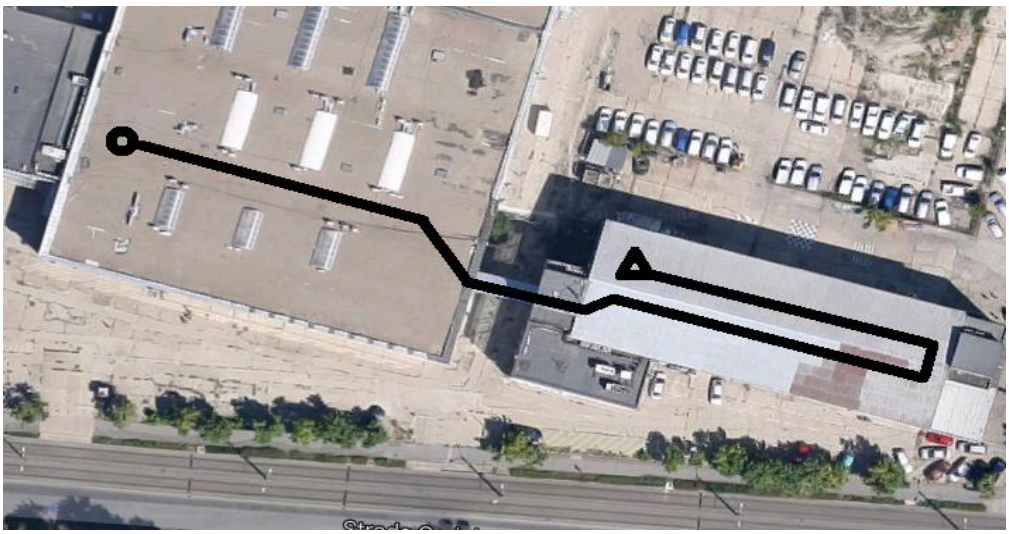

Figure 65: Focus on measurements area

The UE route is indicated in Figure 65 from the starting point marked with a circle to the end point marked with a triangle. The measurement area is located in a congested area. In the building there are hundreds of employees that intensively use the phone. Nearby there are dense residential areas, a high school, business centers and a market. The base stations for the LTE and WCDMA network are located west of the building about 150 m from the start point. The tests are made at busy hours (11 and 16) when the network experiences relatively high load [60].

For all the tests our focus is the analysis of the LTE layer, but we also perform a limited set of 3G measurements to provide a baseline reference. We use UE provided by different vendors (Samsung, LG, and Sony) in order to mitigate the impact generated by the UE category, hardware platform and signal processor type to our final results.

The experimental results suggest that a network densification using small cell technology is highly recommended. We already analyze in different scenarios the benefits for network densification using small cell technologies for the same building in [54]; [73]; [31]. In these papers we analyze the UL, DL and handover (HO) performance in the context of Heterogeneous Networks configuration.

5.1.2 Experimental results

In order to have an accurate view of the end user experience for various services we develop and run the following test types:

- FTP transfer simultaneous on 2 LTE capable UE
- FTP downlink test comparison between 3G capable UE and LTE capable UE
- HTTP downlink test comparison between one 3G capable UE and one LTE capable UE

- Downlink + Uplink FTP test simultaneous on 2 LTE capable UEs

A. FTP transfer in parallel on 2 LTE capable UE

The scenario applied for FTP tests consists in transferring a 100 MB file on each UE. The file transfer is started simultaneous on both UE, the distance between UE is around 0.5 m and the UE are moved in parallel. Both UE have the same subscription type and have similar performance.

The only difference was the fact that during the movement we keep the UE1 in the same position while we change the orientation during the movement for UE2. To increase the accuracy of results we perform 4 iterations. The results for FTP transfer in Downlink (DL) are exposed in Figure 66.

We use the same test configuration for Uplink (UL) transfer keeping the same particularities as in DL but increasing the number of iterations for UL. The results are presented in Figure 67. Analyzing the results, we can conclude that in DL, due to the Multiple Input Multiple Output (MIMO) connection, we facilitate a MIMO dual-layer transition by modifying UE2 orientation. Consequently, we obtain a better average transfer throughput for UE2, even if the results for individual iterations are more fluctuating

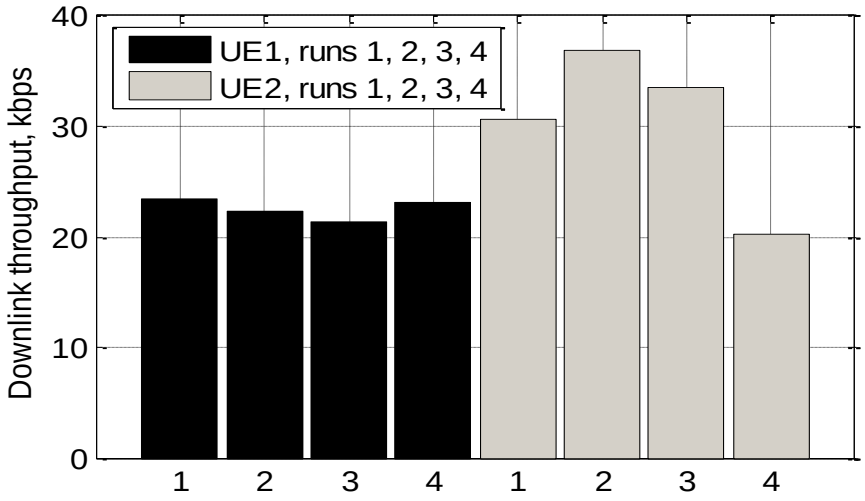

Figure 66: FTP Downlink test simultaneous on 2 LTE capable UEs

For the UL this gain is not obtained because in UL the UE has only one transmit antenna. For UE1, the low throughput for the first two iterations is linked to additional traffic generated by other applications running during the tests. The values reported by DATUM are strictly related to tasks started by the application, and do not monitor all the data exchanged by the UE with the network.

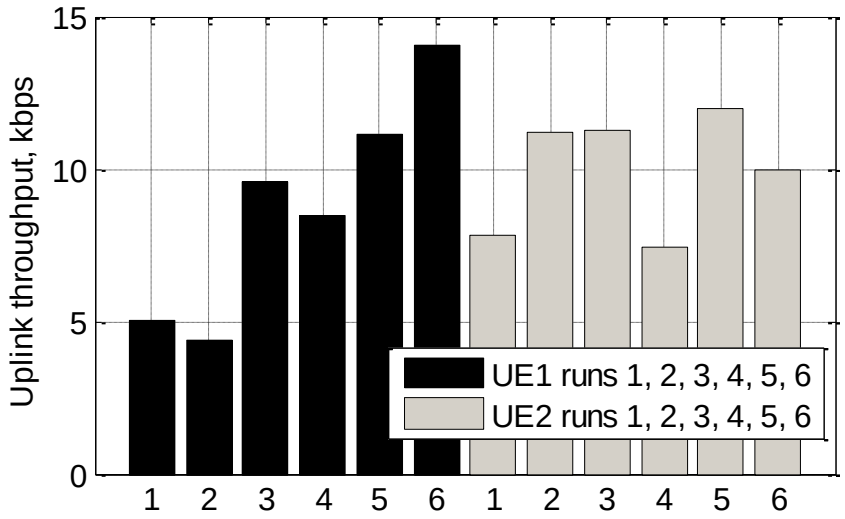

Figure 67: FTP Uplink test simultaneous on 2 LTE capable UEs

B. FTP downlink test comparison between 3G capable UE and LTE capable UE

In the second set of experiments we analyze the DL FTP transfer running the test in parallel on two UE having different capabilities (one LTE and one WCDMA). For these experiments we transfer a 100 MB file and keep both UE in the same position, moving with the same speed, and having less than 20 cm distance between them.

The results are presented in Figure 68. We observe the significant difference between average transfer speeds obtained, in line with theoretical capacity for both systems.

Analyzing the obtained results for DL and UL throughput on LTE network, we observe a low average throughput compared with real eNodeB capabilities. The obtained values were 20-35 Kbps for DL and 5-15 Kbps for UL in the LTE network. In WCDMA network, the corresponding measured throughputs are smaller.

For LTE network, according to the standard specifications, considering a 10MHz bandwidth and MIMO 2X2 capabilities, the maximum value for DL throughput at application level is 61 Mbps in DL and 26 Mbps in UL per cell [16]. For WCDMA (HSDPA+) the maximum DL throughput at application level, for one carrier is 14 Mbps in DL and 5.7 Mbps in UL per cell [75]; [60].

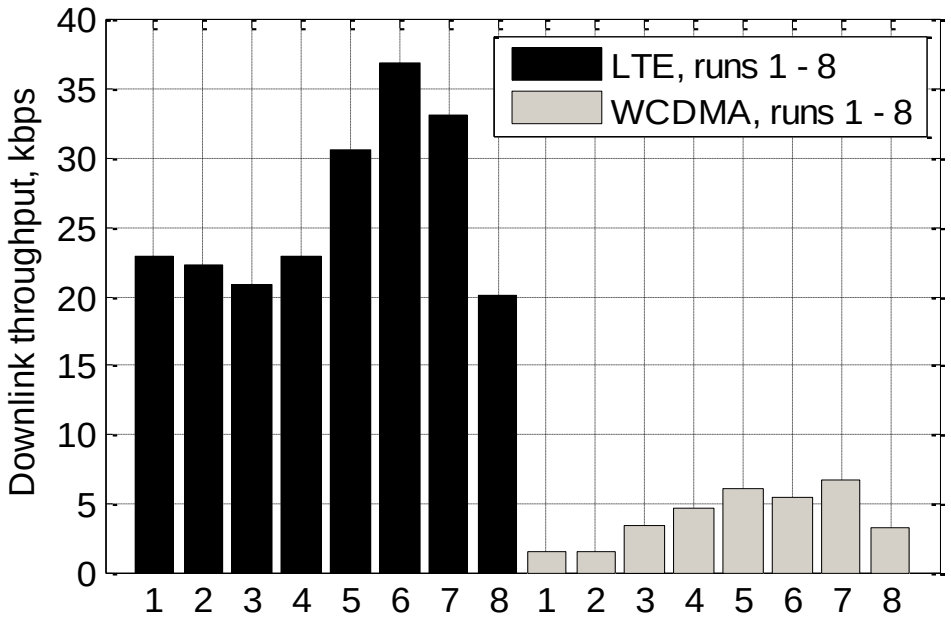

Figure 68: FTP Downlink tests comparison between 3G capable UE and LTE capable UE

These differences between LTE and WCDMA reflect on one hand the maturity of WCDMA network that has a bigger base station density in comparison with the youngest LTE network and on the other hand the load balancing between technologies inside the same network provider.

Taking as reference for analyze the LTE with 61 Mbps DL maximum throughput and considering 400 maximum number of simultaneous active users per cell, characteristic to a dense area, the resulted throughput per user is 152 Kbps. This value is typical for users in cell center proximity, experiencing good radio conditions and using 64QAM modulation and high coding rate. In reality the user's distribution in the cell is random, leading to a lower throughput for the users located at the cell edge due to lower modulation and coding schemes.

C. HTTP downlink test comparison between one 3G capable UE and one LTE capable UE

In order to evaluate the web browsing performance, we chose to analyze the time needed to load an internet page comparing the LTE and WCDMA technologies. The experiment is repeated 10 times in different part of the building for each UE. The results are taken in the same locations for both UE (LTE and WCDMA capable). The loading time for LTE is significantly short compared with WCDMA loading time. The obtained values are displayed in Figure 69.

D. Downlink + Uplink FTP test simultaneous on 2 LTE capable UEs

For Downlink and Uplink FTP test simultaneous on 2 LTE capable UE the results are consistent with the experimental result in previous sections and the related experiments are not included in our work.

For our experiments the user movement is performed from middle cell to cell edge. The area that includes the target building is a dense urban area with high apartment density and office buildings. Based on these observations the experimental values are in line with theoretical limits, but far from end-user expectation, which mostly are based on commercials campaigns made by network operators.

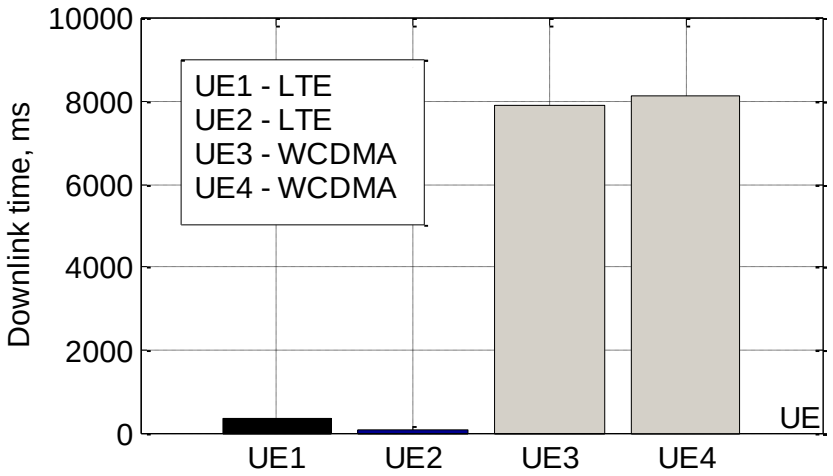

Figure 69: HTTP Downlink test comparison between LTE and WCDMA capable UE

Therefore, in order to meet the customer expectation, the network operators are required to increase the density of the network. In the considered environment the macro layer densification is hard to be performed due to interference and public safety norms. The recommended feasible solution remains the small cells implementation in a Heterogeneous Networks [60].

5.2 Monitoring end-user electromagnetic radiation in a HetNet

In order to be able to reduce the level of radiations, first of all, we need to understand the nature of these, to learn how to evaluate them qualitative and qualitative, and to have a proper tool able to measure them [89].

In the past years the usage of wireless communication devices in close proximity to the human body has been increasing dramatically. The risk of electromagnetic radiation was often considered, and the Specific Absorption Rate is one of important characteristics used to evaluate the EM energy absorbed by human body. The Specific Absorption Rate represents a limiting factor in the high-field Magnetic Resonance. This

paper presents a theoretical approach in analyzing the electromagnetic field penetration and monitoring of network radiation through a dedicated application.

5.2.1 Available radio parameters

Heterogeneous networks differ from traditional homogeneous macrocellular networks in some significant aspects. Unlike the macrocells, which are situated by cell planning to provide complete coverage, small cells are typically located according to the expected density of traffic, in so-called HotSpots or HotZones [90]. This gives rise to different and potentially stronger interference conditions which need to be managed between macro and small cells layers and inter small cells.

To get the most out of small cell deployments, it is important to understand how to optimize the association of user equipment to cells and to balance the load between the macrocells and small cells in a way that maximizes the total system capacity [91].

In a generic cellular network, when a user equipment (UE) moves from a cell to another cell and performs cell reselection, he measures and report two types of indicators, first related to signal strength and the second related to signal quality of the neighbor cells. In Long Term Evolution (LTE) Networks, a UE measures three important parameters regarding signal: Received Signal Strength Indicator (RSSI), Reference Signal Received Power (RSRP) and Reference Signal Received Quality (RSRQ) [92].

RSSI is one of the simplest approaches that was used for estimation of distances between nodes, based on of signal strength received by another node [93]. In this context, a source base station sends a signal with a determined strength that decreases with the propagation. The bigger the distance to the target base station, the less the signal strength when it arrives at that node.

The main advantage of this method is its low cost, since most receivers can estimate the received signal strength.

However, this method is very susceptible to noise and interference, which results in high inaccuracy in distance estimation. Although this approach has been demonstrated to perform poorly, it is the most used solution for distance estimation.

Another aspect that qualify RSSI as first parameter that should be analyze is the fact that RSSI is used for all technologies from GSM to LTE.

RSRP measures the Reference Signal (RS) power, excluding all off the noise and the interference power [94]. RSRP is based on coverage, making it ideally independent of the network load.

RSRP can be defined as the average power of Reference Signal of resource elements.t In order to improve the accuracy of RSRP`s estimates, the UE can also measure the Reference Signal measured from second antenna port.

RSRQ measures the total received signal and the noise power normalized to one physical resource block bandwidth. The e RSRQ is direct depend on the RSRP, thus making the RSRQ redundant as the trigger for intra-frequency handover. In

contrast, the RSRQ ratio can be a useful trigger for inter-frequency handover if it can be used to redirect UE to a less serried layer.

In analog and digital communications, Signal-to-Noise Ratio (SNR), is compute as a report between signal strength and background noise, usually measured in decibels (dB). Communications engineers always tried to maximize SNR. Traditionally, this can be done by using the narrowest possible receiving-system bandwidth consistent with the data speed desired.

SNR can be increased by providing the source with a higher level of signal output power if necessary. In some high-level systems, internal noise is minimized by lowering the temperature of the receiving circuitry. In wireless systems, it is always important to perform a performance optimization of the transmitting and receiving antennas.

5.2.2 Specific Absorption Rate concept

Advanced wireless systems improve day-to-day interconnecting people by imposing a standard of excellence in communication. These advances bring many positive benefits to society, but they also affect the human body in many ways. One form of intervention with the human body is the propagation of radiofrequency waves through biological tissues in the human body. [95].

Propagation of electric fields and electromagnetic waves into the human body and into biological tissues has previously been studied extensively for localized radiation sources such as mobile phones and microwave ovens.

Absorption of RF energy by tissues and the human body is typically used to study both short term and long term impacts caused to the human body but have previously not been studied in detail for other emerging wireless systems. The Radio Frequency concerns regarding the electromagnetic waves absorption in the human body is becoming more and more of a problem.

The extensive use of wireless networks, mobile phones and other devices are the primary sources of electromagnetic radiation and wave absorption into the human body. Therefore, the most important parameter used to in order assess human exposure to Radio Frequency electromagnetic fields emitted from mobile phones is given in terms of absorption rate. Defining the concept, the Specific Absorption Rate (SAR) [2] represents the Radio Frequency (RF) power absorbed per unit of mass of a certain object and is being measured in Watts per body kilogram (W/kg) [54].

SAR can be defined as the average energy deposition in a region of a certain mass over an extended period of time due to the application of an excitation pulse [60]. The SAR describes the potential heating of tissue because of the application of the Radio Frequency energy that is necessary to produce the Magnetic Resonance (MR) signal [96].

The SAR can easily be calculated using the following formula [94]:

SAR = σ E2 / 2

where:

- σ is the conductivity of the material
- E is the Electric Field
- ρ is the mass density.

Nonhomogeneous Radio Frequency fields will lead to local exposure to radiation, where a part of the absorbed radiation is applied to a body region, leading to a concept called local SAR. Hot spots may occur on the tissues and to avoid or to minimize the effects, the frequency and the power of the RF irradiation should be kept at the minimum. Radiation over the whole human body leads to a concept called global SAR.

The precision and the reliability of a SAR value depends directly on three important parameters: tissue density, tissue conductivity and electric field. The most significant parameter is the induced electric field, a complex function of physical and biological variables including the microwave frequency, the radiation source size and the composition of the affected tissue. It is practically impossible to measure the absorbed energy in the human body, as the absorption rate fluctuates from person to person with the age factor and other specific characteristics.

The SAR increases with the electromagnetic field strength, the Radio Frequency power, the transmitter type and the size of the human body. When doubling the electromagnetic field strength from 1.5 Tesla to 3 Tesla, it will lead to a quadruple value of the SAR level. In high and ultrahigh electromagnetic fields, some of the multiple echo's and multiple-slice pulse sequences will be able to create a higher level of SAR than it was initially recommended. The SAR measures exposure to fields between 100 kHz and 10 GHz. SAR is commonly used to measure power absorbed from mobile phones, microwaves and power absorbed during Magnetic Resonance Imaging (MRI) scans.

The value will depend heavily on the geometry of the part of the body that is exposed to the RF energy and on the exact location and geometry of the RF source [97]. Thus, tests must be made with each specific source, such as a mobile phone model, and at the intended position of use. The SAR value is measured at the location that has the highest absorption rate in the entire body. Usually there is no threatening increase in the body temperature that could be measured. In the high magnetic fields is possible for the temperature to increase, but with at most 1°C.

In recent decades, numerous studies have been conducted to understand the occurrence of high risk events due to RF radiation on the human body. Until recently, most radiation exposures used magnetic resonance imaging (MRI) techniques and computed tomography (CT) techniques to thoroughly understand the inside of the human body. The rapid expansion of wireless networks and cell phones has pushed the researchers onto the necessity of studying mobile phones and wireless networks for radiation performance to properly address some of the safety concerns [98].

Nowadays, automatic positioning systems, actual phones and a head-like object filled with the appropriate tissue and equivalent liquid is employed to measure the SAR for mobile phones. Many efforts using numerical methods are aimed to define

human head models, and phone models to allow the comparison between numerical and experimental procedures for SAR evaluation.

It is anticipated that the number of measurements required to properly evaluate the SAR for such types of usage described above will increase and the SAR measurements will become more and more time consuming [99].

5.2.3 SAR Watch – Tracking radiation exposure

The application aims to measure radiation according to the sources of exposure. The classification criterion is defined by the level of control (amelioration) that the user can impose over the sources. Also, account must be taken of the physical capabilities of the phone, which are sometimes limited by manufacturer's constructive decisions.

Depending on the nature of the radiation, two categories are proposed: the effective radiation produced by the mobile phone and the ambient radiation produced by the wireless communication equipment’s. Radiation specific to the mobile phone includes the radiation whose source is strictly limited to the UE. This particular radiation type is the most harmful to the human body and represents the most dominant part of total cumulative exposure to which an individual is exposed.

The frequency of ambient exposure measurements depends on how often the phone’s position changes over time. Measurements are triggered periodically based on a background monitoring mechanism. Furthermore, a measurement can also be launched manually.

The interval between two adjacent measurements is in the order of minutes. Thus, the algorithm adapts dynamically to the distance between the last two measurements and schedules the next measurement considering the user's predisposition to move.

Applying a refining and identification process on the sources that form the overall exposure, we can go further to develop the hypothesis around which the exposure was induced.

Current approach uses metrics that assess the use of the smartphone for its primary purpose (voice call) but also additional activities like data transmissions. Initiating and maintaining a voice call involves a complex exchange of information between the mobile phone and the operator's equipment. In this case we focus only on the mobile phone side. Data packet transmission should not be neglected because it involves intense radio exchange.

Account must be taken of the multitude of factors that directly or indirectly influence the value of the SAR parameter:

- phone characteristics
- user-relative phone position
- distance between phone and operator’s equipment
- cell technology standard

Radiation specific to wireless transmission equipment includes the that form of radiation, which by its nature cannot be controlled by user. It shall be referred to as

ambient exposure because the user is indirectly affected. These radiations have a much lower impact, but they should not be neglected. The specific reason why they are monitored is that the exposure is for a long time, and cumulative over time may have harmful effects on human health. Ambiental exposure analysis is constrained only by the hardware capabilities of a mobile phone.

Regarding the ambiental exposure, the composition of a screen consists of two sources of exposure: operator cells and Wi-Fi networks. Each is represented in the form of an individual graph. The illustrated intervals represent time stamped aggregations of the measurements. Thus, the user can inspect an overview and can make comparisons based on the history of the measurements. Users may decide on the appropriateness of the update and can act by triggering an explicit measurement.

The presentation logic of data gathered from the exclusive use of the phone also follows the source refinement approach. The two areas of interest captures by application's UI are:

- exposure due to initiating a voice call
- exposure due to the mobile data traffic

The highlighting or tinting of an area within which a measurement was executed is done by overlaying a circle that is colored according to the level of exposure. The origin point of the circle is given by the GPS coordinates of that measurement. . The zoom level of a map view is given by the distance between the last measurements and the current user position.

Under the Android operating system, the implementation of the hardware abstraction layer (HAL) that directly make use of hardware resources (GSM modem, sensors etc.) remains a duty for the smartphone manufacturers and not the provider of underlying operating system. Effective testing of the app on Android phones has revealed implementation differences (mostly in HAL) between critical modules and later used by application business rules. Therefore, we are trying to find some complementary solutions to minimize the impact of manufacturer's decisions.

5.2.4 Future directions in developing the SAR Watch application

The perspectives of the paper outline the processing of data gathered through the application. Therefore, the application intends to introduce the concept of global exposure database. This global database can be interrogated for the following reasons:

- building a public map for querying ambient exposures for a particular geographical region
- defining user cohorts
- correlation of information gathered to determine certain factors like diseases, access to information etc.

Currently, we are monitoring only the RSSI parameter in order to determine the radiation level, but in the future we will focus on analyzing the feasibility of introducing additional parameters like RSRP and SNR, in order to improve the accuracy of the analyses, by comparing the level of radiation with the Quality of Services (QoS)

received by the user of the application and constantly trying to find the balance between the radiation exposures and the Quality of Experience.

In the next iteration of the application, we will analyze the level of exposure in several network configurations for the same services. We will compare SAR measurements for the same services (voice, live streaming, video conference and file transfer) and the same QoS, when the user equipment is connected through each technology (GSM, WCDMA, LTE and WiFi) to determine the "best" choice for a specific service, with the lowest radiation exposure.

Another key item to be developed is the user documentation with respect to avoid or reduce exposure to radiation. This module should be interleaved in the presentation of the measurement to the user and must contain prompt advice or solutions. The application is currently available in the online application store [100]. To maximize user adoption rate, a marketing plan should be developed. A possible approach proposes splitting the application into parts with basic functionality offered as free content and user tailored parts offered as purchases.

6. Conclusions

The last decade has seen an exponential increase in the volume of data transmitted over broadband mobile networks, and the trend will probably increase in the coming years. Current cellular networks are poorly equipped to cope with this increase in demand. To meet user demand and maximize profits, a new paradigm for network operation is needed. Heterogeneous networks that implement a small cell overlay with limited coverage and transmission power over a macro coverage area are the solution by providing capabilities and coverage where needed.

Small cells are low-cost, low-power base stations designed to improve wireless network coverage and capability. By deploying small cells on top and in complement to the traditional macro cellular networks, operators are in a much better position to provide the end users with a more uniform and improved Quality of Experience (QoE) [4]. Small cells deployment is subject to service delivery requirements, as well as to the actual constraints specific to the targeted areas. For a good uniformity of service, in dense populated areas where presence of buildings is the main reason for significant radio signal attenuation, small cells may need to be closely spaced, e.g. within a couple of hundred meters from each other. Naturally, the performance of small cells is highly dependent on the environment specific characteristics, such as materials used for building construction, their specific propagation properties and surroundings. It is particularly important to have a proper characterization of an environment where small cells are deployed.

The results presented here were published in a series of papers co-authored by the author of this thesis. The author's contributions are summarized in what follows:

1. **Show trough experimental results the feasibility of using smart antenna array with beamforming capabilities.** With a single small cell using directive antennas and low transmission power we were able to establish good indoor coverage delivering high data rates for large parts of an office building. For each azimuth value we showed that the antenna footprint is well preserved within the building. This result encourages the simultaneous use of multiple narrow beams with high gains to cover indoor environments. Our measurement results indicate low angular spread at the transmitter side and high angular spread at the receiver side. The results are published in paper [31].

2. **We calibrated and validated an analytical 3D signal coverage prediction framework (WiSE) against available field measurements**. The framework allows to determine the number of small cells required to deliver desirable coverage and capacity levels, their most desirable location, transmission power levels, antenna characteristics (beam shapes) and antenna orientation (azimuth, tilt) to serve a targeted

geographical area. The good match between measurements and predictions encourages the use of the 3D performance prediction framework, in complement to field measurements, to support small cell deployments as shown in Figure 36.

3. **Proving the benefits of using small cells to increase the indoor coverage and the end-user experience**. Using a small cell equipped with a directive antenna transmitting at low power we have established good indoor coverage. This architecture has provided high data rates for large parts of the office building and has reduced the uplink interference and UE power consumption by mitigating the UL pathloss. Results are disseminated in [54], [59].

4. **Improve handover performance in HetNET by using RSRQ parameter instead of RSRP parameter.** LTE networks handover performance are of high importance that is why we studied this domain. The results obtained during handover experiments in LTE HetNet considering for handover trigger the A3 event and different parameters: RSSP and RSRQ are presented in Chapter **Error! Reference source not found.**. We also provide some recommendations for parameter tuning for different scenarios. All the measurements are performed in a cabled environment under the conditions characteristic for dense urban settings. The detailed presentation of the results is made in Chapter 4.2 and [73].
5. **eICIC parameters optimization and HetNet cluster capacity increase.** From the analysis of the experimental results, we can conclude that even for the worst case scenario, when the cluster contains only one small cell located in the area covered by Macro, the eICIC mechanism activation increases the spectral efficiently of the cluster. Considering a specific value for ABS and testing several values for eICIC CRE offset we find the optimal offset value equal with 6 dB. The results are presented in [57] and [80].

6. **Specific Absorption Rate analyses in Heterogeneous Networks.** From the perspective of electromagnetic radiation, the high levels of Specific Absorption Rate represent a major concern in parallel transmission of spatially-tailored multidimensional excitation pulses, especially the potential for a relatively high ratio of local SAR to average SAR. The SAR analysis is presented in paper [89].

Measurements validate that the combination of Small Cells and Beamforming improve the radio coverage in indoor environment. Performances depend on bandwidth allocation, adjacent or overlapping, but in both situations a significant improvement on HetNet performance can be ensured.

A decision of what network architecture will be used for each mobile network will be taken by each network operator base on they particularities. The results presented in this thesis create the premises for native Heterogeneous Networks especially through the prism of IoT and 5G specificities.

Appendix A – Results obtained during the PhD studies

A.1 Papers published in ISI indexed publications

- D. Calin, A. Ö Kaya and I. Petrut, "On the in-building performance and feasibility of LTE small cells with beamforming capabilities," 2014 IEEE Globecom Workshops (GC Wkshps), Austin, TX, 2014, pp. 1211-1216.

- I. Petrut, M. Otesteanu, C. Balint and G. Budura, "Improved LTE macro layer indoor coverage using small cell technologies," *Electronics and Telecommunications (ISETC), 2014 11th International Symposium on*, Timisoara, 2014, pp. 1-4.

- I. Petrut, M. Otesteanu, C. Balint and G. Budura, "HetNet handover performance analysis based on RSRP vs. RSRQ triggers," *Telecommunications and Signal Processing (TSP), 2015 38th International Conference on*, Prague, 2015, pp. 232-235.

- I. Petrut, M. Otesteanu, C. Balint and G. Budura, "On the uplink performance in LTE Heterogeneous Network," *2016 International Conference on Communications (COMM)*, Bucharest, 2016, pp. 191-194.

- I. Petrut, M. Otesteanu, C. Balint and G. Budura "HetNet Performance Analysis from the eICIC Parameters Perspective" International Symposium on Electronics and Telecommunications (ISETC), 2016 11th, Timisoara, 2016, pp. 67-71

- I. Petrut, M. Otesteanu, "The IoT connectivity challenges" IEEE 12th International Symposium on Applied Computational Intelligence and Informatics, Timisoara, 2018, pp. 385-388

A.2 Papers published in BDI indexed publications

- I. Petrut, M. Otesteanu, C. Balint and G. Budura, " Cluster Capacity Increase through eICIC Technology – An Experimental Analysis," Buletinul Ştiinţific al Universităţii Politehnica Timişoara, Volume 60 (74), Issue 2, 2015

- I. Petrut, R. Poenar, M. Otesteanu, C. Balint, G. Budura, "User Experience Analysis on Real 3G/4G Wireless Networks", Acta Electrotehnica Volume 56, Number 1-2, 2015, pg 131-134

A.3 Other activities (co-author on book chapter)

- A.ANPALAGAN Ryerson University, M.BENNIS University of Oulu, R.VANNITHAMBY Intel "Design and Deployment of Small Cell Networks" ISBN: 978 1 107 05671 8 **Co-author on chapter 14** "The art of deploying small cells: field trial experiments, system design, performance prediction, and deployment feasibility (Doru Calin, Aliye ¨ Ozge Kaya, Amine Abouliatim, Gonc¸alo Ferrada, and Ionel Petrut" pp. 338-363)

References

[1] L-F Pau, Summary Introduction to Wireless LTE*4G Architecture and Key Business Implications, Proffesor Mobile business , 2011.

[2] "Word Cellular Information Service," 12 07 2018. [Online]. Available: http://www.wcisplus.com.

[3] Health and Safety Authority, A Guide to the Safety, Health and Welfare at Work - Electromagnetic Fields, 2016.

[4] A.Anpalagan, M.Bennis, R.Vannithamby, Design and Deployment of Small Cell Networks, Cambridge: Cambridge University Press , 2015.

[5] L.-F. Pau, "Summary Introduction to Wireless LTE*4G Architecture and Key Business Implications," in *Proffesor Mobile business*, 2011.

[6] J. Erfanian, "Evolution of Wireless Communications," *IEEE Communications Society,* 2013.

[7] P.Lescuyer, Evolved Packet System (EPS): The LTE and the SAE Evolution of 3G UMTS",, John Wiley & Sons Ltd., 2008.

[8] Alcatel-Lucent, "9400 LTE RAN Radio Principles Description," *Alcatel-Lucent University Course TMO18214,* no. 3, 2015.

[9] C. Cox, An Introduction to LTE: LTE, LTE-Advanced, SAE and 4G Mobile Communications, Wiley, 2012.

[10] Telecom Techniques Guide, "www.teletopix.org/," 2018. [Online]. Available: http://www.teletopix.org/.

[11] K.S. Rakesh, "4G LTE Cellular Technology: Network Architecture and Mobile Standards," *International Journal ofEmerging Research in Management &Technology,* vol. 5, no. 12, 2016.

[12] telecom info, "www.telecomsource.net," 2013. [Online]. Available: http://www.telecomsource.net/showthread.php?5881-Event-A3-in-LTE.

[13] A. D. Damini Rai, "LTE PRINCIPLES AND OPTIMIZATION (A 4G WIRELESS TECHNOLOGY)," *INTERNATIONAL JOURNAL OF ENGINEERING SCIENCES & RESEARCH,* vol. 6, no. 9, 2017.

[14] S. Litsyn, "Peak-to-Average Power Ratio Reduction in Multicarrier Communication Systems," in *DIMACS Workshop on Algebraic Coding Theory and Information Theory, Rutgers University*, Piscataway, NJ, 2003.

[15] A. &. B. R. &. U. M. Ulvan, Handover Scenario and Procedure in LTE-based Femtocell Network, 2010.

[16] 3GPP, "3GPP TR 36.814 V9.0.0 (2010-03) Evolved Universal Terrestrial Radio Access (E-UTRA); Further advancements for E-UTRA physical layer aspects, (Rel. 9).," 16 07 2018. [Online]. Available: http://www.3gpp.org/.

[17] J. Acharya, L. Gao, S. Gaur, Heterogeneous Networks in LTE-Advanced, John Wiley & Sons, 2014.

[18] R.Iyer, J. Zeto, D. Schneider et al., Small Cells, Big Challenge: A Definitive Guide to Designing and Deployng HetNets, 2013.

[19] A. Damnjanovic, J. Montojo, W. Yongbin, J. Tingfang, L. Tao, M. Vajapeyam and D. Malladi, "A survey on 3GPP heterogeneous networks," *IEEE Wireless Communications,* vol. 18, no. 3, 2011.

[20] R. Clarke, "Expanding Mobile Wireless Capacity: The Challenges Presented by Technology and Economics," *Telecommunications Policy,* 2013.

[21] A.Ghosh, N.Mangalvedhe, R.Ratasuk, "Heterogeneous Cellular Networks: From Theory to Practice," *IEEE Communications Magazine,* vol. 50, no. 6, pp. 54-64, 2012.

[22] M. Kale, M. Nguyen, "Performance Limits of Network Densification," *IEEE Journal on Selected Areas in Communications,* vol. 35, no. 6, 2017.

[23] A. M. Sadekar, R. H. Hafez, "LTE-A enhanced Inter-cell Interference Coordination (eICIC) with Pico cell adaptive antenna," in *6th International Conference on the Network of the Future (NOF)*, Montreal, QC, Canada, 2015.

[24] Jr., Robert W.Heath, "Research in wireless communication and signal processing," University of Texas at Austin, [Online]. Available: http://www.profheath.org/research/heterogeneous-networks/. [Accessed 01 2019].

[25] A. Tsegaye, "Performance evaluation of eICIC algorithms in LTE HetNets," University of Oslo, Department of Informatics (Ifi), Oslo, 2014.

[26] "What is ICIC(Inter-cell interference coordination) and eICIC (enhanced Inter-cell interference coordination)," 3GPP, 09 2012. [Online]. Available: http://3gppltee.blogspot.com/2012/09/what-is-icic-inter-cell-interference.html. [Accessed 01 2019].

[27] D. Vinayagam, "3gppltee," [Online]. Available: http://3gppltee.blogspot.no/2012/09/what-is-icic-inter-cell- interference.html.

[28] S. Ali, "An Overview on Interference Management in 3GPP LTEAdvanced Heterogeneous Networks," *International Journal of Future Generation Communication and Networking,* vol. 8, no. 1, pp. 55-68, 2015.

[29] H. E. Shaer, Interference Management In LTE-Advanced Heterogeneous Networks Using Almost Blank Subframes, Master's Degree Project, 2015.

[30] M Ali, Md. Shipon, "An Overview on Interference Management in 3GPP LTE-Advanced Heterogeneous Networks," *International Journal of Future Generation Communication and Networking,* vol. 8, no. 1, 2015.

[31] D. Calin, A. Ö Kaya and I. Petrut, "On the in-building performance and feasibility of LTE small cells with beamforming capabilities," in *2014 IEEE Globecom*, Austin, 2014.

[32] S. Fortune, D. Gay, B. Kernighan, O. Landronand, R. Valenzuela, and M. Wright, "WISE design of indoor wireless systems: practical computation and optimization," *IEEE Computational Science and Engineering, vol. 2, no. 1,* pp. 58-68, 1995.

[33] S. Sessia, S. Toufik, and M. Baker, LTE: The UMTS Long Term Evolution: From Theory to Practice: 2nd Edition, Wiley, 2012.

[34] D. Calin, A. O. Kaya, A. Abouliatim, G. Ferrada, P. Richard, and A. Segura, "On the feasibility of outdoor-to-Indoor LTE small cell deployments: Field trial experiments and performance prediction," in *IEEE GLOBECOM*, 2013.

[35] "https://www.icnirp.org/," 2018. [Online]. Available: https://www.icnirp.org/.

[36] J. Peatross and M.Ware, Physics of Light and Optics, Brigham: Brigham Young University, 2013.

[37] D.Calin, A. O. Kaya, "Modeling three dimensional 3D channel characteristics in outdoor-to-indoor LTE small cell environments," in *IEEE MILCOM*, 2013.

[38] D. Calin, A. O. Kaya, B. Kim, K. Yang, and S. Yiu, "On the high capacity lightradio metro cell design for stadiums," *Bell Labs Technical Journal, vol. 18, no. 2,* pp. 77-97, 2013.

[39] T. Müller, "GeoViS—Relativistic ray tracing in four-dimensional spacetimes," *Computer Physics Communications,* p. 2301–2308, 2014.

[40] S.-C. Kim, J. Guarino, B.J., I. Willis, T.M., V. Erceg, S. Fortune, R. Valenzuela, L. Thomas, J. Ling, and J. Moore, "Radio propagation measurements and prediction using three-dimensional ray tracing in urban environments at 908 MHz and 1.9 GHz," *Vehicular Technology, IEEE Transactions on, vol. 48, no. 3,* pp. 931-946, 1993.

[41] V. Erceg, S. Fortune, J. Ling, J. Rustako, A.J., and R. Valenzuela, "Comparisons of a computer-based propagation prediction tool with experimental data collected in urban microcellular environments," *Selected Areas in Communications, IEEE Journal on, vol. 15, no. 4,* pp. 677-684, 1997.

[42] G. Athanasiadou, A. Nix, and J. McGeehan, "A microcellular raytracing propagation model and evaluation of its narrow-band and wideband predictions," *Selected Areas in Communications, IEEE Journal on, vol. 18, no. 3,* pp. 322-335, 2000.

[43] C. Oestges, B. Clerckx, L. Raynaud, and D. Vanhoenacker-Janvier, "Deterministic channel modeling and performance simulation of microcellular

wide-band communication systems," *Vehicular Technology, IEEE Transactions on, vol. 51, no. 6,* pp. 1422-1430, 2002.

[44] A. O. Kaya, L. J. Greenstein, and W. Trappe, "Characterizing indoor wireless channels via ray tracing combined with stochastic modeling," *Wireless Communications, IEEE Transactions on, vol. 8, no. 8,* pp. 4165-4175, 2009.

[45] J. Ling, R. Valenzuela, D. Calin, "Measured and predicted correlation between local average power and small scale fading in indoor wireless communication channels," *Vehicular Technology Conference, 1998. VTC 98. 48th IEEE, vol. 3,* p. 2104–2108, 1998.

[46] V. Erceg, S. Fortune, J. Ling, J. Rustako, A.J., and R. Valenzuela, "Comparisons of a computer-based propagation prediction tool with experimental data collected in urban microcellular environments," *Selected Areas in Communications, IEEE Journal on, vol. 15, no. 4,* p. 677–684, 1997.

[47] G. German, Q. Spencer, L. Swindlehurst, and R. Valenzuela, "Wireless indoor channel modeling: statistical agreement of ray tracing simulations and channel sounding measurements," in *IEEE International Conference on Acoustics, Speech, and Signal Processing*, 2001.

[48] iBwave Solutions, "ibwave," 12 07 2018. [Online]. Available: http://www.ibwave.com/.

[49] Body of Europea Regulators for Electronic Communications, "BEREC Preliminary report in view of a common," 13 07 2018. [Online]. Available: https://berec.europa.eu/eng/.../7415-draft-berec-and-rspg-joint-report-onfaci_0.pdf.

[50] J. G. Anrews, H. Claussen, M. Dohler, S. Rangan, M. C. Reed, "Femtocells: Past, Present and Future," *IEEE Journal on Selected Areas in Communications, April 2012, Vol. 30, Issue 3,* pp. 497-508, 2012.

[51] kathrein, "kathrein.de/en/mobile-communication-antennas/," 17 07 2018. [Online]. Available: http://www.kathrein.de/en/mobile-communication-antennas/.

[52] G. de la Roche, A. A. Glazunov, Ben Allen (Editors), LTE-Advanced and next generation wireless networks. Channel modelling and propagation, John Wiley & Sons, 2013.

[53] S. Sesia, M. Baker, I. Toufik, LTE–the UMTS Long Term Evolution: from theory to practice, John Wiley & Sons, 2009.

[54] I. Petrut, M. Otesteanu, C. Balint, G. Budura, "Improved LTE Macro Layer Indoor Coverage Using Small Cell Technologies," in *International Symposium on Electronics and Telecommunications 2014*, Timisoara, 2014.

[55] A. Damnjanovic, J. Montojo, Y. Wei, T. Ji, T. Luo, M. Vajapeyam, T. Yoo, O. Song and D. Malladi, "A Survey on 3GPP Heterogeneous Networks," *IEEE Wireless Communications Magazine,* pp. 10-21, June 2011.

[56] A. Ghosh, "Heterogeneous cellular networks: From theory to practice," *IEEE Communications Magazine, , vol.50, no.6,* pp. 54-64, 2012.

[57] I. Petrut, M. Otesteanu, C. Balint and G. Budura, "Cluster Capacity Increase through eICIC Technology - An Experimental Analysis," *Buletinul Ştiinţific al Universităţii Politehnica Timişoara, Volume 60(74), Issue 2, 2015,* 2015.

[58] Alcatel-Lucent Wireless department, "Small Cells product portfolio presentation," 2015. [Online]. Available: aww.alcatel-lucent.com/portofolio/small. [Accessed 2016].

[59] I. Petrut, M. Otesteanu, C. Balint and G. Budura, "On the uplink performance in LTE Heterogeneous Network," in *2016 International Conference on Communications (COMM)*, Bucharest, 2016.

[60] I. Petrut, M. Otesteanu, C. Balint and G. Budura, R. Poenar, "User Experience Analysis on Real 3G/4G Wireless Networks," *Acta Electrotehnica, vol. 56, no. 1-2,* pp. 131-134, 2015.

[61] Alcatel-Lucent, "4G Sherpa toll for Air Interface," 2014. [Online]. Available: https://www.scribd.com/document/367318761/Sherpa-User-Guide. [Accessed 2018].

[62] Mrs. Sonia, N. Malik, P. Rekhi, S. Malik, "Uplink Power Control Schemes in Long Term Evolution," *International Journal of Engineering and Advanced Technology (IJEAT) ISSN: 2249 – 8958, Volume-3, Issue-3,* 2014.

[63] D. Calin, A. O. Kaya, B. Kim, K. Yang, and S. Yiu, "On femto deployment architectures and macrocell offloading benefits in joint macro-femto deployments," *IEEE Communications Magazine,* vol. 48, no. 1, pp. 26-32.

[64] 3GPP, " 3GPP TS 36.300, "Evolved Universal Terrestrial Radio Access (E UTRA) and Evolved Universal Terrestrial Radio Access Network (E UTRAN); Overall Description; Stage 2", version 8.7.0," 2008. [Online]. Available: http://www.3gpp.org/dynareport/36300.htm.

[65] H. Holma, A. Toskala, P. Tapia, HSPA+ Evolution to Release 12. Performance and Optimisation, John Wiley and Sons, 2014.

[66] ETSI, "ETSI TS 136 214 "Evolved Universal Terrestrial Radio Access (E UTRA); Physical layer; Measurements (Release 10)," 2011. [Online]. Available: https://www.etsi.org/deliver/etsi_ts/136200_136299/136214/14.04.00_60/ts_136214v140400p.pdf.

[67] 3GPP, "[1] 3GPP TS 36.331 V10.0.0 (2010-12) 3rd Generation Partnership Project; Technical Specification Group Radio Access Network; Evolved Universal Terrestrial Radio Access (E-UTRA); Radio Resource Control (RRC); Protocol specification (Rel. 10)," [Online]. Available: https://3gpp.org.

[68] J. Kurjenniemi, T. Henttonen, J. Kaikkonen, "Suitability of RSRQ measurement for quality based inter-frequency handover in LTE," in *IEEE International*

Symposium on Wireless Communication Systems, ISWCS '08, Reykjavik, 2008.

[69] Hytem, "standard variable atenuators," Hytem, [Online]. Available: http://www.hytem.net/produits/standard-systems/?lang=en. [Accessed 27 02 2019].

[70] ETSI, "ETSI TS 136 211 "Evolved Universal Terrestrial Radio Access (E UTRA); Physical channels and modulation (Release 8)," 2009. [Online]. Available: https://www.etsi.org/deliver/etsi_ts/136200_136299/136211/08.08.00_60/ts_136211v080800p.pdf.

[71] A. Jensen, M. Lauridsen, P. Mogensen, T. B. Sørensen, P. Jensen, "LTE UE Power Consumption Model For System Level Energy and," in *Vehicular Technology Conference,2012*, 2012.

[72] B. Dusza, C. Ide, L. Cheng, C. Wietfeld, "An Accurate Measurement Based Power Consumption Model for LTE Uplink Transmissions," in *Proc. of IEEE INFOCOM 2013, Turin, Italy*, 2013.

[73] I. Petrut, M. Otesteanu, C. Balint and G. Budura, "HetNet handover performance analysis based on RSRP vs. RSRQ triggers," in *38th International Conference on Telecommunications and Signal Processing (TSP), 2015*, Prague, 2015.

[74] A. M. Sadekar, "LTE-A enhanced Inter-cell Interference Coordination (eICIC) with Pico cell adaptive antenna," in *6th International Conference on the Network of the Future (NOF)*, 2015.

[75] 3GPP, "3GPP TR 25.825 (V1.0.0) 3rd GPP Technical Specification Group Radio Access Network "Dual Cell HSDPA Operation"," [Online]. Available: https://www.3gpp.org.

[76] A. Elnashar, M. A. El-saidny, M. R. Sherif, Design, Deployment and Performance of 4G-LTE Networks, A Practical Approach, John Wiley&Sons, 2014.

[77] S. Moon, S. Malik, B. Kim, H. Choi, S. Park, C. Kim, I. Hwang, "Cell Range Expansion and Time Partitioning for Enhanced Inter-cell Interference Coordination in Heterogeneous Network," in *47th Hawaii International Conference on System Sciences (HICSS)*, Waikoloa, 2014.

[78] K. I. Pedersen, Y. Wang, S. Strzyz, F. Frederiksen, "Enhanced Inter-Cell Interference Coordination in Co-Channel Multi-Layer LTE-Advanced Networks," *IEEE Wireless Communications, 20(3),* pp. 120-127, June 2013.

[79] D. V. Bhosale, V. D. Jadhav, "A Reviev of Enhanced Inter-cell Interference Coordination in Long Term Evolution Heterogeneous Netwoks," *Int. Journal of Innovative Science, Enineering and Technology, vol. 2 Issue 2,* 2015.

[80] I. Petrut, M. Otesteanu, C. Balint and G. Budura, "HetNet Performance Analysis from the eICIC Parameters Perspective," in *International Symposium*

on Electronics and Telecommunications (ISETC), 2016 11th, Timisoara, Timisoara, 2016.

[81] A. Daeinabi, K. Sandrasegaran, "A Proposal for an Enhanced Inter-Cell Interference Coordination Scheme with Cell Range Expansion in LTE-A Heterogeneous Networks," 7-10 August 2013. [Online]. Available: https://epress.lib.uts.edu.au/conferences/index.php/ARTIN/warin/paper/viewFile/468/75

[82] M. S. Ali, "An Overview on Interference Management in 3GPP LTE-Advanced Heterogeneous Networks," *International Journal of Future Generation Communication and Networking, Vol. 8, No. 1,* pp. 55-68, 2015.

[83] HS Jo, YJ Sang, P Xia, J. G. Andrews, "Heterogeneous Cellular Networks with Flexible Cell Association: A Comprehensive Downlink SINR Analysis," *IEEE Transactions on Wireless Communications, vol.. 11, no. 10,* pp. 3484-3495, 2012.

[84] J. Goodchild, Integrating data, voice and video – Part II., IP Video Implementation and planning guide, United States Telecom Association, 2005.

[85] B. Chihani, K. Regami, E. Bertin, D. Collange, N. Crespi, T. Falk, "User-Centric, Quality of Experience Measurement," in *Intl Conf Mobile Computing, Applications and Services (MobiCASE)*, 2013.

[86] CelPlan International, "Customer experience Optimization in Wireless Networks," CelPlan International, Inc, 2014.

[87] M. Rumney (Ed), Agilent Technologies, LTE and the Evolution to 4G Wireless: Design and Measurement Challenges, Wiley, 2013.

[88] Spirent, 17 7 2018. [Online]. Available: http://corporate.spirent.com/Site/Home/Products /Datum.

[89] C. I.Petrut, "Monitoring Heterogeneous Networks Radiations Through A Dedicated SAR Application," under preparation.

[90] R. Asif, R.A. Abd-Alhameed, M. Bin-Melha, A. Qureshi, C.H See, Y.I., "Study on Specific Absorption Rate," in *Loughborough Antennas and Propagation Conference (LAPC)*, 2014.

[91] M. Bhat, "Effects on Testis of Human Being with Specific Absorption Rate (SAR) of Mobile Phone," *SJET, vol. 5, issue 10.*

[92] D.J. Panagopoulos, O. Johansson, G.L. Carlo, "Evaluation of Specific Absorption Rate as a Dosimetric Quantity for Electromagnetic Fields Bioeffects," *PLoS ONE, vol. 8, issue 6,* 2013.

[93] I. Graesslin, H. Homann, S. Biederer, P. Börnert, K. Nehrke, P. Vernickel et al., "A specific absorption rate prediction concept for parallel transmission MR," *Magnetic Resonance in Medicine, vol. 68, issue 5,* 2012.

[94] C.Groza, "Aplicație mobilă de monitorizare a emisiilor radio generate de echipamente de comunicatii," Unpublished, 2015.

[95] W. D. Darmindra, "Specific Absorption Rates in the Human Head and Shoulder for Passive UHF RFID Systems at 915 MHz," *URSI,* 2008.

[96] S.C. Satapathy, A. Joshi, "Smart Innovation, Systems and Technologies," *ICTIS 2017, vol. 2,* 2017.

[97] A.M. El-Sharkawy, D. Qian, P.A., Bottomley, W.A. Edelstein, "A multichannel, real-time MRI RF power monitor for independent SAR determination," *Medical Physics, vol. 39, issue 5,* 2012.

[98] N. Slamnik, J. Musovic, A. Okie, F. Tankovic, I. Krijestorac, "An approach to analysis of heterogeneous networks' efficiency," in *2017 XXVI International Conference on Information, Communication and Automation Technologies (ICAT)*, 2017.

[99] "When does your electromagnetic exposure exceed the recommended safety limits?," 17 07 2018. [Online]. Available: https://www.home biology.com/electromagnetic-field-radiation-meters/safe-exposure-limits.

[100] C.Groza, "SAR Watch - Tracking Radiation Exposure," [Online]. Available: https://play.google.com/store/apps/details?id=ro.upt.sarwatch#details reviews.

[101] [Online]. Available: https://www.techopedia.com/definition/28247/.